UNIVERSITY OF SOUTHAMPTON

Assessing potential spatial trade-offs between renewable energy expansion and biodiversity conservation

by

Sebastian Dunnett

ORCID ID 0000-0002-4238-2508

A thesis submitted for the degree of
Doctor of Philosophy

in the
Faculty of Environmental and Life Sciences
Biological Sciences/Geography and Environmental Science

22 September, 2020

This page intentionally left blank.

UNIVERSITY OF SOUTHAMPTON

ABSTRACT

FACULTY OF ENVIRONMENTAL AND LIFE SCIENCES
BIOLOGICAL SCIENCES/GEOGRAPHY AND ENVIRONMENTAL SCIENCE

Doctor of Philosophy

ASSESSING POTENTIAL SPATIAL TRADE-OFFS BETWEEN RENEWABLE ENERGY EXPANSION AND BIODIVERSITY CONSERVATION

by Sebastian Dunnett

Total word count (excl. figures, tables, footnotes and bibliography): 30,506

Energy systems need decarbonisation in order to limit global warming to within safe limits. Unfettered climate change has the potential to greatly exacerbate species extinctions already much higher than historic baselines. Renewable energy technologies, especially solar photovoltaic and wind, have the potential to greatly aid in this decarbonisation but there are concerns as to the land required when compared to conventional, energy-dense, fuels. This is especially true given the urgent need to demarcate more land for biodiversity conservation. However, attempts to evidence these land concerns are hindered by lack of quality spatial data. This thesis shows, using newly generated spatially explicit data, that the expansion of renewable energy and biodiversity conservation do not necessarily conflict. I find, using a novel global, open access, harmonised dataset of onshore wind and solar photovoltaic installations, that although there are currently numerous overlaps with areas of conservation importance worldwide, echoing previous studies, when historic distributions are taken into account there is no evidence that energy-biodiversity conflict is set to increase in the future. I also find that although priority areas for biodiversity conservation have been identified well in prior work, identification of priority areas for renewable energy needs improvement. The results presented here suggest that more thoughtful planning of renewable energy can ensure no more potential impact on biodiversity than expected under a business as usual development scenario. I anticipate the data will support more research into what drives renewable energy siting, as well as providing a potential avenue for civil society to assess governmental progress towards clean energy objectives, for example Target 7.1 and 7.2 of the Sustainable Development Goals. Furthermore, the methods here provide a framework into which local impacts of renewable energy on biodiversity can be incorporated when they are better known.

This page intentionally left blank.

Contents

This page intentionally left blank.

List of Figures

List of Tables

This page intentionally left blank.

Acronyms

AUC	area under curve
AZE	Alliance for Zero Extinction
CBD	Convention on Biological Diversity
DBSCAN	density-based spatial clustering of applications with noise
DPI	development potential index
EU	European Union
FAO	Food and Agriculture Organisation of the United Nations
GEO	Global Environment Outlook
GIS	geographic information system
GLM	generalised linear model
GWh	gigawatt hour
HBASE	Human Built-up and Settlement Extent
IBA	Important Bird and Biodiversity Area
IEA	International Energy Agency
IPBES	Intergovernmental Panel on Biodiversity and Ecosystem Services
IPCC	Intergovernmental Panel on Climate Change
IRENA	International Renewable Energy Agency
ISO	International Standards Organisation
IUCN	International Union for the Conservation of Nature
KBA	Key Biodiversity Area
LSA	Land System Archetype
LPI	Living Planet Index
MAE	mean absolute error
MEA	Millenium Ecosystem Assessment
NET	negative emissions technology
OSM	OpenStreetMap
PA	protected area
PV	photovoltaic
PADDD	protected area downgrading, downsizing and degazettement
RF	random forest
RMSE	residual mean standard error
ROC	receiver operating characteristic

SDG	Sustainable Development Goal
TWh	terawatt hour
UKREPD	United Kingdom Renewable Energy Planning Database
UNFCCC	United Nations Framework Convention on Climate Change
USGS	United States Geological Survey
USWTD	United States Wind Turbine Database
WDPA	World Database on Protected Areas
WGS84	World Geodetic System 1984
ZINB	zero-inflated negative binomial

Declaration of Authorship

I, Sebastian Dunnett, declare that this thesis entitled *Assessing potential spatial trade-offs between renewable energy expansion and biodiversity conservation* and the work presented in it are my own and has been generated by me as the result of my own original research.

I confirm that:

1. This work was done wholly or mainly while in candidature for a research degree at this University;
2. Where any part of this thesis has previously been submitted for a degree or any other qualification at this University or any other institution, this has been clearly stated;
3. Where I have consulted the published work of others, this is always clearly attributed;
4. Where I have quoted from the work of others, the source is always given. With the exception of such quotations, this thesis is entirely my own work;
5. I have acknowledged all main sources of help;
6. Where the thesis is based on work done by myself jointly with others, I have made clear exactly what was done by others and what I have contributed myself;
7. Parts of this work have been published as Dunnett, S., Sorichetta, A., Taylor, G., & Eigenbrod, F. 2020. Harmonised global datasets of wind and solar farm locations and power. *Scientific Data*: *7*(130). `https://doi.org/10.1038/s41597-020-0469-8`.

Signed:

Date:

This page intentionally left blank.

Acknowledgements

I wish to gratefully acknowledge the Natural Environment Research Council (NERC) and the University of Southampton for funding my research.

I would first like to thank my primary supervisor, Prof. Felix Eigenbrod. His unwavering support and guidance seemed to fly in the face of everything I had ever read about PhD supervisors. Secondly, I would like to thank Dr Rob Holland for his positivity and encouragement in the past few months. I would also like to thank my other supervisors Prof. Gail Taylor and Dr Richard Pearson for their support, as well as Dr Alessandro Sorichetta for his help getting the first chapter published. Thanks also to Dr Michael Harper, Shackleton goalkeeper extraordinaire, for turning me on to OpenStreetMap as a potential data source and also for taking the time to produce the sotonthesis R package, with which this thesis was written.

I wish to thank all the members of the ADVENT research project, staff and PhD students, for the supportive environment in which to conduct my research. I also thank the members of my lab for their intelligent and engaging debates; early on I wondered whether I would ever be able to understand them!

In addition, I would like to thank my unofficial funders: my parents. You set the standard for inter-generational equity and I am immensely privileged to have you in my corner. Happy retirement!

Finally, I would like to thank my partner Jessie J, for being my good bad cop. I am looking forward to a lifetime of learning with you.

This page intentionally left blank.

Introduction

Accelerating biodiversity loss

Catastrophic global biodiversity decline is continuing and, in many cases, accelerating in almost every assessment of recent history and future projections (Leadley et al., 2010; Pimm et al., 2014; Newbold et al., 2015). A mid-term assessment of progress towards the 2020 Aichi Targets, developed under the umbrella Convention on Biological Diversity (CBD), used a Pressure State Benefit Response model and a diverse selection of indicator datasets for evaluation. Despite 21 out of 33 (64%) *response* indicators showing an increase, e.g. a marked increase in conservation effort, 5 of 7 (71%) of *pressure* indicators and 11 of 17 (65%) *state and benefit* indicators showed a decrease in the period 2010-2015 (Tittensor et al., 2014).

In modern times, biodiversity loss has been linked with a number of facets of globalisation, both directly and indirectly. One analysis linked threats in the IUCN Red List of Threatened Species (hereafter Red List) and BirdLife threatened species database to a global multi-regional input output model that describes international trade. The study concluded that up to 30% of threats to threatened species are due to international trade, with the vast majority of threats generated by demand from the USA and Japan (Lenzen et al., 2012). A more recent study suggests that world regions are starting to displace their impact on biodiversity from the electricity sector along international supply chains (Holland et al., 2019). Whilst historic intrusions into species habitat were from local demands for food, fibre, fuel and living space, the new globalised world order means that developed countries increase threats to global species through demand for products that are ultimately produced in developing countries. However, one analysis suggests that the impact of humans (mid-Holocene) on species habitat and the natural environment was much larger than previously thought. Impact had before been demonstrated locally at site-level but not regionally. Deforestation for cropland and pasture was significant Europe-wide as early as 1000BC (Kaplan, Krumhardt, & Zimmermann, 2009); humans may even have had an impact on the climate system since this time. The vastly increased impact of human demand on the terrestrial system post-1950 is labelled by land scientists as "The Great Acceleration" – a rapid uptick in socio-economic metrics and resource use (Steffen, Broadgate, Deutsch, Gaffney, & Ludwig, 2015). This has led to some calls for the prioritisation of re-establishing biome and Earth system functions

left lacking after the extinction of global megafauna (Norris, Terry, Hansford, & Turvey, 2020).

Energy demand is an important driver of threats to species (Holland et al., 2015, 2016, 2019), and business as usual demand for non-renewable fuel to drive industry and technology risks worsening any decline. Fossil fuel reserves (petroleum and coal deposits) overlap areas of high ecoregional species richness and number of threatened species (Butt et al., 2013; Harfoot et al., 2018). As not all fossil fuel reserves, even recoverable ones, will be exploited, this type of analysis only works to highlight future risks of continued demand for non-renewable fuel. The most imperilled regions were identified as the western Pacific Ocean (around Indonesia and the Coral Triangle) and northern South America. Significant trade-offs may need to be made in these regions if both demand for fossil fuels and conservation continue. Other studies have tried to link the proliferation of fossil fuel extraction with biodiversity decline, but most settle for non-causal implications. One simple overlap analysis in the Western Amazon, looking at both leased and non-leased blocks, identified 180 oil and gas blocks covering $\sim$ 688,000km^2, intersecting with some highly speciose regions and many indigenous areas (Finer, Jenkins, Pimm, Keane, & Ross, 2008). In Ecuador and Peru, these blocks cover two thirds of their national share of the Amazon. Another, lacking serious inferential power, suggests that oil price inelasticity may be able to affect deforestation rates by driving agricultural intensification and extensification through petrochemical fertiliser price shifts (Eisner, Seabrook, & McAlpine, 2016). With more studies asserting that fossil fuel demand is driving extraction in more and more remote locations with high biodiversity (Leach, Brooks, & Blyth, 2016), there is an even more urgent need for an expedited shift to renewable technologies.

Arresting rapid biodiversity loss requires considering multiple drivers – both synergistic and antagonistic. A new framework for "New Conservation", where both regulatory *and* monetary valuation and non-use values can contribute to conservation, has been suggested (Pearson, 2016). These can differ in their importance when looking at different levels of biodiversity: whether it is genetic, population, species, or ecosystem level. This is further complicated when different facets of biodiversity are non-congruent (Orme et al., 2005). Hotspots of species richness, endemism and threat are only present in the 2.5% of global hotspot areas; over 80% of hotspots are idiosyncratic, i.e. contain high levels of only one of the three. More complicated still is that any one index of biodiversity only explains up to 24% of variation in the other facets, meaning that a different mechanism is responsible for the creation of species richness, endemism, and threat. However, recent work suggests that large gains in biodiversity conservation can be achieved through small, targeted increases in the global protected area estate (Pollock, Thuiller, & Jetz, 2017).

Fortunately, the number of robust datasets and tools that can support conservation decisions are growing. The PREDICTS dataset contains more than 3.2 million records sampled at over 26,000 locations and representing over 47,000 species. The dataset can be used to ask pertinent questions as to how well conservation science is protecting global biodiversity

(Hudson et al., 2016; e.g. Newbold, Hudson, et al., 2016a, 2016a; Gray et al., 2016). Furthermore, to aid regional biodiversity assessments like the Global Environment Outlook (GEO) and the Intergovernmental Panel on Biodiversity and Ecosystem Services (IPBES), three global knowledge products - the Red List, Protected Planet, and Key Biodiversity Areas (KBAs) - have been disaggregated and presented alongside fourteen other datasets: numbers of species occurring and percentages threatened; numbers of endemics and percentages threatened; downscaled Red List Indices for mammals, birds, and amphibians; numbers, mean sizes, and percentage coverages of IBAs and AZE sites; percentage coverage of land and sea by protected areas; and trends in percentages of IBAs and AZE sites wholly covered by protected areas (Brooks et al., 2016). It has also been suggested that three extant indices, the Red List, WWF's Living Planet Index (LPI), and the Biodiversity Intactness Index (BII) (Newbold, Hudson, et al., 2016a), can adequately measure progress towards an ambitious post-2020 CBD goal (Mace et al., 2018).

Land change drives global biodiversity loss

One of the strongest identified drivers of biodiversity decline is land use and land cover change (hereafter referred to as land change) (Leadley et al., 2010; B. McGill, 2015). Despite this, the majority of studies overwhelmingly focus on climate change projections at the expense of land change projections, despite the latter two directly driving decline of biodiversity. The Millennium Ecosystem Assessment (MEA) reported that land change has been the most important driver of biodiversity decline in the last 50 years. The LPI suggests that habitat destruction and/or degradation due to land change constitutes an ongoing threat to 44.8% of vertebrate populations listed; climate change in only 7.1% of them. The Red List has a ratio of 85%/20%. Of 2,313 articles published in 1990-2014 that draw on either climate change or land change for projections, 85.2% made use of climate change projections alone and only 14.8% used either a combination of both (10.7%) or only land change (4.1%) (Titeux et al., 2016).

Land use has a demonstrably strong impact on all levels of biodiversity. A study using the PREDICTS dataset demonstrated that while compositional turnover within land uses does not differ strongly between land use category, human land uses and secondary vegetation in an early stage of recovery are poor at retaining species that characterise primary vegetation (Newbold, Hudson, et al., 2016b). Another study, also using the PREDICTS dataset, looked at the efficacy of the global protected area network by comparing four different facets of biodiversity (species richness, species abundance, rarefaction-based richness, and endemicity) across paired sites within and outside of protected areas. Globally, species richness was found to be 10.6% higher and abundance 14.5% higher in protected sites, with rarefaction-based richness and endemicity not differing significantly (Gray et al., 2016). Whilst this may seem encouraging for the existence of protected areas, the study showed that for the large part the observed difference between protected and non-protected sites could be explained by

differences in land use: protected areas were most effective when protecting primary habitat from conversion to human-dominated land uses. If we were to use the planetary boundaries framework, with a boundary of 10% loss of abundance and 20% loss of species richness, land use change has contributed significantly to the overshooting of these boundaries (Newbold, Hudson, et al., 2016a), although the approach of using the planetary boundary framework for something as complex as biodiversity has been heavily criticised (Montoya, Donohue, & Pimm, 2018). When land use, land use intensity, distance to nearest road and human population density are all set as fixed effects, these factors have already reduced local biodiversity intactness across 58.1% of the global surface where 71.4% of the world's human population live.

It is clear that we live on a planet now predominately covered by human land uses, and also that this is not confined to recent history. Not only can significant human modification be demonstrated as early as 1000BC (Kaplan et al., 2009), but between 1700 and 2000, 55% of Earth's ice-free land was transformed into rangelands, croplands, villages and densely settled land uses (Ellis, Goldewijk, Siebert, Lightman, & Ramankutty, 2010). Two processes drove this transformation: expansion into wildlands (95% of ice-free land was wildlands and semi-natural biomes in 1700), but also intensification of the semi-natural lands already converted from wildlands. Global pastures meanwhile increased six-fold between 1800-2000. With sustainable, species-friendly farming "*rare in reality*", expansion of modern agriculture causes an "*incontrovertible*" loss of biodiversity (Lanz, Dietz, & Swanson, 2018, p. 274). Studies into the intensity and length of anthropogenic impacts on Earth's natural habitats have led to calls for the recognition of a new type of land classification: *anthromes* (Ellis et al., 2010).

Anthromes, and explicitly accounting for human impacts in all biomes, allow for important research into conservation efficacy. One study, looking at the distribution of conservation effort relative to anthromes, found that protected areas are not equally distributed across anthromes and that protected areas were more prevalent in less populated anthromes (Martin et al., 2014). Secondly, biodiversity hotspots are also not equally distributed: they are more common at either end of the anthromes spectrum, in densely settled anthromes and wildlands with sparse human populations. The authors suggest that there are significant conservation opportunities in understudied anthromes: rice villages, irrigated villages, and remote rangelands.

Integrating socio-economic data into land classifications arguably allows for more accurate representations of land systems, especially as human influence on Earth is increasing (Ellis et al., 2010; Steffen et al., 2015). One such system is *land system archetypes* (LSAs). Whilst previous efforts to classify archetypal land systems concentrated on dominant land cover, with limited consideration of land use intensity, LSAs are based on 30 high resolution datasets on land use intensity, environmental and socio-economic conditions for the year 2005 (Václavík, Lautenbach, Kuemmerle, & Seppelt, 2013). The extensive croplands archetype in Eastern Europe, China, Argentina and India appear strikingly similar, whilst

there is demonstrable diversity of land systems at a sub-national scale in China and India. These findings challenge previous studies that use integrated assessment models at national or macro-regional scales, and suggest that finer scale tools should be used. The LSA concept has been extended to provide a methodology to transfer research project outcomes to geographically separated landscapes. A proof of concept study estimated the transferability of twelve regional sustainable land management projects. Results showed that areas with high transferability are typically clustered around the project site, but for some projects they are geographically distant (Václavík et al., 2016).

Unsurprisingly, with a significant impact on biodiversity, land change can have repercussions for global conservation efforts. One study looked at how land change may impact the global protected area network using the CLUMondo land change model (Van Asselen & Verburg, 2013; Pouzols et al., 2014). CLUMondo allows for distinguishing between intensively and extensively managed systems in more detail, as well as more adequately accounting for mosaic systems that generally house higher levels of biodiversity. Pouzols and colleagues used CLUMondo to look at Red List distributions for current day and 2040, discounted by land cover. Taking the Aichi Target of expansion to 17% global terrestrial protected area by 2020, the team looked at the optimal species ranges possible to cover with expansion to 17%, then 30% and upwards. The analysis showed that projected global land change by 2040 would reduce species ranges covered by 12% if 17% of land were protected. This land use change requires 4% more land protected (to 21% globally) to protect the same amount of species ranges as 17% land with no land change.

Climate change threatens global biodiversity

Climate scientists warn that global temperature rise caused by greenhouse gas emissions should not exceed 2°C (UNFCCC, 2016). To have 50% chance of doing this for the 21st Century, cumulative carbon emissions between 2011-2050 need to be limited to 1,100Gt of CO_2. Globally, one third of oil reserves, half of gas reserves, and over 80% of current coal reserves should remain unused (McGlade & Ekins, 2015). There is significant concern that territorial ambitions to exploit fossil fuel reserves are inconsistent with temperature commitments. Whilst land change may be the dominant driver of many population declines, climate change is still a significant driver and the two are very much synergistic. Even with mid-range climate projections, some studies suggest that 15-37% of all species will be "committed to extinction" (Thomas et al., 2004). One study used MEA scenarios to evaluate exposure of all 8,750 land bird species to projected land cover changes due to climate and land use change. Even under environmentally benign scenarios, at least 400 species are projected to suffer >50% range reductions by the year 2050 (over 900 by 2100). Expected climate shifts at high latitudes are significant, but the species most at risk are range-restricted endemic species of the tropics, where contractions are driven by anthropogenic land conversions (Jetz, Wilcove, & Dobson, 2007). Another uses a dynamic global vegetation model and an

aggregated metric of simultaneous biogeochemical, hydrological and vegetation-structural shifts to investigate impacts of climate change and land change on the terrestrial biosphere in the last 300 years. Within three centuries, the impact of land change has increased thirteen-fold. Since the advent of the 20th century, the impact of climate change has caught up (Ostberg, Schaphoff, Lucht, & Gerten, 2015).

There is a rich literature on climate impacts on species, including much evidence from the paleoecological archives (Nogués-Bravo et al., 2018). A recent review of different approaches for modelling species vulnerability to climate change highlighted different analytical approaches (Pacifici et al., 2015). A correlative approach is best when there are only occurrence data and you can model fossil species' paleoclimatic niche, or model future suitable areas. Mechanistic models have the greatest power to assess species vulnerability to climate change and identify conservation actions, but the technique is restricted to well-studied species for which detailed demographic and physiological data are available. Trait-based approaches are less resource-intensive and ideal to conduct regional assessments in the absence of specific distribution data (Urban et al., 2016). Whilst there are many approaches, Pacifici et al. (2015) caution future analyses not to neglect the indirect effects of climate change on human use and biological communities.

All three approaches – correlative, mechanistic and trait-based – have been used to answer the important question of how current conservation actions will change with future climate and how best to quantify climate risk. Using a combination of species spatial and demographic variables, one study showed that current data compiled for the Red List are sufficient to accurately predict extinction risk from climate change and there is no need to revamp species threat assessments as previously thought (Pearson et al., 2014). This has given rise to research into quantifying the "warning time" for species extinctions, i.e. the time between a species being listed as threatened, and its extinction. The warning time for any species must be longer than the latency time (the time between a species being listed as threatened and conservation action starting) and response time (time taken for the species to respond to conservation action) (Akçakaya, Butchart, Watson, & Pearson, 2014). Using multiple criteria can give the longest possible warning time. One study used ecological niche models and generic life history models to project population distributions for 36 North American endemic reptiles and amphibians to 2100. Modelled 'populations' were assessed at various time intervals using all, one or combinations of two of the Red List criteria. When all criteria are used, there is ample warning time (median 62 years, with 99% of replicates giving over 20 years' warning) (Stanton, Shoemaker, Pearson, & Akçakaya, 2015).

More recent studies have used trait-based approaches to look at the impact that climate change has already had on species populations. One review looked at published studies providing causal evidence of negative impacts of climate change on species populations and identified intrinsic and spatial traits most associated with declines. Using these traits, the authors identified species in the Red List likely to have been impacted by climate already. The analysis suggests that as many as 47% of terrestrial non-volant threatened mammals

(N=873) and 23.4% of threatened birds (N=1,272) may have already been impacted in at least part of their distribution (Pacifici et al., 2017).

Projected climate change can also contribute to large shifts in global vegetation cover: up to one tenth of land may be highly to very highly vulnerable, using Intergovernmental Panel on Climate Change (IPCC) scenarios and uncertainty treatments. Temperate mixed forest, boreal conifer and tundra and alpine biomes were the biomes most at risk, whilst tropical evergreen broadleaf forest and desert biomes showed the lowest vulnerability (Gonzalez, Neilson, Lenihan, & Drapek, 2010). Further research assessed the vulnerability of ecosystems to biome shifts at two spatial scales (Eigenbrod, Gonzalez, Dash, & Steyl, 2015): the global extent of climate refugia depends on the definition of habitat intactness and the spatial scale of analysis. 28% of terrestrial vegetation can be considered refugia if all natural vegetated land cover is considered, but this drops to 17% if only areas with >50% wilderness at scale of 48 by 48km are considered, and down to 10% if done at 4.8 by 4.8km.

Species distribution shifts caused by a changing climate also have ramifications for the efficacy of conservation measures. Analysis of African Important Bird Areas (IBAs) suggests that the network is remarkably climate resilient. If sub-Saharan avifauna ranges are projected to 2085, 88-92% of priority species retain suitable climate space in one or more IBAs in the network; only 7-8 species lose climatic representation in the network. Species turnover will likely vary regionally, but will be substantial at many sites (>50% at 42% of IBAs for priority species) (Hole et al., 2009). In fact, setting aside land for conservation can have synergistic benefits. For example, in the UK, with a (now modified) commitment to reduce emissions 50% by 2025 and 100% by 2050 (compared to 1990 levels), it has been shown that land sparing with concurrent land restoration can sequester enough carbon by 2050 to offset emissions from agriculture. Not only will these land areas provide potential refugia for climate refugees, but the land areas themselves may help reduce the *need* for climate refugia (Lamb et al., 2016).

Impacts of renewable technologies

As a result of the need to abate anthropogenic emissions, alternative energy systems are growing rapidly that may allow continued development whilst maintaining or reducing carbon emissions – the so-called "decoupling" of the economy and emissions. Interesting research on resource exploitation time series of 27 renewable and non-renewable resources sought to identify peak years of extraction and provides evidence for why renewable alternatives should be explored (Seppelt, Manceur, Liu, Fenichel, & Klotz, 2014). 21 of 27 resources have already experienced a peak year, with 20 of them occurring in the period 1960-2010 – a relatively narrow period in human history. The authors express worry at the synchrony evident in the peaks of 16 resources occurring in the year 2006, and call for a paradigm shift from resource exploitation to more sustainable use. There has not yet been a peak year for

renewable energy, but the study puts forward little evidence that renewable energy provides a robust substitute for conventional fuels.

However, renewable energy, in its many forms, remains an important research avenue due to the potential to vastly reduce emissions whilst increasing energy supply to meet rising demand. Life cycle assessment of alternative energy pathways to 2050, analysing freshwater ecotoxicity and eutrophication, particulate matter, and climate change, suggests a doubling of electricity supply of renewable technology whilst stabilising or even reducing emissions is feasible (Hertwich et al., 2014). The same study warns that this may come with displaced pressures on resource extraction: renewable energy uses 11-40 times more copper than conventional fossil fuels (solar photovoltaic) and 6-14 times more iron (wind). Two years' copper production and one year's current iron production would produce a system capable of supplying electricity needs in 2050. A recent study emphasised that this increased mining effort could negatively impact global biodiversity (Sonter, Dade, Watson, & Valenta, 2020).

However, there are fierce criticisms of these overly optimistic analyses. One review assessed 24 studies that forecast 100% renewable energy generation at regional, national or global scale with sufficient detail (Heard, Brook, Wigley, & Bradshaw, 2017). The analysis used four criteria for feasibility: consistency with mainstream energy demand forecasts, simulating at a range of timescales with resilience to climate change, identifying necessary transmission and distribution requirements, and maintaining the provision of necessary ancillary requirements. The highest unweighted score was four (out of seven); eight studies (33%) provided no form of system simulation, twelve (50%) relied on unrealistic forecasts of energy demand. While four (17%) provided transmission and distribution requirements, only two (drawn from the same study) addressed ancillary requirements. More than anything, these systems need evaluation with multiple criteria; not just carbon emissions. For example, while renewable energy produces fewer emissions than conventional fossil fuels, they are more land extensive (Smil, 2008, 2010; Trainor, McDonald, & Fargione, 2016; Fritsche et al., 2017; United Nations Convention to Combat Desertification, 2017; Miller & Keith, 2018; Zalk & Behrens, 2018). In another multicriteria analysis of seven energy sources of electricity generation (coal, gas, nuclear, biomass, hydro, onshore wind, and solar), nuclear energy was ranked as having the smallest land footprint (as well as the greatest overall benefit-to-cost ratio), followed by gas and coal, and then the renewable sources (Brook & Bradshaw, 2015). However, a working paper for the Global Land Outlook recommends land be separated into *spatial* footprint, i.e. land occupied, and *functional* footprint, i.e. functional aspects of the land like soil (Fritsche et al., 2017, p. 5).

Decarbonisation pathways need strong empirical evidence, which is currently lacking for even well-established technologies. One review looked at 220 published studies on the effects on wildlife of onshore wind. Whilst research into the impacts of offshore wind is now catching up with those analysing onshore wind, there are still hypotheses being debated (e.g. the determination of wildlife corridors), and impacts that remain unknown (e.g. population level effects) (Schuster, Bulling, & Köppel, 2015). Another calls for more research into marine

renewable energy infrastructure (MREI) (Inger et al., 2009). Potential negative effects on biodiversity of MREI include habitat loss and degradation, especially of low energy environments, collision and entanglement with associated infrastructure, noise and electromagnetic fields. However, there are plenty of potential positive benefits: MREI can act as artificial reefs for benthic sessile organisms, fish aggregation devices and safe nurseries for pelagic species, as well as *de facto* protected areas safe from the more mechanised of fishing effort. Paradoxically, if it can be proven that MREI ameliorate biodiversity, it may be most efficient to site infrastructure *within* conservation areas.

Gasparatos, Doll, Esteban, Ahmed, & Olang (2017) provide an excellent review of the impacts of renewable energy technologies on biodiversity using the five direct drivers of ecosystem change and biodiversity loss defined in the MEA: habitat loss/change, overexploitation, introduction of invasive species, pollution and climate change. Renewable energy technologies can affect ecosystems in myriad ways throughout their lifecycles (i.e. construction, operation, decommissioning). The vast majority of studies focus on the *operation* of renewable energy or highlight the land change and disturbance associated with construction; as renewable energy is still in its infancy, very few studies assess the impacts of *decommissioning* (it is mentioned only three times in the entirety of the Gasparatos et al. (2017) review).

There are known local negative effects of renewable energy on wildlife. The direct impact of wind energy operational mortality on birds and especially bats is well known (Northrup & Wittemyer, 2013; Thaxter et al., 2017). Northrup & Wittemyer (2013) demonstrate that wind turbine collisions are likely to have contributed to the decline of the Egyptian vulture (*Neophron percnopterus*), and impacted breeding and fecundity in the griffon vulture (*Gyps fulvus*) and the white-tailed eagle (*Haliaeetus albicilla*) in Europe. Outside of birds and bats, the review found only six studies: two on ungulates, three on gopher tortoises and one on a species of ground squirrel. All showed no significant effects of wind turbine development. One of the world's oldest wind energy plants, the Altamont Pass Wind Resource Area in the Diablo Mountains in California, kills >1000 raptors annually, including over 60 federally protected golden eagles (*Aquila chrysaetos*). Other species (grouse, songbirds and waterbirds) are impacted in Norway, Spain, and Scotland (Katzner et al., 2013). Bats are also killed in greater numbers than birds in many cases. Thaxter et al. (2017) conducted a review of 9,538 bird and 888 bat species worldwide to characterise the trait-driven vulnerability of species. The review was designed to aid land planners in siting wind installations in low risk regions. The most important need for wind turbines is to link continual siting of wind turbines with migratory volant species, but the importance of indirect impacts of habitat loss, fragmentation and degradation cannot be ignored. Mitigation for wind largely revolves around not siting wind farms near high densities of either birds or bats or food sources, as well as timed shutdowns depending on activity levels. Painting one turbine black has also been shown to decrease turbine mortality (May et al., 2020).

Direct impacts of bioenergy are largely limited to tropical bioenergy, where conversion from primary or secondary forest is often needed as opposed to temperate regions where *Populus*

spp., *Salix spp.*, and *Miscanthus* are often grown on land already used for agriculture. Furthermore, global price signals of temperate bioenergy can have indirect effects on tropical land clearance (Northrup & Wittemyer, 2013). Bioenergy mitigation is ensuring large tracts of virgin habitat are not converted, whereas in temperate bioenergy the best mitigation option is to maintain as much habitat heterogeneity as possible with structural variation. Regardless of biome, there are also concerns as to the amount of land required for bioenergy in order to act as an efficient negative emissions technology, i.e. removing CO_2 from the atmosphere (Slade, Saunders, Gross, & Bauen, 2011; Fuss et al., 2018). Both wind and bioenergy require the ability to site locally but in the context of the wider landscape (Allison, Root, & Frumhoff, 2014).

Solar impacts have been hypothesised to be habitat loss and fragmentation during construction, and alteration of the microclimate when operating, but are vastly understudied: "*many of the effects of [utility scale solar energy] are hypothesised with little peer-reviewed evidence*", and are often erroneously "*assumed to be negligible*" (Gasparatos et al., 2017, pp. 162–163). Hernandez et al. (2014) also highlight habitat loss and fragmentation as the leading threats to biodiversity from solar PV, however this obviously hinges on the siting and specifics of the installation. Solar PV sited on existing built infrastructure can be safely assumed to have little or no relevant impacts on wildlife. Emerging research on agrivoltaics – food production under the shade of solar PV – suggests that the concept needs few adaptations from traditional food production, and may even be more productive (Marrou, Guilioni, Dufour, Dupraz, & Wery, 2013; Barron-Gafford et al., 2019; Marrou, 2019). Other research in the UK provides evidence that well managed solar PV siting can even benefit wildlife, with study installations *increasing* vegetation diversity and butterfly abundance (Randle-Boggis et al., 2020). This possibility for co-benefits is explored by a proposal for a techno–ecological synergy (TES) framework to specifically engineer mutually beneficial relationships between solar energy and "competing" land uses (Hernandez et al., 2019).

Impacts of renewable energy on biodiversity are also heavily dependent on the spatial context within which they are sited (Allison et al., 2014; Yohe, 2014). Solar PV can be sited with negligible land change impacts on existing built infrastructure, or could be sited (with strong enough economic incentives) on land converted for the purpose from primary vegetation. Furthermore, ecosystem resilience is important to consider. Highly disturbed ecosystems like agricultural (or formerly agricultural) land offer an opportunity to provide benefits to species (Randle-Boggis et al., 2020), whereas any impact in low energy environments (e.g. MREI impacts on low energy, benthic environments) is likely to have a disproportionately negative impact on sessile species (Gasparatos et al., 2017). There is also the potential for non-linear scaling of landscape impacts: a wind installation placed within a landscape of similar wind installations may have marginal impacts on biodiversity when compared to the first commission. However, the cumulative effects cannot be ignored. This has been shown to be important for roads, where "*deforestation first spreads along an initial road and then proliferates to an expanding spider web of illegal secondary and tertiary roads*" (Laurance & Arrea, 2017, p.

444). Roddis, Carver, Dallimer, Norman, & Ziv (2018) reference "*hazard havens*", where energy infrastructure becomes clumped as it becomes easier to secure planning permission next to similar existing infrastructure. The importance of place for renewable energy also impacts different *facets* of biodiversity (species, phylogenetic, and functional diversity). A wind installation sited within an area of high biodiversity may affect *species* diversity through direct mortality, but an installation sited on the boundaries of the area may also significantly impact *functional* diversity by restricting influx of more widely dispersed species. These are all concepts that need addressing as the renewable energy and biodiversity literature grows.

Katzner et al. (2013) identified four grand challenges for the expansion of renewable deployment whilst minimising impact on biodiversity:

1. Mainstreaming life cycle analysis: implementing any energy programme requires inputs of land and materials to manufacture, install, maintain generators, and transport electricity;
2. Best management practices for each renewable energy;
3. More analysis needed on the "elephant in room" of species-specific indirect effects to wildlife of renewable generation;
4. A central assumption of renewable energy is that over the short term ($<$100yrs), the impacts of deployment are lesser than the business as usual scenario of continuing fossil fuel generation. Renewable energy may have an impact lessening climate change but they may also convert more habitat than fossil fuels so there is a need to explicitly define which implementation scenarios this central assumption is and is not met.

The speed of technology development of renewable energy infrastructure exacerbates the problem of insufficient global data on impacts. Whilst the impacts of horizontal axis wind turbines (HAWTs) are only now reaching acceptable evidence levels, one paper calls for proportional research into vertical axis wind turbines (VAWTs) (Santangeli & Katzner, 2015). The environmental impacts of HAWTs were only evaluated late and as such development was often prohibitively expensive. VAWTs have the efficiency bonus to potentially dominate the wind market in coming decades as they can generate in a wider range of wind conditions and could better match local energy demand whilst requiring less land. Proponents say VAWTs have lesser wildlife impacts but the sparse evidence base is patchy, and this was originally thought to be the case with HAWTs.

The frontier of renewable energy research has twice been identified in conservation horizon scans. In 2016, the changing costs of energy transport and storage was identified as a potential long term issue for conservation (Sutherland et al., 2016). Improvements in storage and transmission would likely rapidly increase renewables deployment, which could happen before knowledge of the full life cycle impacts of renewable energy infrastructure on wildlife is sufficient to minimise negative effects. There are also concerns of renewable energy integrating into current energy systems. In 2017, the horizon scan identified a number of

potential issues with renewable energy deployment (Sutherland et al., 2017). Average wind speeds at sea surface have increased from 24.8kmh^{-1} to 27.4kmh^{-1}; this could represent a long-term trend, or long-term oscillation. If it is a trend, it could affect sediment movement, bird migrations and offshore windfarm siting. Development of floating wind farms was also identified: fixed base wind turbine development is hampered by the need to be shallower than 50m. In 2016, Statoil was granted a seabed lease to develop the largest floating wind farm in the world (five 6-megawatt turbines) off the Scottish coast (maximum water depth 95-120m). The project was completed in 2017. More than 40 global floating projects are in development but the ecological effects are still unknown. Other issues demonstrate the difficulty in securing evidence for mitigation options before deployment: fuel from bionic leaves, reverse photosynthesis and mineralising anthropogenic carbon are all being investigated.

An enabling policy environment

As global sustainability commitments multiply to address a suite of environmental problems, there is a pressing need to quantify land-use impacts of policy scenarios in order to inform landscape planning at much larger scales than ever attempted before. A recent study selected ten targets from six goals of the Sustainable Development Goals (SDGs) with some discernible land requirement (Gao & Bryan, 2017). These targets were then scaled to three different ambitions (weak, moderate, and ambitious) and two time frames (2030 and 2050). Running 648 plausible future environmental, socio-economic, technological and policy pathways using the Land-Use Trade-Offs (LUTO) integrated land systems model, suggested accelerating land use dynamics post-2030, requiring a longer-term view of land systems sustainability. "*Simultaneous achievement of multiple targets is rare owing to the complexity of sustainability target implementation and the pervasive trade-offs in resource-constrained land systems*" (Gao & Bryan, 2017, p. 217). The authors go so far as recommending a priority for land system assessments: first food/fibre production, biodiversity and land degradation components of sustainability; and secondly emissions abatement, water and energy targets by capitalising on co-benefits derived from tier one priorities.

Integrated policy assessment is a priority to achieve this type of ranking system. For energy and the environment specifically, one study identified 22 ecosystem services scenarios, 6 UK-focussed, with 18 energy scenarios, 13 of which were UK-focussed (Holland et al., 2018). Ecosystem services scenarios use highly aggregated versions of energy scenarios, whilst energy scenarios rarely consider implications of ecosystem services excluding water and air pollution. Another UK study, part of the Addressing the Value of Energy and Nature Together (ADVENT) research project, criticises the emphasis on carbon emissions in energy pathway assessments (Holland et al., 2016). The paper proposes a framework that takes a broader look at energy systems to include ecosystem services, both market and non-market goods and services, and recommends assessments look at full life cycle impacts. The disparity of temporal and spatial scales of energy and the environment is highlighted. Renewable

energy looks to address the global, long-term effect of climate change at the possible expense of short-term localised impacts on biodiversity. It is incredibly difficulty to equate the two to consider an objective benefit-to-cost ratio for new projects. Integrated assessments are starting to address the problem posed by local solutions for global challenges (Gasparatos et al., 2017); one study linked domestic demand for energy to international water use by integrating a hydrological model with multiregional input output analysis (Holland et al., 2015).

Integrating policy assessments are further complicated by the scenarios used for even single-issue assessments. One study looked at scenarios used in Global Environmental Assessments (GEAs) (Vuuren, Kok, Girod, Lucas, & Vries, 2012). There has been a shift since 2007 from using explorative scenarios to policy-based scenarios. Policy-based scenarios usually centre on one baseline pathway, with scenarios based on different realistic policy decisions. The authors recommend expanding the baseline outcomes used for policy-based projections to include other exploratory outcomes in order to provide some kind of sensitivity analysis and to provide a believable spectrum of counterfactuals.

Even with the best available evidence and intentions, there will inevitably be some tough decisions to make regarding renewable energy and the need to arrest global climate change, land change and the need to prevent global biodiversity decline with local actions. One interesting case study looks at European law (Jackson, 2011). The European Union's (EU) Natura 2000 network covers $\sim 18\%$ of EU territory and is strictly protected. As member states move towards their 2020 emissions reductions targets, necessary large infrastructure projects were likely to overlap with protected sites and face rejection as a matter of EU law. "*In developing climate change law*", writes Hodas (2008) (p. 399), "*we must not forget the need to protect and enhance biodiversity. . . Instead we should seek win–win sustainable development solutions that reduce [greenhouse gases] while protecting and enhancing biodiversity*". The study highlights two case studies: a hydroelectric dam in Portugal's Sabor valley, and the Severn barrage. The Severn barrage was largely rejected for cost, and the fact that it would struggle to contribute to the UK's 2020 emissions reductions as it would only become operational post-2020. A very important factor, however, was "*regulatory barriers. . . [would] create uncertainties that would add to the cost and risk of construction*". The authors argued that this dilemma introduces the possibility of negative feedbacks for the rule of law, nature conservation in the EU, and by precedent, globally. Rather than water down commitments to either, open, frank talks are recommended to decide projects on a case-by-case basis.

Finally, in order to provide an enabling policy environment for the achievement of multiple development goals, targets must be quantifiable and well understood. The mid-term assessment of progress towards the Aichi Biodiversity Targets suggested that most targets "*lack explicitly quantifiable definitions of 'success' for 2020*", so authors were forced to use projected values for 2020 against modelled 2010 values (Tittensor et al., 2014). Similarly, a more recent study warns of a "*pyrrhic victory*" of 17% land area coverage if ecologists

don't sensibly define what constitutes important, representative and effective protected areas, including what *other effective area-based conservation measures* (OECMs) are (Watson et al., 2016). Current lack of definition opens doors for national governments to designate areas by least social and economic cost and/or objection. Important areas can be established using species-specific life history characteristics, strengthened by expert knowledge; climate smart targets based on habitat suitability can also be incorporated. Increasing protected area coverage with inadequate increases in management effectiveness can mask serious declines in biodiversity. Realistic counterfactual use and development of conservation balance sheets accounting for biodiversity loss and protected area coverage, alongside protected area management improvements, should be encouraged. Clear policy goals and targets allow for better monitoring and tracking of progress, with less scope for national interpretation. Biodiversity conservation needs a science-informed clear goal akin to 2°C warming put forward by the UNFCCC, which can be underpinned by extant indices already discussed (Mace et al., 2018).

Renewable energy data availability

Adequately integrating different sustainability objectives requires sufficient availability of quality data. There are good improvements in the data available at a global scale for assessing the cumulative impact of some renewable technologies. For example, large hydroelectric projects have been shown to threaten river basins (Mekong, Amazon and Congo) that together contain one third of freshwater fish species (Winemiller et al., 2016). The vast majority of hydroelectric infrastructure is small upstream installations, but as there are >450 dams planned in these basins alone, the cumulative effects may be severe. The authors call for better regional coordination of environmental assessments and integration of climate and land change. A spatially explicit and hydrologically linked database is available for assessments: the Global Reservoir and Dam database (GRanD) (Lehner et al., 2011). Global reservoirs >0.01ha contribute an additional 305,000km^2 to surface water, and 46.7% of large rivers with average flows above 1,000m^{3}s^{-1} are affected by dams in some regard. Sensitivity analysis using GRanD suggests that smaller reservations, despite their small contribution to global areas, have a significant impact on river flows.

While data may be good for hydropower infrastructure, there are no such data available for more dispersed technologies like onshore wind and solar photovoltaic (PV). Instead, there are a plethora of geographically, functionally or financially restrictive datasets. For example, there are good data for the UK, through the UK Renewable Energy Planning Database (UK REPD – all types of renewable energy), curated by the Department for Business, Energy & Industrial Strategy (BEIS, 2019). The data are evidently geographically restricted, and the spatial data is functionally restricted to approximate postcodes. There are also good data for US wind energy, with the creation of the excellent US Wind Turbines Database (Hoen et al., 2019), and other national examples – Sweden and Germany, for example – where the data are

easy to view, but difficult to access. Eichhorn et al. (2019) provided a snapshot of renewable energy installations in Germany, with open access to their data. The dearth of renewable energy data on global human development mapping intiatives like the United Nations' MapX (`http://www.mapx.org/`) and WWF SIGHT (`http://wwf-sight.org/explore`) serves to highlight the pressing need for open access global data for wind and solar PV, two of the fastest growing renewable technologies.

There are a number of proprietary datasets kept behind paywalls which may hinder the estimation of the global renewable energy estate: Rehbein et al. (2020) recently used data from GlobaData (retrieved from `https://power.globaldata.com`), which they estimated contains 90% of the world's hydropower, wind and solar PV capacity. The Wind Power (`https://www.thewindpower.net/`), with global data available for EUR1250, provides a similar service solely for wind. Wiki Solar, used in 1, provides global solar installation data for a fee but notably provided data without charge for academic purposes. However, academic analysis with paywalled data is not conducive to *post hoc* evaluation of results, and reduces the replicability of studies by erecting financial barriers to studies.

Artificial intelligence and machine learning provide a fruitful new direction for efforts to map renewable energy. DeepSolar, an initiative to map solar PV in the US, published a Random Forest derived dataset of installations in the contiguous US (Yu, Wang, Majumdar, & Rajagopal, 2018); they intend to update the data annually, as well as adding other countries and regions of the world. The United Kingdom Research and Innovation (UKRI) funded solar 'nowcasting' project run by the Alan Turing Institute (available at `https://www.turing.ac.uk/research/research-projects/solar-nowcasting-machine-vision`), aims to provide a similar service for the UK. As these types of deep learning approaches are incredibly computationally intensive, extant crowdsourced data may be able to bridge the data gap until more high-fidelity data (e.g. Yu et al., 2018) becomes more globally comprehensive. OpenStreetMap, (available at `https://www.openstreetmap.org/`) an open source collaborative global mapping project generated by a commmunity of millions of users, contains records describing energy infrastructure, and has already been used to amalgamate data for other sectors – e.g. the Oil and Gas Infrastructure WikiProject (OpenStreetMap, 2020).

For the moment, quality data describing renewable resource potential exist (e.g. the World Bank's Solar and Wind Atlases), as well as geographically aggregated capacity statistics (e.g. from the International Renewable Energy Agency – IRENA), but spatially explicit, open access infrastructure data are lacking. Generation of such data would greatly improve civil society's ability to interrogate the siting of installations locally and globally.

Renewable energy deployment and biodiversity conservation

There is an urgent need to accurately quantify impacts on biodiversity of all forms of renewable energy at a local level. However, a more urgent need is to transform our energy

systems to more sustainable alternatives, using multicriteria analyses and genuine impartiality regarding energy mixes. Concurrently, therefore, there is an equally urgent need to use best available methodologies and data to research the potential global impact on biodiversity conservation of shifting to low carbon economies.

Santangeli et al. (2015) looked at three types of renewable energy technologies: solar PV, onshore wind and *Miscanthus* biofuel and where their areas of highest generation potential overlap with protected areas and areas of high biodiversity. Central America, Africa, and Southeast Asia were flagged as areas likely at high risk from renewable energy expansion. Offshore wind and hydropower were excluded from the analysis – the former due to terrestrial focus and the latter because "*most of the potential sites have already been exploited*" (p. 943). Local energy demand was by far the most restrictive factor, meaning that as transmission and storage restrictions are gradually lifted with improving technology, solar may well be the most attractive option to minimise conflict with global biodiversity. The restricted scenario increased the fraction of energy potential in the top 30% biodiversity areas from 31 to 44% for wind, and 32 to 41% for solar. As only roughly half of this area is set to be protected by 2020, the future of biodiversity remains still very much dependent on measures outside of protected areas.

The current spatial overlap of renewable energy and areas of importance for biodiversity has been found to be surprisingly extensive: Rehbein et al. (2020) identified 2,206 fully operational installations of onshore wind, hydropower and solar PV generation spread across 886 protected areas (seemingly independent of IUCN Category), 749 KBAs and 40 distinct wilderness areas. They also found 922 overlapping installations under development that could represent a 30% increase in protected areas and KBA affected and a 60% increase in impacted wilderness areas. The authors warn that coordinated planning of renewable expansion and biodiversity conservation is needed to "*avoid conflicts that compromise their respective objectives*" (Rehbein et al., 2020, p. 3040). The study used a proprietary renewable energy dataset and, although the authors dissolved overlapping protected areas, overlapping areas of conservation importance were not taken into account. The authors also highlight Western Europe as a hotspot of historic overlaps which, while unfortunate, is not unlikely – the Natura 2000 protected area network covers $\sim 18\%$ of EU land alone, before considering KBAs and wilderness areas, and Western Europe is currently one of the world's renewable energy powerhouses.

More work is needed in the areas flagged as high risk to investigate local factors constricting renewables development. Actual renewables development can depend on national priorities, requirements for domestic agriculture, and even harder to predict factors like viewshed, land rights, and direct nimbyism. A second analysis by Santangeli et al. (2016) conducted beta regressions of the proportion of renewable energy potential inside and outside the top 30% of biodiversity areas (0-1) against a variety of national factors including human development index (HDI), political stability, air pollution mortality, and national biodiversity potential. The results were extremely variable and showed little discernible relationships. Under the

global protection scenario, where protected areas are designated globally as opposed to nationally, most challenges and opportunities concentrate in the developing world, where renewable energy can also contribute to improving human health, whereas in the national scenario, they concentrate in developed countries with good governance and high population density.

One UK-based study moved from looking at correlations to how national factors would affect actual renewable energy infrastructure siting (Gove et al., 2016). The study assessed the deployment potential of field-scale solar, offshore and onshore wind, bioenergy, tidal and wave at three different levels of ecological sensitivity, based on distributions of protected areas and sensitive species. The energy potential of lowest ecological risk was estimated at 5,547 $TWhyr^{-1}$ – sufficient to meet projected UK energy demand. However, some of the energy investigated is not commercially deployed, and further local ecological monitoring is needed. Validating global integrated assessments of renewable energy and biodiversity with national realities is a priority. More knowledge about what actually predicts renewable energy siting locally would allow for more accurate identification of areas at high risk of difficult trade-offs between policy goals. For example, the latest attempt to provide comprehensive development likelihoods for a suite of human land uses included some forms of renewable energy (concentrated solar power, solar PV, wind power, bioenergy, and hydropower), as well as conventional fuels (Oakleaf et al., 2019). The study generated 1-km^2 resolution land suitability maps for each technology using multicriteria decision analysis to support research into cumulative impacts. However, the data were largely based on resource availability, with the implicit assumption that resource availability is the driver of spatial distribution without really testing this assumption with spatially explicit infrastructure data.

There are concerns that ecology is losing its ability to predict (Houlahan, Mckinney, Anderson, & Mcgill, 2016). Prediction allows for more quantifiable hypotheses to exist. Integrated assessment models researching the impact of global renewable energy deployment need to rapidly move from exploratory modelling to predictive modelling if they are to assist in building the evidence base for sustainable energy system transformations. Predictive models need to explicitly account for confounding factors like spatial autocorrelation (Lennon, 2000). Evaluating early efforts at assessing the trade-offs between renewable energy and biodiversity with competing policy priorities (e.g. food/fibre/living space), national realities (e.g. nimbyism, political factors), as well as emerging technologies and their potential to ease terrestrial pressure (e.g. offshore wind/tidal/wave) are critical to improve the predictive power and realism of policy goals and targets.

The aim of this thesis is to assess the potential for significant trade-offs between two crucial pillars of a sustainable future: our ability to supply and markedly expand renewable energy, and our ability to protect global biodiversity. Chapter 1 first addresses significant shortcomings in research to date by generating a novel, spatially explicit, open access database of onshore wind and solar PV locations globally. Chapter 2 builds on these data to assess

previous attempts at identifying priority areas for renewable energy and biodiversity to inform new, more accurate likelihood maps of renewable energy expansion and their potential co-occurrence with areas of conservation importance. Finally, Chapter 3 provides baseline land change scenarios to 2040 in response to food crop, housing and livestock demands, and describes renewable energy's place in human-dominated landscapes and how this may change with projected land changes.

Chapter 1

Harmonised global datasets of wind and solar farm locations and power

This chapter was published as:

> Dunnett, S., Sorichetta, A., Taylor, G., & Eigenbrod, F. 2020. Harmonised global datasets of wind and solar farm locations and power. *Scientific Data*: *7*(130). https://doi.org/10.1038/s41597-020-0469-8

Author contributions are as published and reprinted here:

> "*S.D. conceived the research, conducted data processing and analysis, and wrote the manuscript. A.S. and F.E. edited the manuscript. G.T. and F.E. wrote the grant application for the NERC funding outlined above.*"

1.1 Abstract

Energy systems need decarbonisation in order to limit global warming to within safe limits. While global land planners are promising more of the planet's limited space to wind and solar photovoltaic, there is little information on where current infrastructure is located. The majority of recent studies use land suitability for wind and solar, coupled with technical and socio-economic constraints, as a proxy for actual location data. Here, we address this shortcoming. Using readily accessible OpenStreetMap data we present, to our knowledge, the first global, open access, harmonised spatial datasets of wind and solar installations. We also include user friendly code to enable users to easily create newer versions of the dataset. Finally, we include first order estimates of power capacities of installations. We anticipate these data will be of widespread interest within global studies of the future potential and trade-offs associated with the global decarbonisation of energy systems.

1.2 Background & Summary

The estimated share of renewables in global electricity generation was more than 26% by the end of 2018 (REN21, 2018). Moreover, many national, regional and international policies mandate for ever larger renewable shares of electricity generation (UNFCCC, 2016).

Solar photovoltaic (PV) panels and wind turbines are by far the biggest drivers of the rapid increase in renewable energy electricity generation. Globally, in 2018, 100 gigawatts of solar PV were installed, contributing 55% of new renewable energy capacity; wind contributed the second largest share, with 28% of new renewable capacity (REN21, 2018). Both technologies are well established and feature heavily in decarbonisation scenarios as proven concepts to generate emission-free electricity. Indeed, myriad studies present the goal of 100% renewable energy as eminently achievable with current technology (Heard et al., 2017). For example, available wind power in Europe alone may be able to produce enough electricity for global demand to 2050, whilst replacing US hydroelectric dams with solar PV could produce equivalent power output on just 13% of the land (Enevoldsen et al., 2019; Waldman, Sharma, Afshari, & Fekete, 2019).

Despite this widespread interest in solar and wind, policy makers and governments have struggled to maintain robust geospatial information on the rapid expansion of renewable energy technologies. This lack of spatial data is problematic for several reasons. For example, the impacts of wind and solar installations on biodiversity are far from well known (Santangeli & Katzner, 2015), even at the local scale. The mortality effects of wind turbines on volant species are relatively well studied (Thaxter et al., 2017), however ancillary effects such as noise, visual and landscape impacts are less well known. Furthermore, there may be significant trade-offs between increasing expansion of renewable energy globally, and efforts to reduce biodiversity decline through protected areas (Hernandez, Hoffacker, Murphy-Mariscal, Wu, & Allen, 2015; Santangeli et al., 2015, 2016). Another recent study suggests small-scale deployment of renewables has a lower impact on biodiversity than conventional energy, but the implications of scaling up renewable generation on biodiversity remain unknown (Holland et al., 2019). Local-scale studies do show that siting of utility scale solar energy can have significant impacts on soil degradation and water availability (Hernandez et al., 2014); and wind turbines can have significant effects on market prices (Jensen et al., 2018). However, hitherto studies have largely relied on the use of suitability maps for renewable energy which are not derived from historic placement of energy infrastructure but are rather based on purely climatic characteristics. As a result, they implicitly assume that the climatic characteristics will be the largest driver of installation placement (Kiesecker et al., 2011; Pogson, Hastings, & Smith, 2013; Santangeli et al., 2015, 2016; Enevoldsen et al., 2019; Oakleaf et al., 2019; Waldman et al., 2019). At the global scale, a recent study used human influence as a proxy for where energy generation is occurring (Holland et al., 2019). Both approaches are likely insufficient, as two UK-based studies showed that when location data are available, a variety of socio-economic factors affect the siting of wind turbines and solar

PV (Roddis et al., 2018; Harper, Anderson, James, & Bahaj, 2019). Sufficient location data would allow researchers to interrogate the socio-economic drivers of renewable energy infrastructure siting at a global scale to produce probability surfaces for energy development (Evans & Kiesecker, 2014).

Despite the evident utility of location data, spatially explicit national data are only publicly available for a handful of countries (BEIS, 2019; Eichhorn et al., 2019; Hoen et al., 2019; Rand et al., 2020). Furthermore, often when they are available they are not open access. Global renewable energy data are readily available when spatially aggregated and summarised at the national scale (e.g. through the International Renewable Energy Agency - IRENA), but there is an urgent need for spatially explicit, global data describing the distribution of solar and wind installations. A harmonised spatial database could support data-driven indicators to track progress towards Sustainable Development Goals (SDGs) (UN, 2020), especially SDG 7 (Affordable and Clean Energy) and SDG 13 (Climate Action). A database would also allow the integration of global wind and solar installations with other geospatial datasets supporting SDGs, e.g. the World Database on Protected Areas informing the expansion of terrestrial protected areas for conserving threatened species supporting SDG 15 Life on Land.

Here, using OpenStreetMap infrastructure data, we present the first publicly available, spatially explicit, harmonised dataset describing global solar PV and wind turbine installations. These data are available in vector format, either as geopackages, shapefiles, or comma-delimited and describe groupings of wind turbines or solar PV, i.e. energy 'farms', as well as lone installations, i.e. a single wind turbine or solar panel. These data include metadata describing whether the location is urban or beside/on a water body, as well as an estimate of its power output, created using a predictive model detailed in this paper.

1.3 Methods

1.3.1 Data Collection

1.3.1.1 OpenStreetMap structure

OpenStreetMap (OSM) is an open-source, collaborative global mapping project generated by a community of millions of users that can provide a unique insight into energy infrastructure locations. OSM data have an analogous structure to other geospatial data in that they describe the physical world with three different elements: points (e.g. street lamps, phone boxes), lines (e.g. roads, power lines), and polygons (e.g. parks, buildings). However, in OSM, point data are referred to as nodes, lines as ways, and polygons are described as closed ways. These georeferenced data are then given tags to ascribe the spatial data with meaning. Tags consist of two text fields, a key and a value. For example, a service road for a wind turbine or set of wind turbines could be a way tagged with key 'highway' and value

TABLE 1.1: OpenStreetMap key/value pairs used for the sample 50 global solar installations.

Key	Values
barrier	fence; wall
building	yes
frequency	50
generator:method	photovoltaic
generator:output:electricity	10MW; 3.5MW; 5MW; yes
generator:source	solar
generator:type	horizontal_axis; solar_photovoltaic_panel
highway	track
landuse	industrial
plant:output:electricity	250MW; 290MW; yes
plant:source	solar
power	generator; plant
wall	no

TABLE 1.2: OpenStreetMap key/value pairs used for the sample 50 global wind installations.

Key	Values
generator:method	wind_turbine
generator:output:electricity	1.75MW; 2.1MW; 2.3MW; 3MW; 800kW; 900kW; yes
generator:source	wind
generator:type	horizontal_axis
power	generator

'service' to give a key/value pair `highway:service`. The value field provides more detail to the key classifier. More information on the structure of OSM data can be found on the OSM Wiki (OpenStreetMap, 2019).

1.3.1.2 OpenStreetMap key/value pair selection and extraction

To overcome the problem of inconsistent tagging in the OSM feature metadata, we conducted a preliminary analysis to determine the best key/value pairs to use as search terms for data extraction. We recorded the key/value pairs used for 50 randomly selected solar installations and 50 randomly selected wind installations with known locations. 50 random solar installations were selected from the Wiki Solar dataset (Wolfe, 2013), a dataset comprising 4,129 solar projects. The wind installations were selected from a study into bird and bat mortality around wind turbines at 134 onshore sites (Thaxter et al., 2017). 13 unique keys and 21 unique values were used to tag the solar sites in our test dataset (Table 1.1), with 5 unique keys and 11 unique values used to tag the wind sites (Table 1.2). The most common

key/value pair for solar was `power=generator` paired with `generator:source=solar`. Frequently, OSM tags work in hierarchies; in this instance, features tagged `power=generator` should be further categorised to describe what type of energy is used for electricity generation. Moreover, anecdotally, it appears that the most common approach to tagging solar installations is to tag the entire area (closed way or polygon) as `power=plant`, while tagging groups of PV panels as `power=generator` and `generator:source=solar`.

For the sample of wind installations, tagging was much more straightforward. Again, the most common key/value pair to use was `power=generator`, this time coupled with `generator:source=wind`. However, there is one more use of `power=generator` without a corresponding `generator:source` tag within the sample of known wind installations. In reality, in most instances this sort of tagging omission would not be a problem with these data, as features generally occur together, and so any untagged elements are highly likely to be tagged by a different element within the same project.

Given that tag omissions were rare in the sample dataset, it was judged that using `generator:source` as a search key would capture most target features, with either solar or wind as the corresponding value. We therefore selected `generator:source=solar` and `generator:source=wind` as two of our search terms. We coupled these with `plant:source=solar` and `plant:source=wind` as the OSM Wiki suggested that the outer boundaries of renewable energy installations should be tagged thus.

Data were extracted using the **R** package `osmdata` (Padgham, Rudis, Lovelace, & Salmon, 2017) to build queries to send to the Overpass API, a read-only API (available at overpass-turbo.eu) that allows for customised access to OSM data. For example, to search for solar PV OSM elements tagged as either `generator:source=solar` or `plant:source=solar` in a geographic area bound by bounding box `bbx`, a query can be built as follows:

```
query = opq(bbox=bbx, timeout=5000) %>%
    add_osm_feature("generator:source", "solar") %>%
    add_osm_feature("plant:source", "solar")
```

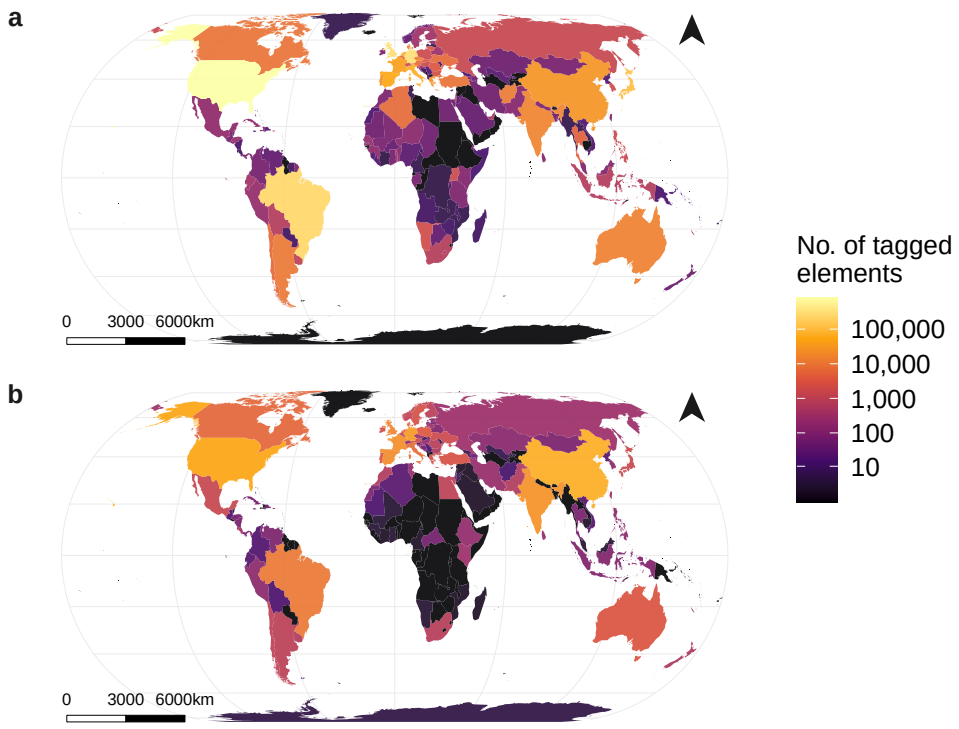

FIGURE 1.1: Numbers of OSM elements per country (point and polygon data) returned by search query for solar PV (a) and wind (b).

Applying this query globally resulted in four initial datasets: 326,234 solar polygons, 1,808,585 solar point data, 1,889 wind polygons, and 305,306 wind point data (Figure 1.1).

1.3.2 Data processing

1.3.2.1 Land cover

The first stage of data processing was to classify data located in areas identified as either water (both sea and inland bodies), or an urban centre. Offshore, rooftop and residential installations are very different in structure to field-scale solar and wind installations. Offshore turbines tend to be larger than onshore turbines to counteract high development costs (Enevoldsen & Valentine, 2016), while groups of residential buildings with single solar PV panels could conceivably be grouped as one solar installation, but do not act as one. Processing was done using the 2015 Global Human Settlement Layer (GHSL) in World Mollweide projection at 1-km^2 resolution, reprojected to Eckert IV equal-area at 1-km^2 resolution (Pesaresi, Florczyk, Schiavina, Melchiorri, & Maffenini, 2019). Urban areas were considered as any of the following municipal level categories in the GHSL dataset: *City*, *Dense town*, *Semi-dense town* and *Suburbs*. *Water* was taken straight from the GHSL categorisation.

1.3.2.2 Aggregating individual elements to installations

The raw OSM data extract contains sole polygons, sole points, as well as polygons and points within wider polygons. To counteract the potential for mis-tagging of these data as identified in our key/value pair analysis (Data Collection), we looked at the spatial clustering of the raw datasets to amalgamate any point and polygon data clearly referring to the same installation. Firstly, we filtered any point already contained within a wider polygon, and the number of these points intersecting were recorded (strictly, the OSM guidance suggests tagging the wider installation as `power:plant` and `plant:source:<source>`, but in reality contributors tend to focus on the lowest unit: either a group of PV panels, or one wind turbine, tagging them with `power:generator` and `generator:source:<source>`). We then performed bespoke spatial clustering for each technology to group the remaining points that occur close together in space, as outlined below.

1.3.3 Determining the scale for spatial clustering: spatial distribution of wind and solar features

In order to justify spatially clustering the remaining renewable energy point data into 'farms' based on their position in space relative to other points, we analysed the spatial characteristics of two large wind and solar databases, the United States Geological Survey (USGS) Wind Turbine Dataset (USWTD) and Wiki Solar (Wolfe, 2013; Hoen et al., 2019; Rand et al., 2020), to check whether they were significantly clustered in space.

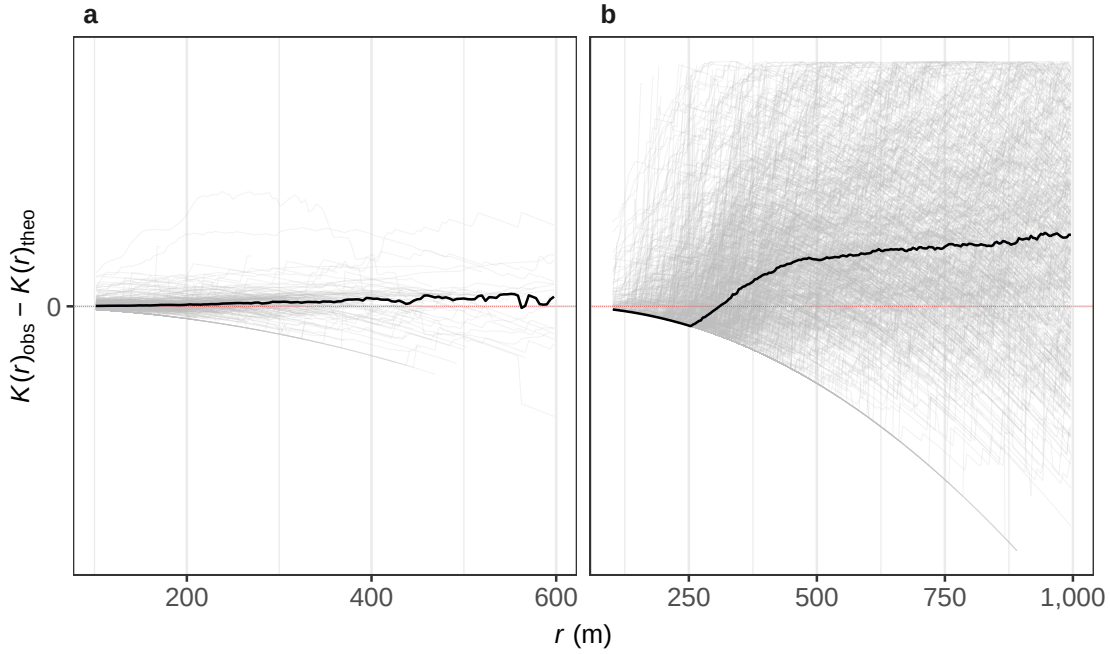

FIGURE 1.2: The difference between $K(r)_{obs}$ and $K(r)_{theo}$ per installation for the Wiki Solar dataset (a) and the USWTD (b) within different search radii, r. $K(r)_{theo}$ represents the number of neighbours found within search distance r for a completely random Poisson point process. $K(r)_{obs}$ represents the observed value of Ripley's K. Where $K(r)_{obs} > K(r)_{theo}$, data are clustered at that search radius; where $K(r)_{obs} < K(r)_{theo}$, data are ordered. The horizontal dotted red line indicates a difference of 0, i.e. no different from a random process. Dark lines indicate the median differences of all projects.

We performed Ripley's K function on both datasets (Ripley, 1977). Ripley's K function returns a measure, K, for the spatial characteristics of a point pattern for a range of neighbourhood search radii, r. The function can be used to estimate whether a point pattern is clustered, dispersed, or distributed randomly in space. A theoretical K value, $K(r)_{theo}$, is calculated based on a completely random Poisson point process at search radius r. If the observed K value at r, $K(r)_{obs}$, is above $K(r)_{theo}$, the point pattern is clustered at that spatial scale. If $K(r)_{obs}$ is below $K(r)_{theo}$, data are dispersed at that spatial scale. A difference of 0 suggests a completely random distribution.

In order to be calculated, the function requires a sensible study area. For the USWTD, this meant grouping the turbines by project (54,481 turbines in 1,311 projects). For Wiki Solar, we only had the point location of the installations. To address this, we applied circular buffers of the reported installation areas to the point locations and assumed all points from the OSM dataset in these areas belonged to the buffered project (63,901 points in 1,270 projects).

Next, we applied Ripley's K function to the point data in every project in both datasets. The result of this can be seen in Figure 1.2. At shorter neighbourhood distances, we would expect our point patterns to be dispersed: wind turbines and solar panels require at least

some dispersion from one another in order to work (e.g. to avoid wind wake for turbines, and shade for solar panels). For solar, the relationship is not clear, but for r values between 200 and 400m, there appears to be a slight tendency towards clustering over dispersion (Figure 1.2a). However, as r increases, we see a pronounced increase in clustering for wind; where 400m $< r <$1,000m, the majority of projects exhibit clustering over and above a random point process (Figure 1.2b).

1.3.4 Determining the neighbourhood radius for spatial clustering

Spatial clustering was achieved by running a density-based spatial clustering of applications with noise (DBSCAN) algorithm (Ester, Kriegel, Sander, & Xu, 1996). Given a set of points in space, DBSCAN groups together points that are closely packed together (points with many nearby neighbouring points), classifying as noise points that lie alone in low-density regions (whose nearest neighbours are too far away). The algorithm takes two parameters as arguments: ε, a neighbourhood search parameter, and *minPts*, the minimum number of points to form a cluster.

DBSCAN clustering is more appropriate than, for example, k-means clustering for these spatial data for two main reasons. Firstly, you do not need to specify the number of clusters *a priori*. As we are explicitly searching for the number of clusters in the data, this suits our needs. Secondly, DBSCAN can find arbitrarily shaped clusters. This is important as many wind farms are linear in shape and may be overlooked by more conventional clustering methods. In order to run this algorithm, two parameters need to be set: the neighbourhood radius (i.e. the search distance), ε, and *minPts*, the minimum number of points for the algorithm to consider a cluster. It is usually recommended that for setting parameters, *minPts* should usually be $>$2 so as to specifically look for *density*-based clusters. However, in order to extract linear clusters (which can occur for energy installations), *minPts* was set to 2. When *minPts* is set to 2, DBSCAN acts as a single-linkage hierarchical clustering algorithm truncated at ε. Whilst this avoids some of the pitfalls associated with DBSCAN of choosing an appropriate density (Kriegel, Kröger, Sander, & Zimek, 2011), single-linkage clustering is not without its disadvantages: this implementation can produce large clusters joined by one lone point. As a sensitivity analysis to this single-linkage effect, we repeated the analysis for *minPts* values of 3, 5 and 10 (Technical Validation). Values of 1 were not considered, as a lone wind turbine or solar panel cannot be considered a 'farm'.

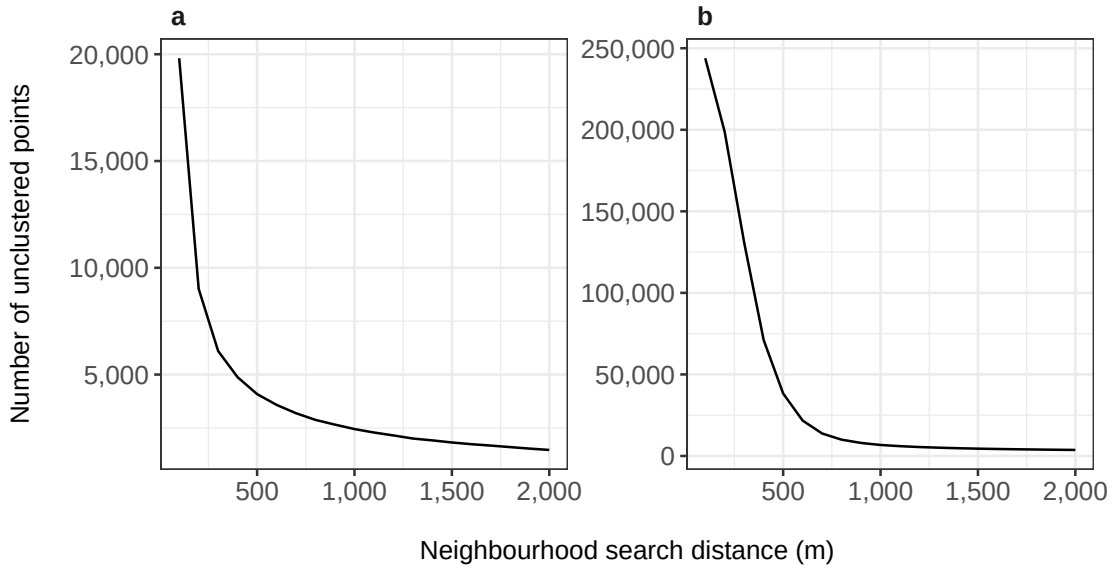

FIGURE 1.3: "Knee" plots for OSM solar (a) and wind (b) point data showing the number of unclustered points remaining for differing neighbourhood search radii. As the neighbourhood search distance increases, the number of unclustered points will eventually tend towards 0. Where the plot 'turns' indicates a sensible neighbourhood distance which captures the majority of points; for wind, this corroborates the previous analyses at c.800m. For solar, it is more unclear but looks to lie in the range 300-500m.

For wind, the neighbourhood radius (ε) has been discussed at length in the energy literature through the lens of the optimal spacing of wind turbines in order to maximise wind speed for each turbine. This varies widely but is largely considered to be in the range of 3-10 rotor diameters (Meyers & Meneveau, 2012). The median rotor diameter in the US and German turbine datasets were 87 and 71m respectively, thus ε was set to 800m. This also falls within the range 400-1,000m suggested by the Ripley's K function analysis. Running DBSCAN on the OSM wind point data with differing values of ε suggests that 800m is a sensible neighbourhood size (Figure 1.3).

For the solar data, this proved much more difficult as there is no theoretical basis for spacing of panels in solar farms. There is recommended spacing at the very lowest level, as rows of panels are required to be a certain distance apart (dependent on their solar incidence slope) so as not to shade each other. However, we are interested in spatial clustering at the higher level of panel architecture, i.e. an array of multiple panel rows, on which there are no restrictions. The Ripley's K function analysis suggested an optimal clustering distance of 200-400m. Again, running DBSCAN with differing values of ε it appears there is no optimal value (Figure 1.3).

We ran DBSCAN on the wind point dataset with *minPts* set to 2 and ε to 800m, which yielded 23,534 clusters and 9,980 noise points (here representing single turbines or polygons intersecting no point data). We ran DBSCAN on the solar point dataset, again with *minPts*

set to 2, and ε set to 400m, which yielded 30,394 clusters and 4,878 noise points. 400m was selected for solar as the mid-range value suggested by Figure 1.3.

1.3.5 Estimating power output of installations

The vast majority of variables (including capacity, rotor diameters, and areas) that would ordinarily provide a straightforward way of calculating power were >99% missing values in geospatial data from OSM. We overcome this limitation and provide first order power estimates derived solely from the area of the polygon and the number of original points contained within the OSM data, using regression equations derived from independent datasets.

The processed wind and solar OSM datasets were spatially joined with three independent datasets each. A spatial join combines the characteristics of any data that overlap each other in space. Using this technique, we can assign more descriptive metadata from national databases to the spatial information gleaned from the processed OSM data. For wind, these validation datasets were the USWTD, the United Kingdom Renewable Energy Planning Database (UK REPD), and data from a German renewable energy study (BEIS, 2019; Eichhorn et al., 2019; Hoen et al., 2019; Rand et al., 2020). Solar also utilised the German and UK data (these databases provide more than one type of renewable energy), swapping in data from Wiki Solar (Wolfe, 2013) in place of the USWTD.

Spatial joins were performed using the `sf` package (Pebesma, 2018). Duplicate matches, where more than one record spatially overlaps, were discarded in order to keep the model setup as simple as possible. This, for example, excluded instances where DBSCAN considered an area as one contiguous wind (or solar) farm and the corresponding national dataset considered the area as several different projects. This often happens when one larger installation is installed in successive funding rounds. Spatial joining with this caveat yielded 3,096 instances for solar and 3,457 for wind where we knew the OSM characteristics, but also other descriptors provided by the validation datasets, such as the power capacity.

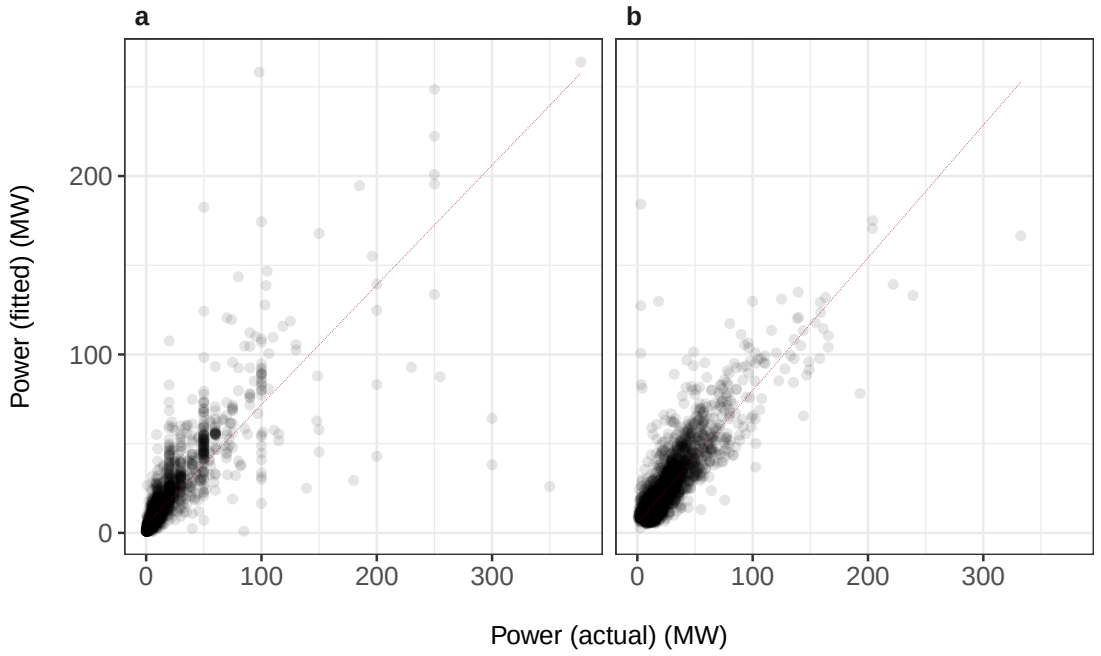

FIGURE 1.4: Fitted vs actuals for the solar (a) and wind (b) power models. Slope represents y∼x, i.e. perfect prediction. 5-repeat 10-fold cross validation models: solar (RMSE=14.29, R^2=0.70, MAE=4.93, n=3,280) and wind (RMSE=11.12, R^2=0.734, MAE=6.22, n=3,574).

Two 5-repeat 10-fold cross validation models were trained on these data (Figure 1.4) and used to predict power for the larger processed OSM solar and wind datasets. For solar, power was predicted from the installation panel area only, whereas for wind, power was predicted from both the number of turbines and the area of the installation. The power of a wind installation is dependent on the type of turbines installed: larger turbines require larger wake distances so are likely to be more sparsely spaced in an installation. Including landscape area as well as turbine number allowed us to create a *de facto* measure of turbine density. Predicting power solely from number of turbines implicitly assumes the same turbine type occurs at all global installations; predicting power from number of turbines only was inferior to the full model (RMSE 14.24 $>$ 11.24).

The power estimates are the best available currently, but should be viewed with caution as, for example, the Wiki Solar dataset only records solar installations >100MW. Furthermore, these datasets are from three early-adopting countries, where wind and solar projects are more established, engineering expertise is more readily available, and higher power projects are more likely. All three – USA, UK, and Germany – are in the top ten countries for solar and wind capacities in 2018. We understand that predicting power beyond the geographical range of the input data can be problematic. However, there is no reason to think that the relationship between solely geospatial predictors (area, number of points) and power would change with geography with the limited wind and solar technology currently available, and hence we feel that our extrapolation is reasonable and defensible given data limitations.

There were also 9 instances where the solar power model predicts power capacities in the larger OSM dataset beyond the power range present in the solar power model input data (where the maximum power capacity is 377MW). However, the solar power model input data capture 99.9% of the variation in panel area in the larger OSM dataset, so we opted to include these 9 extrapolated points as a justifiable small extension of the model. The wind power model captured 100% of the variability in turbine numbers and 99.95% of the variation in landscape area in the larger OSM dataset, with no power capacities beyond the range found in the independent datasets.

1.4 Data Records

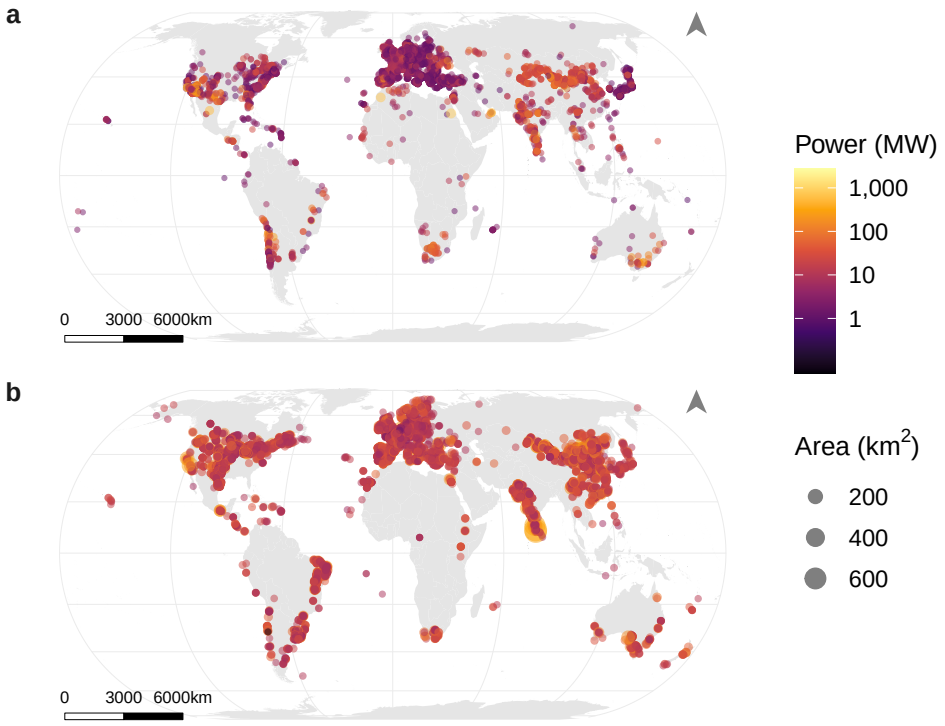

FIGURE 1.5: The global distribution of solar (a) and wind (b) installations. Solar installations represent those outside of urban cells and more than 1 hectare in panel area. Wind installations represent those outside of urban and water cells and with more than four turbines. 'Area' refers to landscape area for wind and panel area for solar.

This dataset is stored in three different formats: shapefiles for use with GIS software, geopackage for open-source usage, and .csv format for ease of use in any statistical software. Two final datasets were produced that represent the best publicly available global, harmonised geospatial data for field-scale solar PV and wind installations (Figure 1.5). We provide vector data (point and polygon) for grouped installations (more than two features; Methods), in Eckert IV equal area projection (an update to the data since publication now also presents the data in WGS84 after repeated requests from users).

1. Global solar PV installations
    - global_solar_2020.gpkg
    - global_solar_2020.csv
    - global_solar_2020 layer in global_wind_solar_2020.gdb
2. Global wind installations
    - global_wind_2020.gpkg
    - global_wind_2020.csv
    - global_wind_2020 layer in global_wind_solar_2020.gdb

Both datasets include the following variables:

1. *x_id*; unique ID for data record
2. *GID_0*; country ISO-3 code
3. *panels* or *turbines*; the number of OSM tagged features that occurred within the boundaries of the cluster
4. *panel.area* (solar only); the (estimated) area of panels in the cluster in km^2
5. *landscape.area*; the area of the site in km^2, i.e. the area bounded by the outermost points or polygons, buffered by 800m for wind
6. *water*; binary indicator of whether the feature occurs in an area classified as water (Methods)
7. *urban*; binary indicator of whether the feature occurs on land classified as urban (Methods)
8. *power*; estimated power output in MW

The .csv and .shp files, in lieu of detailed spatial information, contain the X and Y coordinates of the data centroid. The geopackage format can contain multiple geometries and is the preferred option. To comply with Esri field name specifications, landscape area and panel area are renamed as *p_area* and *l_area* in the Esri geodatabase.

The final, downloadable format of both databases is available from *figshare* (Dunnett, 2020).

1.5 Technical Validation

1.5.1 Data completeness assessment

To assess whether the OSM data truly reflect global solar (Figure 1.1a) and wind (Figure 1.1b) built infrastructure, or simply sampling bias (most observations are in developed countries with large OSM user communities (Barrington-Leigh & Millard-Ball, 2017)), we ran regressions for the raw number of solar and wind features extracted from OSM per country

as explained by their respective reported solar PV and onshore wind capacities per country in 2018, as well as other variables known to influence the completeness of OSM data.

While reported onshore wind capacity alone explains the number of wind feature observations relatively well ($R^2 = 0.8961$), the relationship between solar capacity and number of observations is much weaker ($R^2 = 0.1306$). However, removing data for China improves the solar correlation considerably ($R^2 = 0.5218$) due to an apparent dearth of OSM data compared to the enormous reported capacity.

One previous study assessing the OSM global road network identified three significant factors driving the completeness of a country's data: land area, the number of Internet users, and the country governance (Barrington-Leigh & Millard-Ball, 2017). We used the same World Bank variables from that analysis for the latter two: Internet users per 100 people in 2015, and the Voice and Accountability Governance indicator for 2018. This allowed us to assess whether the geographic variability in OSM features is driven primarily by the existence of wind and solar infrastructure (using reported capacity as a proxy), or factors relating to the completeness of OSM.

As number of observations represents count data, we looked at fitting Poisson general linear models. However, the number of observations per country for both solar and wind were heavily zero-inflated; i.e. the majority of countries worldwide do not have any renewable-tagged OSM data. Log transforming count data to correct for zero-inflation has previously been shown to have little use over alternative methods (Zuur, Ieno, Walker, Saveliev, & Smith, 2009; O'Hara & Kotze, 2010), thus we decided to fit a zero-inflated negative binomial (ZINB) regression model. A ZINB regression model was selected over the similar hurdle approach as we expect two types of zeros in the data: structural zeros, where a country with no renewable energy capacity could never have any renewable infrastructure, and sampling zeros, where a country may have national renewable energy capacity, but no data in OSM. A ZINB first fits a binomial regression to the data to produce an estimate of the count being positive, then fits a truncated negative binomial model to produce an estimate of the count. The predictors do not have to be the same in both models. For our application, the models fitted solely with reported capacity outperformed the models with only the three OSM completeness metrics (Likelihood ratio test, p value $= 0$ and p value $= 0.001911$ for wind and solar respectively). However, the most parsimonious models are presented in Table 1.3, and these include some measures of OSM data completeness. National capacities and land area were both modified with a Yeo Johnson transformation to correct for heavy negative skew. All variables were scaled.

Although country governance and land area contribute towards the variability in OSM observations for both wind and solar, the coefficients for the national capacities clearly suggest that the observed pattern is largely reflective of the true distribution of renewable infrastructure. Furthermore, the sole driver of whether a country has any OSM data at all, e.g. the binomial models, in both cases, is the reported national capacity.

	Solar	Wind
Count model: (Intercept)	0.93^{*}	-0.62^{*}
	(0.44)	(0.32)
Count model: solar.cap	1.41^{***}	
	(0.18)	
Count model: governanceVoice2018	1.13^{***}	0.27^{**}
	(0.19)	(0.10)
Count model: land	0.86^{***}	0.35^{**}
	(0.19)	(0.12)
Count model: Log(theta)	-1.11^{***}	0.56^{***}
	(0.12)	(0.15)
Count model: wind.cap		2.61^{***}
		(0.12)
Zero model: (Intercept)	-0.27	0.40
	(0.79)	(0.53)
Zero model: solar.cap	-1.77^{*}	
	(0.78)	
Zero model: wind.cap		-2.56^{***}
		(0.69)
AIC	2253.36	1351.29
Log Likelihood	-1119.68	-668.65
Num. obs.	178	128

$^{***}p < 0.001$; $^{**}p < 0.01$; $^{*}p < 0.05$.
Whether a country has any observations at all is driven by the respective national capacities, after which the capacity, governance and land area of the country explain the count.

TABLE 1.3: Zero-inflated negative binomial regression fitted for OSM wind and solar observations.

Moreover, after data processing, the aggregated estimated power capacities of our datasets per country correlate even better with reported capacities ($R^2 = 0.8178$ and 0.9707 for solar and wind respectively).

TABLE 1.4: Performance measures for 5-repeat 10-fold cross validation models fitted to predict the power capacity of wind installations. Here, *n* is the sample size for the spatial join with independent datasets (Methods) after processing the raw OSM data with the presented values of *minPts* and ε.

minPts parameter	ε (m)	RMSE	R^2	MAE	*n*
2	800	11.22133	0.7308343	6.233574	3574
3	800	10.80424	0.7516774	6.134675	3571
5	1000	11.68232	0.7308547	6.776778	2678
10	2000	19.71299	0.6271118	11.547240	848

TABLE 1.5: Performance measures for 5-repeat 10-fold cross validation models fitted to predict the power capacity of solar installations. Here, *n* is the sample size for the spatial join with independent datasets (Methods) after processing the raw OSM data with the presented values of *minPts* and ε.

minPts parameter	ε (m)	RMSE	R^2	MAE	*n*
2	400	18.42949	0.6482381	5.367391	3280
3	400	17.90751	0.6519353	5.263504	3396
5	400	17.60908	0.6473003	5.254524	3558
10	400	17.55904	0.6446935	5.211948	3621

1.5.2 DBSCAN minPts parameter

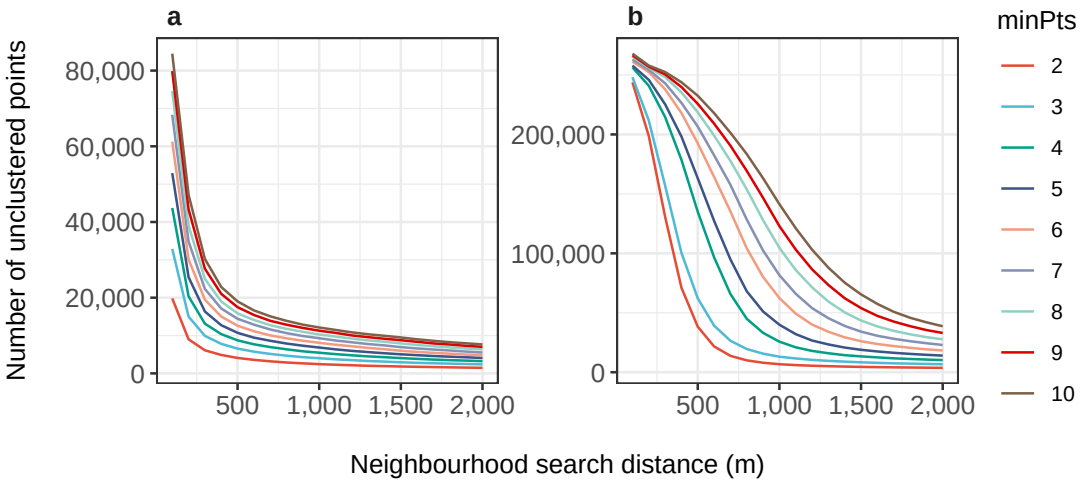

FIGURE 1.6: "Knee" plots for OSM solar (a) and wind (b) point data showing the number of unclustered points remaining for differing neighbourhood search radii and values of *minPts*. For wind, the optimal value of ε changes as *minPts* increases, but the value for solar remains relatively constant.

To assess the functioning of DBSCAN when passed a *minPts* argument of 2 over more explicit density-based clustering, and to check whether the model fits were adversely affected by the *de facto* single-linkage clustering needed to identify some linear wind installations, we repeated the power analyses for different values of *minPts* and ε. Figure 1.6 shows the

"knee" plots for solar (a) and wind (b). For solar, the value of *minPts* does not appear to affect the appropriate value for the neighbourhood search radius (ε) of 400m. The optimal neighbourhood search radius does appear to change with *minPts* for wind. The values selected for ε are shown in Table 1.4 and Table 1.5.

As the primary purpose of our fitted power models is prediction, and not explanation, the root mean square error (RMSE) and mean absolute error (MAE) are the most appropriate performance measures for these models. The RMSE and MAE of the wind models are highest as the *minPts* parameter is increased to 10 (Table 1.4), but notably the models trained on *minPts* 2, 3 and 5 are very similar, suggesting that the wind data are not significantly affected by the lack of specifically density-based clustering. The solar data appear to be robust against different values of DBSCAN parameters (Table 1.5).

1.6 Usage Notes

Location data for wind and solar installations worldwide can be used to support a range of applications, including analysing the land impact of current infrastructure, measuring progress towards global goals, and informing future energy planning scenarios.

Ongoing work involves the integration of these datasets with socio-economic and biophysical predictors to produce probability surfaces for the likely development of wind and solar infrastructure in order to more accurately highlight potential trade-offs with other important sustainable land uses (Oakleaf et al., 2019). While potential regions of conflict have been highlighted in previous studies, for example biodiversity and renewable energy (Santangeli et al., 2015, 2016), these new data allow analysis at whatever resolution there are readily accessible global predictors (currently 1 by 1km grids). This is especially important as it has been suggested that the wider social and environmental impacts of energy scenarios are typically overlooked because the majority of scenarios are aspatial (Howard et al., 2013).

Additionally, there are many applications of these data outside a purely renewable energy context. While this analysis focuses on renewable energy infrastructure, there is no reason why the methodology cannot be replicated for other types of infrastructure lacking in openly accessible data. For example, conventional fuels also lack such consistent data. Appropriate tags for oil and gas can be found at the site of the Oil and Gas Infrastructure WikiProject (OpenStreetMap, 2020). We would caution that the specific methodology of this study was designed with renewable energy in mind, and some thought would be needed to recalibrate some of the analysis parameters, e.g. the neighbourhood distance.

R scripts are provided that allow users to generate and process their own raw OSM data at a future date. All model data are also provided so that users can recreate the power models and compare to reported national capacities.

We highly recommend using the geopackage data, which can be easily read into **R** with the `sf` package and has the advantage of holding multiple geometries, i.e. point, multipoint, polygon and multipolygon data. For ease, the shapefiles and comma-delimited files were restricted to point geometries by taking the centroid of each data record.

The datasets contain all data and require filtering in order to be meaningful for different use cases. For example, the power models in this paper were trained on a subset of the raw data: solar farms not in urban centres, and with a panel area of >1ha, and wind farms not in urban centres or in water and with more than four turbines (the median number of turbines in the three independent datasets was 5). For this reason, power capacity is missing for all data that do not meet these criteria.

1.7 Code Availability

The code used to extract and process the OSM data is publicly available through the *figshare* repository (Dunnett, 2020). The code consists of four **R** programming language scripts (**R** version 3.6.2) numbered 1-4: the first extracts the latest OSM data; the second processes the data into wind and solar farms; the third contains the power models, and the fourth conducts the technical validation. Each script includes text that guides the user through the process and details the functions being performed. The README file, included with the scripts, provides more detail on rerunning the analyses.

We regret that we cannot provide the full, geospatial Wiki Solar dataset as it was provided on the condition of confidentiality. We have provided a copy of the spatial join between the Wiki Solar dataset and the processed OSM data, with all geospatial data stripped out. This can be used as an input to the power estimations on its own. However, the power estimation can be rerun omitting these data if users require models trained on truly open access data (alternatively, users can contact the Wiki Solar data provider). When we ran this analysis, the accuracy of the solar model to predict unseen data in the two remaining independent datasets increased (RMSE=3.153742, R^2=0.7442277, MAE=1.386226, n=1889). However, the input data for this model only managed to capture 96.8% of the variation in panel area in the wider OSM dataset and subsequently predicted 253 occurrences of power capacities outside of the model range. For this reason, we elected to keep the Wiki Solar data in the final model.

This page intentionally left blank.

Chapter 2

Predicting future energy and biodiversity trade-offs globally

2.1 Abstract

Protected areas and renewable, emissions-free energy generation are our most important tools to combat biodiversity loss and unprecedented climate change respectively. With other pressing needs for land use emerging from requirements for adequate food and housing for the global population, there are concerns that hierarchies of needs may force lower priority land uses, like renewable energy and protected areas, to co-occur in space if priority areas overlap. Renewable energy infrastructure has demonstrably negative effects on wildlife, and co-occurrence may contribute to emissions targets only at the expense of conservation objectives. Expansion of both may exacerbate this issue but identification of potential conflicts is hampered by limited data and methodologies. Here, using newly generated spatially explicit wind and solar photovoltaic data, I assess how accurately priority areas for renewable energy and biodiversity conservation expansion are identified, and evaluate the potential risk of near-future trade-offs between the two land uses. I show that while research has done well predicting priority expansion areas for protected areas, solar PV and wind models can be improved with distribution data. I also present results that demonstrate there is no significant spatial correlation between likely expansion areas at a regional level, suggesting a low risk of conflict in the near future. Finally, I demonstrate that the current co-occurrence bears this out: 3,666 installations occur in 1.247% of protected areas, 3.852% of Key Biodiversity Areas, and 0.7769% of wilderness areas. Unlike previous studies, I identify countries of the world where this overlap is greater or less than expected using models taking into account land areas. Although any overlap with such vastly different management objectives is unfortunate, I show there is no reason to believe that the overlap between renewable energy and biodiversity conservation is set to worsen with expanding area targets.

2.2 Introduction

The global renewable energy generation capacity was up to approximately 2,537GW by the end of 2019, an increase of 7.4% on 2018. Wind and solar energy comprised 90% of new capacity in 2019 (IRENA, 2020a). With commitments from multilateral environmental agreements like the Paris Agreement (UNFCCC, 2016), it is clear that the march of renewable energy expansion is set to continue: the International Energy Agency (IEA) has forecast that renewable energy capacity may increase by over 50% by 2024 (IEA, 2019). It has long been pointed out that renewable energy technologies possess energy densities orders of magnitude below conventional fossil fuels (Smil, 2008; Trainor et al., 2016; Fritsche et al., 2017; United Nations Convention to Combat Desertification, 2017; Miller & Keith, 2018; Zalk & Behrens, 2018): while coal and gas can reach power densities of as high as 2000Wm^{-2}, the most power-dense renewable technology (concentrating solar power – CSP) peaks at just 10Wm^{-2} (Smil, 2010).

As a result, the expansion of renewable energy capacity joins a plethora of other sustainability concerns that have enormous repercussions for global land systems and planning (Holland et al., 2019). For example, it is oft mentioned that many estimates of bioenergy assume an area of grasslands and marginal lands the size of India will become available for energy crops (Slade et al., 2011; Fuss et al., 2018); wind energy area requirements were forecast to be six times the size of Great Britain by 2020, and solar PV the size of New Zealand (Scheidel & Sorman, 2012). At the same time, food production may need to increase 100% on 2005 levels by 2050 (Eitelberg, Vliet, & Verburg, 2015); much of this may be achieved by agricultural intensification, but croplands continue to expand regardless (Grassini, Eskridge, & Cassman, 2013; Seppelt et al., 2014; Eigenbrod et al., 2020). Furthermore, protected area designation to protect dwindling global biodiversity needs to increase to demarcate at least 17% of global land area (the Biodiversity Aichi Targets) (Pouzols et al., 2014; Tittensor et al., 2014). The targets are due for review in 2020, with some conservation scientists pushing larger targets; some even suggest that half of Earth's area should be protected in some way or other (Dinerstein et al., 2017). Thus, three important concepts for global sustainability: energy, biodiversity, and food production, all demand ever larger shares of terrestrial area with an increasing risk of conflict.

The direct impacts of renewable energy technologies on biodiversity are relatively well known (Fritsche et al., 2017; United Nations Convention to Combat Desertification, 2017). Wind turbines have significant effects on volant species (Schuster et al., 2015; Thaxter et al., 2017; Thompson, Beston, Etterson, Diffendorfer, & Loss, 2017; Miao, Ghosh, Khanna, Wang, & Rong, 2019), while solar PV can also have significant local effects (Lovich & Ennen, 2013; Hernandez et al., 2014; Moore-O'Leary et al., 2017). Solar PV largely completely precludes its immediate area from any other land use, whereas wind energy can accommodate some forms of agriculture (Smil, 2010). Bioenergy has much the same negative impacts on land as agriculture (Slade et al., 2011; Fritsche et al., 2017).

Due to these inherent trade-offs between different land uses, and the diminishing availability of global land area for each function respectively, it is important for land planning to evaluate where these trade-offs might occur (Köppel, Dahmen, Helfrich, Schuster, & Bulling, 2014; Gasparatos et al., 2017; Gibson, Wilman, & Laurance, 2017; Baruch-Mordo, Kiesecker, Kennedy, Oakleaf, & Opperman, 2019; Kiesecker et al., 2019).

This task is made even more difficult when there is a lack of harmonised global data to support analyses. Even in the field of agricultural land systems, where global data coverage is actually now very good with a number of high resolution datasets (HarvestChoice, 2014; Fritz et al., 2015), estimates of available cropland vary from 1,552 to 5,131 Mha (Eitelberg et al., 2015). Furthermore, although the drivers of current cropland extent are relatively well known, it is much harder to predict agricultural frontiers, where many factors not historically considered drive the expansion of croplands (Eigenbrod et al., 2020). As outlined in Section 1.2 of Chapter 1, spatially explicit renewable energy data are sparse, available only for select countries (BEIS, 2019; Eichhorn et al., 2019; Hoen et al., 2019; Rand et al., 2020), and rarely open access. Biodiversity conservation data, on the other hand, is relatively comprehensive and the subject of many global analyses (Pouzols et al., 2014; Brooks et al., 2016).

Previous research has looked at the potential for conflict between three types of renewable energy, bioenergy (*Miscanthus*), solar PV and wind, and areas of high priority for biodiversity protection (Santangeli et al., 2015, 2016). The research highlighted regions of the world thought to be most at risk by assuming that areas high in physical suitability for the different energy technologies would be the most likely areas for installation of additional capacity. The distinct lack of quality renewable energy spatial data means that this is an assumption that is rarely tested. However, even with readily-available biodiversity conservation data, retrospective assessment of various identified priority areas for biodiversity are similarly rarely tested.

More recent research has attempted to increase the precision of using suitability maps to predict areas with a high probability of development for land uses related to renewable energy (Oakleaf et al., 2019). These development potential indices (DPIs) represent the best available estimates as to where the pressure from these sectors (including wind and solar) will be and combine resource availability with development feasibility. For wind, development feasibility included traditional constraints: excluding 1-km^2 grid cells with a wind speed of below 6ms^{-1}, a slope greater than 30%, elevation above 3,000m, and unsuitable land cover (wetlands, rock/ice, etc.). For solar PV, constraints included a slope greater than 30% and unsuitable land cover. For wind development feasibility, Oakleaf et al. (2019) did include some measure of current wind installations, choosing to exclude grid cells with $\geq$ 3 wind turbines (i.e. $\geq$ 3 turbines/km^2). No such constraint was added for solar PV, *"given lack of global data"* (2019, p. 2). The authors deliberately did not include any administrative constraints (e.g. excluding protected areas).

Other studies have made use of proprietary renewable energy data to evaluate the current renewable energy estate's footprint in areas of importance for biodiversity. Rehbein et al. (2020) used paywalled data from the GlobalData Power Database for solar PV, onshore wind and hydropower generators to conduct spatial overlap analysis with protected areas, Key Biodiversity Areas (KBAs) and wilderness areas. The study found a large number of overlapping renewable energy facilities: 169 renewable energy facilities were found to exist inside the strictest category of protected area (IUCN categories I-IV), where no development should occur. Wind power was found to overlap with the largest number of conservation areas. As with previous studies (Santangeli et al., 2015, 2016), the conflict between renewable energy and conservation areas was decidedly heterogeneous: Western Europe contained the vast majority of overlaps (although this is likely because Western Europe has large amounts of both protected areas and renewable energy facilities), whereas Africa and the Middle East had the greatest *proportion* of overlaps (again, likely because both have far fewer facilities). Wilderness overlaps are found largely in China and North America, whereas protected area overlaps are found mostly in Europe and Japan.

The Rehbein et al. (2020) study also looked at renewable energy facilities *under development*, which is extremely important – as available land comes under increasing pressure from differing land uses in the future, land system planners have to look at maximising the benefit for each land use. This heavily relies on our ability to identify priority areas for each land use. Rehbein et al. (2020) used renewable energy facilities under development as a proxy for future threat. While this works as a proxy for *immediate* threat, identifying priority areas beyond this relies on the use of suitability-based maps like those produced by Oakleaf et al. (2019). However, these need to be further corrected for how renewable energy infrastructure has historically been placed as it has been shown that a host of seemingly innocuous local socio-economic factors affect siting of facilities (Roddis et al., 2018; Harper et al., 2019).

Here I focus on the global renewable energy (wind and solar PV) estate to answer the following question: do identified priority areas for expansion of biodiversity protection and renewables suggest future conflict? To do this, I assess the literature's current ability to identify priority areas for renewable energy as exemplified by Oakleaf et al. (2019) when compared to a novel spatially explicit dataset of wind and solar installations worldwide (Dunnett et al., 2020), and compare to the much more established protected area priorities literature (Pouzols et al., 2014). I conclude with comparing suggested levels of conflict with current distributions and overlap, as shown by Rehbein et al. (2020).

2.3 Methods

All analyses were performed in **R** (version 3.6.2).

2.3.1 Renewable energy data

Spatially explicit infrastructure data

The spatially explicit wind and solar data represent 12,581 and 12,043 installations worldwide in 153 countries, totalling 322.8 and 125.6GW of capacity respectively (Dunnett et al., 2020). They currently represent the best available data for wind and solar infrastructure globally. These datasets were created by extracting features from OpenStreetMap, an open-source collaborative global mapping project. Data were extracted from OpenStreetMap that were tagged in a manner representing either a wind turbine or solar PV. Data were then spatially aggregated to approximate utility-scale installations. Power estimates were provided based on prediction models trained on independent data. For full methodology please see either Chapter 1 or the accompanying paper (Dunnett et al., 2020). As suggested by the authors, these data were filtered to remove any wind installations with fewer than 5 turbines and not in cells identified as water, and any solar installations with less than 1 hectare ($0.01km^2$) in panel area. However, wind and solar installations in cells identified as an urban centre were not filtered – it is likely that distance to urban centres (or accessibility) is a strong signal for the development of renewable energy probability surfaces (Harper et al., 2019). Removing installations in urban centres would therefore mask a potentially important effect.

Development potential data

Renewable energy development indices were taken from the Oakleaf et al. (2019) study assessing land suitability for 13 sectors related to renewable energy. The study produced gridded 1-km^2 resolution development potential indices (DPIs) for each sector, using multicriteria decision analyses that took into account resource potential and development feasibility. Here I use the wind and solar PV DPIs.

2.3.2 Biodiversity conservation data

Protected areas

Protected area data used were from the December 2019 release of the World Database on Protected Areas (WDPA) (UNEP-WCMC & IUCN, 2020). Protected area data were processed according to accepted practice (see UNEP-WCMC, n.d.; Visconti et al., 2013; Pouzols et al., 2014; Rehbein et al., 2020). Point locations for protected areas were excluded, as well as polygons $< 5km^2$ in reported area. Only terrestrial protected areas were considered, and those with status *Designated*, *Inscribed* or *Established*. Protected areas are, where possible, assigned an IUCN Management Category (Dudley, Shadie, & Stolton, 2013). While they are often considered to be hierarchical, the IUCN explicitly cautions against this. When looking at infrastructure/development impacts on protected areas, users, including Rehbein et al. (2020), routinely categorise areas generally into the stricter categories – I-IV – and those that allow some form of land development – V-VI. IUCN categories of *Not Reported*,

Not Applicable and *Not Assigned* are recommended to be amalgamated into one group (Bingham et al., 2019) – these categories do not indicate that these areas are any less well managed than I-VI areas, but for individual reasons they cannot be designated a specific category. Global protected areas are reasonably equally distributed between these three classes (I-IV, V-VI, and no category), with 17,985, 10,601, and 18,563 areas respectively.

Preparing the data as such resulted in a global total of 47,149 polygon data for 28,586 sites with 13.37 million km^2 reported area designated IUCN Category I-VI, and 13,701 with 14.48 million km^2 area in the strictest categories, I-IV, where no development should occur.

Key Biodiversity Areas

As with the Rehbein et al. (2020) study, I obtained data on KBAs (BirdLife International, 2019). KBAs are designated by the International Union for Conservation of Nature (IUCN), and signify *sites contributing significantly to the global persistence of biodiversity*. These comprise, in the September 2019 iteration, 13,041 sites globally with a total reported area of 1,214 million km^2. Crucially, 10,393 (79.69%) of these sites are designated as Important Bird and Biodiversity Areas (IBAs) – primarily with the intention of identifying and protecting sites for the conservation of naturally occurring bird populations. As with protected areas, I excluded KBAs with only point data as well as those designated as *marine* IBAs.

Wilderness areas

Areas of 'wilderness' were collected from a previous study identifying the remaining large, conterminous areas of the world with the lowest human footprint. The authors made efforts to ensure these areas were representative of the Earth's Biogeographic Realms (Venter et al., 2016; Allan, Venter, & Watson, 2017). The areas identified were split by country but otherwise used without modification.

Priority expansion areas for protected areas

Priority expansion areas for protected areas were obtained from a previous study looking to assess the effects of land use change and national versus global priorities on the efficacy of the global protected area estate, available at `https://avaa.tdata.fi/web/cbig/gpan` (Pouzols et al., 2014). Pouzols et al. (2014) used range maps of all threatened terrestrial vertebrates identified by the IUCN Red List of Threatened Species at the time (24,757 species globally) and the world's 827 World Wildlife Fund (WWF) ecoregions. The analysis took the 2013 protected area network and identified areas outside these that represented the best opportunities for expansion, with rankings weighted on species numbers and ecoregion representativeness using the conservation spatial planning tool Zonation (v4). The data are available at 0.008333 resolution, WGS84 projection.

Protected area downgrading, downsizing, and degazettement data

Data on protected area downgrading, downsizing, and degazettement (PADDD) were downloaded from PADDDTRACKER (available at `https://www.padddtracker.org/`). These

data were collated in a study that originally identified 3,749 PADDD *events* (instances where a protected area has been downgraded, downsized or degazetted) (Golden Kroner et al., 2019). Between 1892 and 2018, 519,857km^2 has been removed from protection, with 1.660 million km^2 downgraded.

For the purposes of this (spatial) study, these data were filtered by events with **known** locations, as recommended by the authors. This stipulation removed 61 events. As with other conservation data, events with point data were excluded: this exclusion removed 23.89% of the total area affected by PADDD events. Furthermore, events were filtered by the event cause: only events where the cause was identified as "Infrastructure" were included. This generated 10 PADDD events of interest, totalling 24.84km^2.

2.3.3 Global independent variables

The following global datasets were used where all were reprojected, and in some cases aggregated, to Mollweide equal-area projection, 1-km^2 resolution:

- 2015 accessibility (travel time to cities) (Weiss et al., 2018);
- 2005 gridded data of cattle, goats, and sheep derived from the Gridded Livestock of the World datasets (Robinson et al., 2014);
- 2005 percentage cropland per pixel (Fritz et al., 2015);
- Elevation (and calculated slope), available from `http://viewfinderpanoramas.org/dem3.html`;
- Gridded distance from protected areas, calculated on the same dataset as described in Section 2.3.2;
- 2015 population density from the Gridded Population of the World v4 (Doxsey-Whitfield et al., 2015);
- Total road density from the Global Roads Inventory Project – GRIP – dataset (originally in WGS84 0.08333-resolution and simply disaggregated to 0.008333-resolution) (Meijer, Huijbregts, Schotten, & Schipper, 2018);
- Global horizontal irradiance from the Global Solar Atlas, available from `https://globalsolaratlas.info/`;
- Global wind speed at 100m height from the Global Wind Atlas, available from `https://globalwindatlas.info/`

2.3.4 Priority protected areas

To assess the identification of priority areas of expansion for the protected area network, I used the WDPA data prepared as detailed in Section 2.3.2. The original Pouzols et al. (2014) analysis used protected area data from the June 2013 WDPA release; to be certain I was assessing the placement of protected areas *after* this date, I only considered areas with

STATUS_YR $\geq$ 2014 as the database does not provide the month and year of designation. This identified 1,344 protected areas of interest, with a total reported area of 659,556km^2.

The post-2013 protected area layer was then rasterised to a resolution of 0.008333 degrees. Rasterisation describes a process where data in vector format, e.g. the boundary of a protected area, are converted to a gridded format. A pre-2014 protected area layer was then used as a mask layer to remove cells that were already protected. This reduces the risk of false positives due to the resolution of the data. The data were also masked with a global land layer, producing a binary raster of the global surface presenting each 1-km^2 cell as either protected post-2013, or not. This layer was then used to extract values from all four scenarios produced by (Pouzols et al., 2014): national with 2000 land use, national with 2040 projected land use, and global with both 2000 and 2040 land use.

10,000 values were then randomly selected from the protected cells and from the unprotected cells using `sample_n` in the `dplyr` **R** package (Wickham, François, Henry, & Müller, 2020) to give a total sample of 20,000. Pairwise two-tailed t tests were then performed between the protected and unprotected samples for each scenario to determine whether protected cells were ranked on average higher or lower than unprotected (background) cells. To measure effect size, Cohen's *d* was also calculated for each pair (Cohen, 1992). In order to exclude cells that were artificially forced into high or low rankings (for full details see Pouzols et al. (2014)), values were trimmed below 0.1 and above 0.89.

2.3.5 Priority renewable energy areas

To assess the identification of priority areas for the *renewable energy* network, I used data from (Oakleaf et al., 2019) (Section 2.3.1). Spatially explicit wind and solar data were first reprojected to Mollweide equal-area (the projection of the Oakleaf et al. (2019) data). These datasets were then used to extract values from the DPI rasters for wind and solar respectively, as well as a suite of independent variables (Section 2.3.3). This produced a dataset (n = 12,249 for wind and 11,830 for solar PV) where for each wind and solar installation I had values for the DPI, nine global independent variables, and installation variables from the renewable energy datasets (four for solar, three for wind).

The DPI layers were masked by a number of constraints (see Online-only Table 2 in Oakleaf et al. (2019)). In cells where this occurs, the cell is assigned a no data value, indicating zero development potential. Thus, a number of the extracted DPI values for wind and solar installations (3,675 and 1,516 respectively) are missing. One of these constraints attempted to exclude global 1-km^2 cells which already contained a wind or solar PV installation. For solar PV, this was not attempted due to lack of global data (Introduction). For wind, cells with ≥ 3 wind turbines were excluded. However, the data used for this only covered the United States (Refs 59, 147 and 148 in Oakleaf et al. (2019)). For the purposes of this analysis I reclassified the no data values DPI rasters as 0.

Here, I compare all wind and solar PV installations with an equally sized selection of background point values to determine whether cells with installations in them present on average higher or lower DPIs than cells without installations (background cells). As with Section 2.3.4, I randomly sampled an equally sized selection of background points to presences and performed pairwise two-tailed t tests and calculated Cohen's *d*.

2.3.6 Renewable energy probability layers

Global and regional wind and solar PV probability layers were created using the `zoon` and `raster` **R** packages (Hijmans, 2017; Golding et al., 2018). The `zoon` package allows users to create reproducible workflows for species distribution modelling. Species distribution models, as explained by Araújo & Peterson (2012), use *"associations between aspects of climate and known occurrences of species across landscapes of interest to define sets of conditions under which species are likely to maintain viable populations"* (p1527). They are essentially correlative models with no biological mechanisms (such as species dispersal) involved and are widely used in the field of ecology (Barbosa & Schneck, 2015; Golding et al., 2018). One of the overriding principles of species distribution modelling is that there is an "environmental envelope" of multivariate space that best matches a species' observed distribution. In a very similar way, wind and solar PV siting is predicated on a number of environmental variables: namely resource potential (solar irradiance and wind speed), but also, as implemented by Oakleaf et al. (2019) with simple land constraints, slope, elevation, land cover, etc. (Kiesecker et al., 2011; Pogson et al., 2013; Santangeli et al., 2015, 2016; Enevoldsen et al., 2019; Oakleaf et al., 2019; Waldman et al., 2019). Furthermore, renewable energy is subject to anthropogenic drivers such as population density, distance to roads and urban areas (Roddis et al., 2018; Harper et al., 2019). As such, I can estimate the "socio-environmental envelope" of wind and solar PV using their occurrence data and a suite of environmental and social predictors, in a similar manner to a recent study that characterised the climate niche of humans (Xu, Kohler, Lenton, Svenning, & Scheffer, 2020). I did not consider the wind and solar PV DPIs as a potential predictor as they are wholly based on resource availability, a factor already considered by the included wind speed and global horizontal irradiance variables. Whilst previous studies create probability layers by layering constraints atop resource potential maps, this method uses no constraints – except for land surface – and allows me to scrutinize what *actually* drives the distribution of the renewable energy estate.

For the observed occurrence of renewable energy facilities, I use a new spatially explicit global database of wind and solar PV (Section 2.3.1). I chose not to exclude installations tagged as urban as I wanted to capture potential socio-economic drivers associated with urban centres. Filtering the data in this way presents 12,753 and 14,350 wind and solar PV occurrences worldwide. With no formal absence data, and because group discrimination species distribution models (those with presence/absence data) tend to perform better than

profile methods (presence-only) (Elith et al., 2006; Liu, Newell, & White, 2019), I looked to generate sensible pseudo-absences, a well-established technique in species distribution modelling (Barbet-Massin, Jiguet, Albert, & Thuiller, 2012; Liu et al., 2019).

There are myriad models to select from in the species distribution field (Elith et al., 2006; Barbosa & Schneck, 2015; Golding et al., 2018). The highest ranking group of these includes MARS community (MARS-COMM), boosted regression trees (BRTs), generalised dissimilarity (GDM and GDM-SS) and maximum entropy (MAXENT and MAXENT-T) (Elith et al., 2006; Marmion, Luoto, Heikkinen, & Thuiller, 2009; García-Callejas & Araújo, 2016). Combining the results and recommendations of prior studies with model techniques readily available in existing `zoon` modules, I selected GBM (Generalised Boosted Model), GLM (Generalised Linear Model – logistic) and a machine learning technique, Random Forest (RF) (Breiman, 2001), to investigate for their predictive capacities. For more details of each model's use in species distribution modelling, see Marmion et al. (2009).

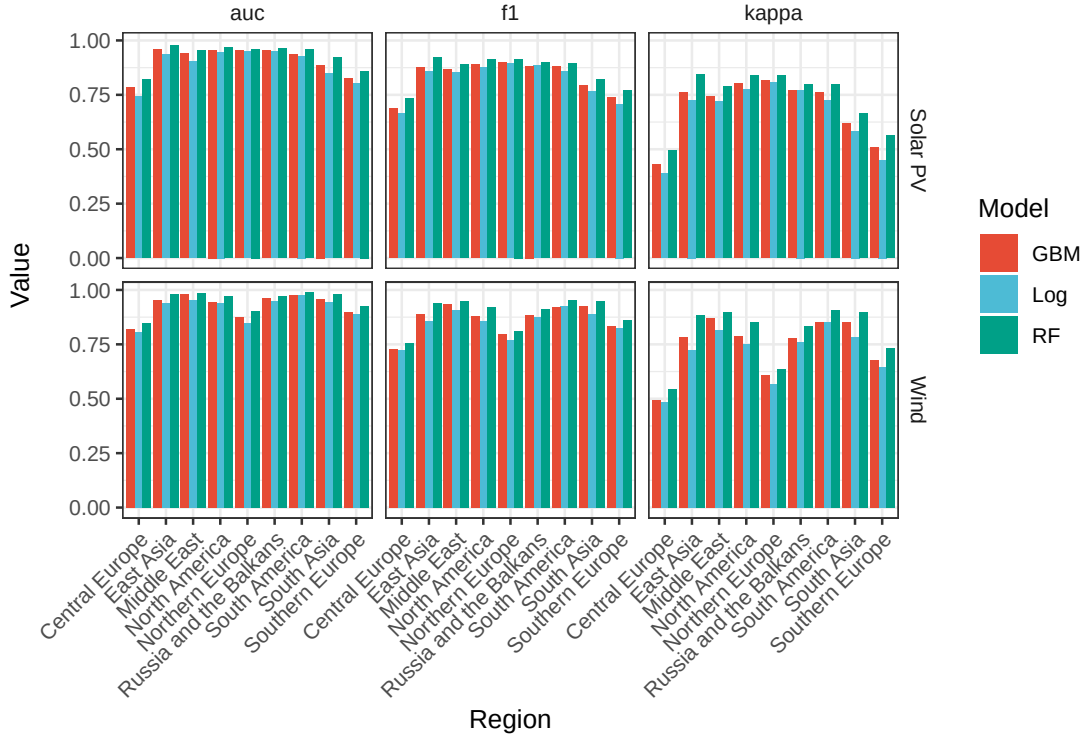

FIGURE 2.1: Performance measures for 5-fold cross validation species distribution models fitted to wind and solar PV occurrence/pseudo-absence data: area under the curve (AUC), F1 score, and Cohen's kappa (κ).

World regions with greater than 100 observations of wind and solar PV occurrences were selected. These regions were Middle East, Southern Europe, South America, North America, South Asia, Russia and the Balkans, East Asia, Northern Europe, Central Europe with sample sizes for wind and solar PV respectively of 146, 1453, 635, 2466, 714, 280, 2518, 861, 2624 and 425, 3639, 208, 1533, 332, 1287, 1413, 1465, 3327. For this preliminary analysis, I used a ratio of 1:1 pseudo-absence points to presence points, as suggested by Barbet-Massin

et al. (2012) for classification models like Random Forest. The threshold for classifying predictions as presences was the mean of the presences occurring in the input data, i.e. 0.5 (our presence and absence classes were deliberately balanced).

Area under the curve (AUC), or more precisely area under the *receiver operating characteristic* (ROC) curve, is a widely used performance metric for classifiers and gives an indication of how well a model accurately predicts two classes. However, it is less useful for models where one class is of more interest than the other. This is the situation here, where I am most interested in how accurately the models predict *presence* of a renewable energy facility.

Cohen's kappa (κ) is an improvement that assesses the *observed accuracy* of a classifier against the *expected accuracy* (also known as *random accuracy*). While there are no quantitative assessments of κ, Landis & Koch (1977) first suggested that a $\kappa >$ of 0.41-0.60 is "Moderate", a value of 0.61-0.80 is "Substantial" and 0.81-1.00 is "Almost Perfect".

Finally, the F1 score is a good metric for assessing a model's ability to distinguish the positive class and is calculated as a function of *precision* and *recall*. *Precision* describes a model's performance when the prediction is positive (i.e. a presence):

$$\text{Precision} = \frac{\text{True positives}}{\text{True positives} + \text{false positives}}$$

Recall describes a model's ability to correctly predict the actual occurrences:

$$\text{Recall} = \frac{\text{True positives}}{\text{True positives} + \text{false negatives}}$$

The F1 score is then calculated as

$$\text{F1 score} = 2(\frac{Precision * Recall}{Precision + Recall})$$

and is scaled from 0 (poor) to 1 (perfect).

As shown in Figure 2.1, all models performed relatively well classifying renewable energy installations by region. Random Forest performed the best, with mean scores for AUC, κ, and F1 of 0.9418, 0.7674 and 0.8783 respectively. Although larger, these were not significantly different from the next best performing model, GBM ($p = 0.1257$). However, the Random Forest models were run using the default parameters; these can be further tuned to increase accuracy thus Random Forest was selected to produce regional and global probability surfaces.

Variable importance values were calculated for the Random Forest models with the `varImp` function from the `caret` **R** package (Kuhn, 2020). The documentation for `varImp` describes how variable importance is calculated for Random Forest classification models:

> *For each tree, the prediction accuracy on the out-of-bag portion of the data is recorded. Then the same is done after permuting each predictor variable.*

The difference between the two accuracies are then averaged over all trees and normalized by the standard error.

As a reference point for the accuracy of our probability layers, I also performed 10-fold 5-repeat binomial regressions on wind, solar and an equal number of randomly selected background points with only the wind and solar DPIs as predictors.

In order to test the spatial relationship between priority areas for biodiversity conservation and those for renewable energy, global and local Pearson's correlation coefficients were calculated for the study regions with >100 observations of wind and solar. This was done using the `corLocal` function in the `raster` **R** package (Hijmans, 2017). The biodiversity priority areas layer (global 2040 land use scenario) was masked with current protected cells at 1-km^2 resolution, and the solar PV and wind probability layers were masked with current wind and solar installations at 1-km^2 resolution. For the global coefficients, a systematic sample of 1,000 cells was taken. For the local correlation coefficient layers, each cell's coefficient was calculated using the values from the 9 by 9 cell neighbourhood around the cell.

2.3.7 Spatial overlaps

Simple spatial overlaps of renewable energy installations and conservation areas were performed using the `sf` and `raster` **R** packages. Data were reprojected to Mollweide equal-area projection to ensure comparability of areas at all latitudes. Spatial overlaps were based on the predicate `st_contains_properly` – a function that ensures only installations *completely* contained within conservation areas were considered. This was done to minimise the risk of boundary inaccuracies flagging false overlaps where an installation and a conservation area merely intersect each other.

Of course, overlaps are more likely to occur in countries with large areas of both renewable energy and conservation areas, especially small countries. To identify countries where there is a larger (or smaller) area of overlap than expected from their size and renewable energy/-conservation estates, I fit a simple linear model (or the most parsimonious version of this model): overlap area $\sim$ renewable area + conservation area + land area.

The same overlap process was performed for renewable energy installations and the PADDD events of interest. However, as point data comprised a significant portion of the PADDD data (27.9%), I opted to include buffered point data in this analysis: the radii for the circular buffers were calculated from the reported area of the PADDD event.

2.4 Results

2.4.1 Development potential of onshore wind and solar PV deployment for selected regions using Random Forest

Figures 2.2 and 2.3 show probability surfaces generated with 10-fold 5-repeat Random Forest models for solar PV (mean accuracy = 0.776, mean $\kappa = 0.5518$, $N = 3{,}327$) and wind (mean accuracy = 0.786, mean $\kappa = 0.5719$, $N = 2{,}624$) respectively. Central Europe here refers to France, Germany, Liechtenstein, Belgium, Luxembourg, Monaco, Netherlands, Switzerland and Austria, as defined in the basemap from the `maptools` **R** package (Bivand & Lewin-Koh, 2019). The other test regions (also as defined in `maptools` – Southern Europe, South America, North America, South Asia, Russia and the Balkans, East Asia, Northern Europe and the Middle East) had a mean accuracy for wind of 0.9115 ($\kappa = 0.8227$) and for solar PV of 0.8857 ($\kappa = 0.7602$).

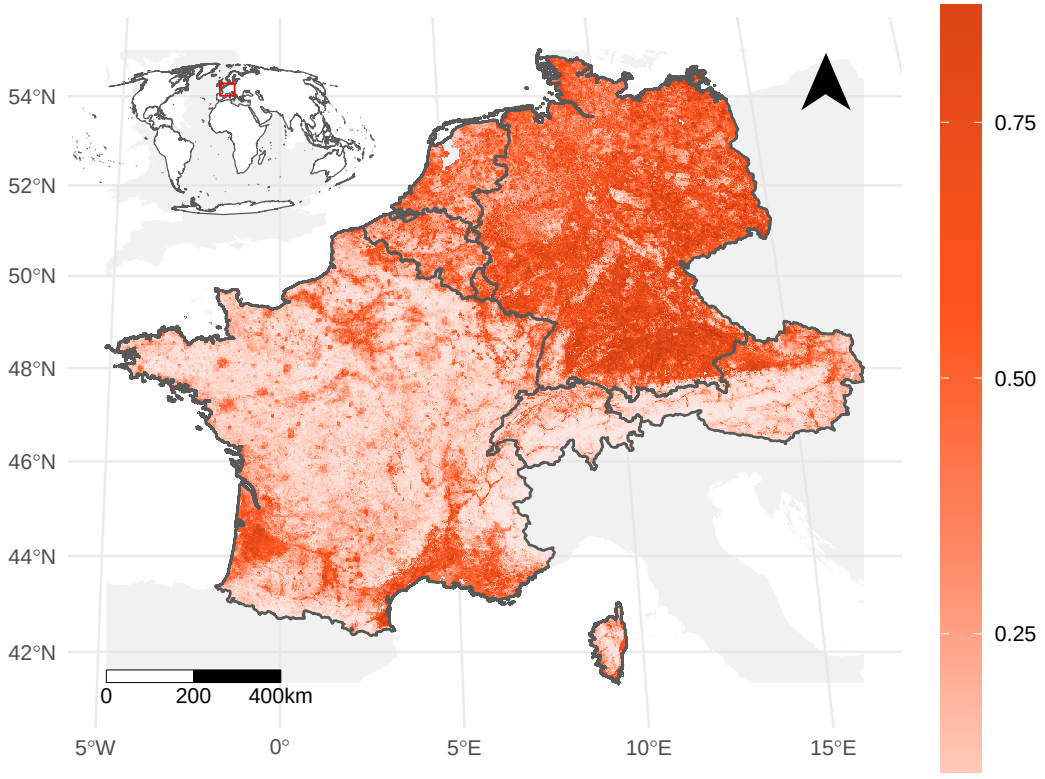

FIGURE 2.2: Solar PV probability layer generated with Random Forest for Central Europe (10-fold, 5-repeat; mean accuracy = 0.776, mean $\kappa = 0.5518$, $N = 3{,}327$).

The usual latitudinal divide between solar PV and wind is evident in Figures 2.2 and 2.3. Wind installations are much more likely to be found in the Netherlands, Belgium, and northern France and Germany. Solar PV is more likely to be found in southern France. However, also evident is that solar PV is much more likely to occur in Germany, especially the South. The impact of the slopes of the Alps are shown with the stark divide in likelihood for solar

PV across northern Austria. High likelihood for wind installations appears heavily correlated with the northern coasts of Central Europe, and the Alps are also visible with very low wind likelihood across Switzerland, southeast France and southern Austria.

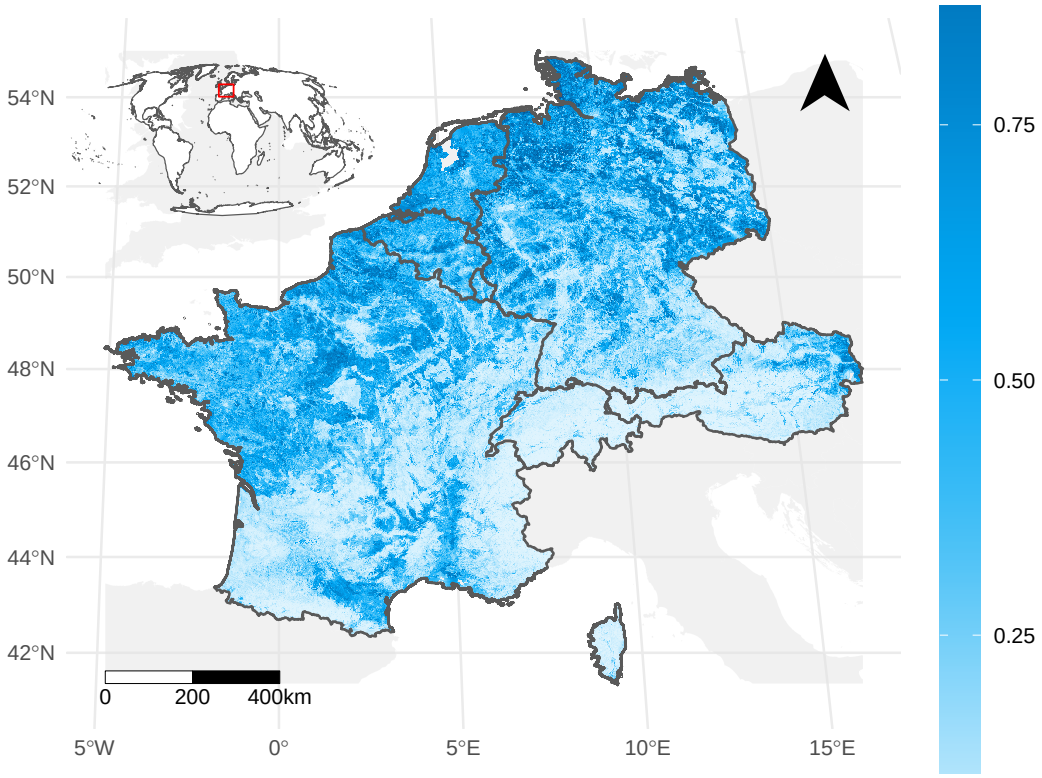

FIGURE 2.3: Wind probability layer generated with Random Forest for Central Europe (10-fold, 5-repeat; mean accuracy = 0.786, mean $\kappa = 0.5719$, $N = 2{,}624$).

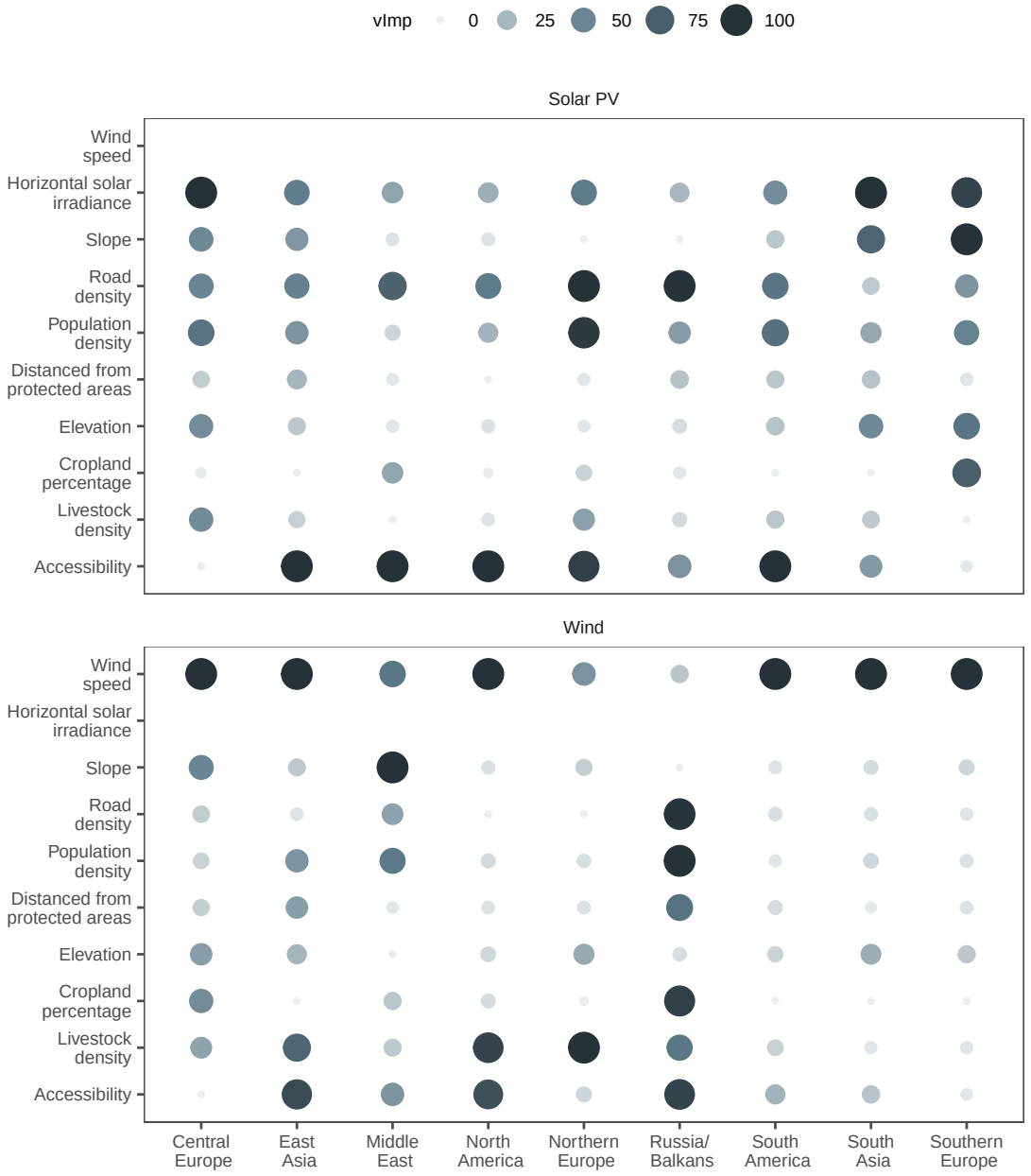

FIGURE 2.4: Variable importance values from Random Forest models

Variable importance values from the Random Forest models for all regions are shown in 2.4. For solar PV, accessibility appears to be the most important variable across all model regions; horizontal solar irradiance is largely unimportant for all regions bar Central and Southern Europe, and South Asia. Road density also appears to be an important predictor across the majority of model regions. For wind, encouragingly, wind speed appears to be the most important predictor in all but Russia and the Balkans. Accessibility is not as universally important as with solar PV, although for important predictors for all model regions, accessibility, wind speed and livestock density appear to be the most influential. Despite

their traditional use in energy suitability models, slope and elevation appear less important for predicting cells containing installations.

Both Central European Random Forest models, using the newly generated spatially explicit data, outperformed our reference models that used only the (solar and wind) DPIs as predictors (Accuracy = 0.672, κ = 0.3419, N = 5,341 for solar PV and Accuracy = 0.4868, κ = -0.02624, N = 5,292 for wind). The reference models perform surprisingly well, but this is likely reflective of the somewhat bimodal nature of the DPI data. For example, for wind in Central Europe, a large portion of the land is missing data. Where data are not missing DPI values are uniformly high, with a mean DPI (excluding missing values) of 0.7882. Reclassifying the missing values to 0s lowers this mean DPI to 0.3306.

Globally, 78.44% of renewable installations occur in cells deemed *suitable* for that technology, with a gentle slope or low elevation (<30% or <3,000m respectively) (Oakleaf et al., 2019). Thus 21.56% of installations worldwide are present in grid cells that were classified by Oakleaf et al. (2019) as *unsuitable* for development of that renewable energy at 1-km^2 resolution.

Using Germany as a case study, 81.62% of wind and solar installations were not considered in the original analysis but are present in grid cells deemed suitable for development. As the maximum slope and elevation for the installations present in *unsuitable* cells were 23.87% and 895.6 respectively, they were likely excluded either due to unsuitable land cover or for other installations being present in the cell. However, as the study only considered US wind turbines and no solar PV (Section 2.3.5), they were most likely excluded due to unsuitable land cover. Wind and solar DPI coverage for Germany can be seen in Figure A.2, Appendix A.

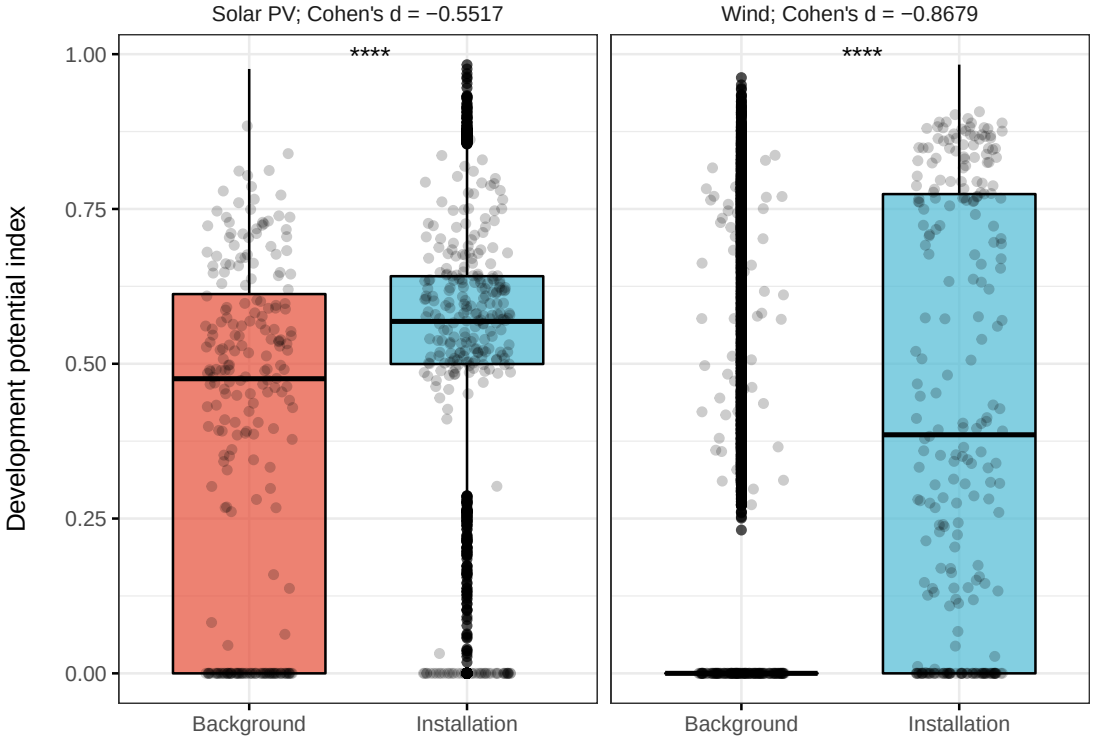

FIGURE 2.5: Boxplots showing differences in development potential indices for installations (n = 12,043 for solar PV, 12,581 for wind) versus background points (n = 11,111 for solar PV, 11,595 for wind). Jittered points represent random samples of 1,000 points from the data for readability. Values for Cohen's d are also presented, where effect size $|d| < 0.2$ is "Negligible", $|d| < 0.5$ is "Small", $|d|$ is "Medium", and $|d| \geq 0.8$ is "Large" (Cohen, 1992). *Note*: *ns* p>0.05; $*p \leq 0.05$; $**p \leq 0.01$; $***p \leq 0.001$; $****p \leq 0.0001$.

Pairwise comparisons of DPIs between 1-km^2 cells with wind or solar installations, and a random sample of background values (simulating a random distribution of installations, with missing values reclassified as 0) both exhibit low p values (t-test, two-tailed). However, this will mostly be driven by the large sample size. Cohen's d suggests that only installation cells for wind have a notable effect on DPI (-0.8679, "Large"); the effect size for solar PV installations is -0.5517, "Small". Cells with wind installations have a larger wind DPI value than a random selection of cells (Figure 2.5).

2.4.2 Future conflict between expansion areas for renewable energy and biodiversity conservation

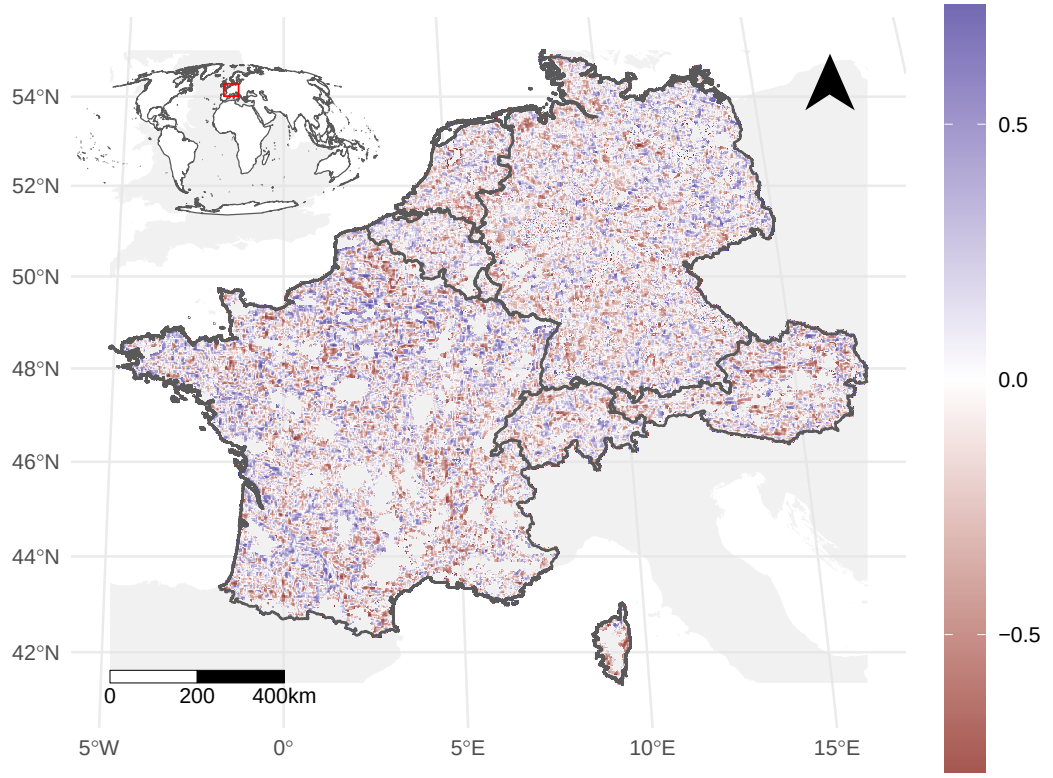

FIGURE 2.6: Local raster correlation between (Pouzols et al., 2014) cell rankings for the global 2040 land use scenario and solar probability layer generated in Figure 2.2. For each cell, Pearson's correlation coefficient is calculated for the 9 by 9 cell neighbourhood surrounding the cell. Global correlation coefficient for the region was 0.07826, based on a systematic sample of 1,000 cells. Cells with protected areas are masked, as well as cells with solar PV installations already.

Local Pearson's correlation coefficients for solar PV and the protected area priority expansion areas (global 2040 land use scenario) from Pouzols et al. (2014) are shown in Figure 2.6. The global coefficient for the whole region, using a systematic sample of 1,000 cells, was 0.07826. For the other study regions, global correlation coefficients range from -0.3418 to 0.1227 for solar PV and from -0.1782 to 0.2053 for wind. Figure 2.6 suggests that there are no notable regional-scale spatial relationships between priority areas for biodiversity conservation and priority areas for renewable energy in Central Europe.

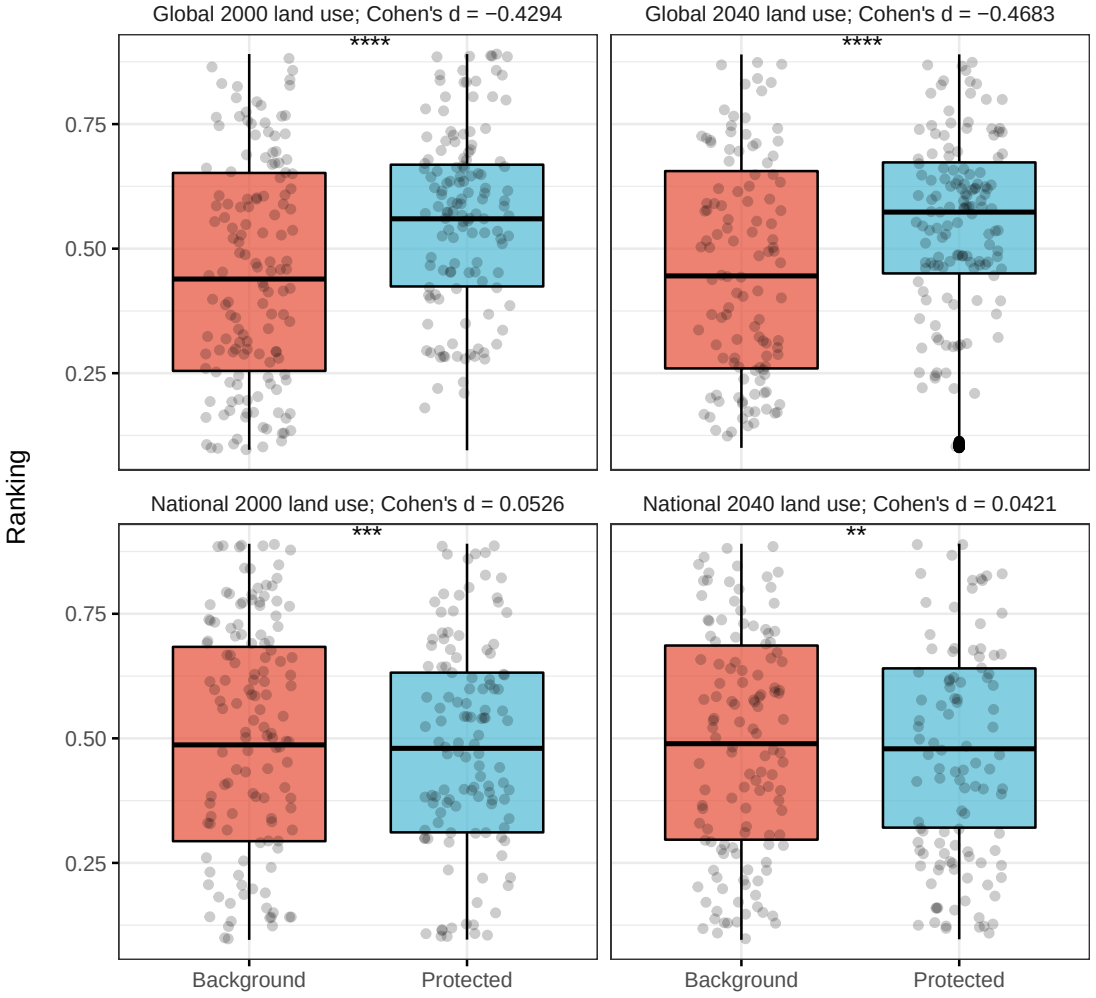

FIGURE 2.7: Boxplots showing differences in mean cell ranking of protection (n = 10,000) versus background points (n = 10,000) for the four scenarios presented in Pouzols et al. (2014). Jittered points represent random samples of 1,000 points from the data for readability. Values for Cohen's d are also presented, where effect size $|d| < 0.2$ is "Negligible", $|d| < 0.5$ is "Small", $|d|$ is "Medium", and $|d| \geq 0.8$ is "Large" (Cohen, 1992). *Note*: *ns* p>0.05; $*p \leq 0.05$; $**p \leq 0.01$; $***p \leq 0.001$; $****p \leq 0.0001$.

Analysis of protected areas post-2013 and the Pouzols et al. (2014) priority expansion area data suggests that the identified priority expansion areas are a good predictor of future protected area designation. A background sample of 1-km^2 cells not protected since 2014 form a randomly dispersed distribution with respect to their rankings for priority expansion. However, cells protected since 2014 exhibit a significantly higher ranking for global biodiversity conservation versus nationally (+0.09942 in global ranking, $p < 0.001$ – Figure A.1 in Appendix A), i.e. generally, 1-km^2 cells protected since 2014 do more for biodiversity conservation than if they were designated randomly (one of the most important findings in the Pouzols et al. (2014) paper was that biodiversity conservation was more effective if protected areas were designated *globally* as opposed to *nationally*). All four scenarios present very low p values (t tests, two-tailed) when comparing cells protected since 2013 and those

	pa	kba
(Intercept)	476.50	453.19
	(247.36)	(268.62)
re_area	−447.85**	−1046.30***
	(151.14)	(262.01)
land_area	−103.85*	−97.78
	(47.76)	(52.24)
re_area:pa_area	87.41***	
	(22.44)	
re_area:kba_area		148.89***
		(32.58)
R^2	0.49	0.43
Adj. R^2	0.45	0.40
Num. obs.	41	62

$^{***}p < 0.001$; $^{**}p < 0.01$; $^{*}p < 0.05$.
Note: standard errors are in parentheses; re_area denotes the total area of wind and solar installations in the country, land_area the total land area of the country, and pa_area and kba_area the total areas of protected areas and Key Biodiversity Areas respectively.

TABLE 2.1: Simple linear model explaining the area of overlap between protected areas and renewable energy installations by country.

not (Figure 2.7). Cohen's *d* values for all comparisons suggest that only protected cells in the global 2000 and 2040 land use scenarios demonstrate a notable effect on cell ranking – "small", as opposed to "negligible" for national scenarios (Cohen, 1992).

2.4.3 Current wind and solar PV spatial overlap with important conservation areas

The results of two simple linear models explaining the overlapping area of renewable energy and conservation areas by country are presented in Table 2.1 (Protected areas $R^2_{\text{adj}} = 0.4463$ and KBAs $R^2_{\text{adj}} = 0.3956$). Figure 2.8 presents the standardised residuals for protected areas (2.8a) and KBAs (2.8b). Wilderness area overlaps occurred in too few countries to provide a meaningful sample size for modelling.

The five countries with the highest standardised residuals for the protected areas model were Spain, Portugal, Brazil, Uzbekistan, France, whereas for KBAs they were China, Spain, Venezuela, Germany, Guadeloupe. Spain had the highest standardised residual for the protected areas model by a factor of 2.421, whereas China had the highest standardised residual in the KBAs model by a factor of 2.443. The five countries with the lowest standardised residuals in the protected areas and KBAs models respectively were Poland, United Kingdom, Martinique, China, Australia and Australia, Japan, India, Brazil, United States.

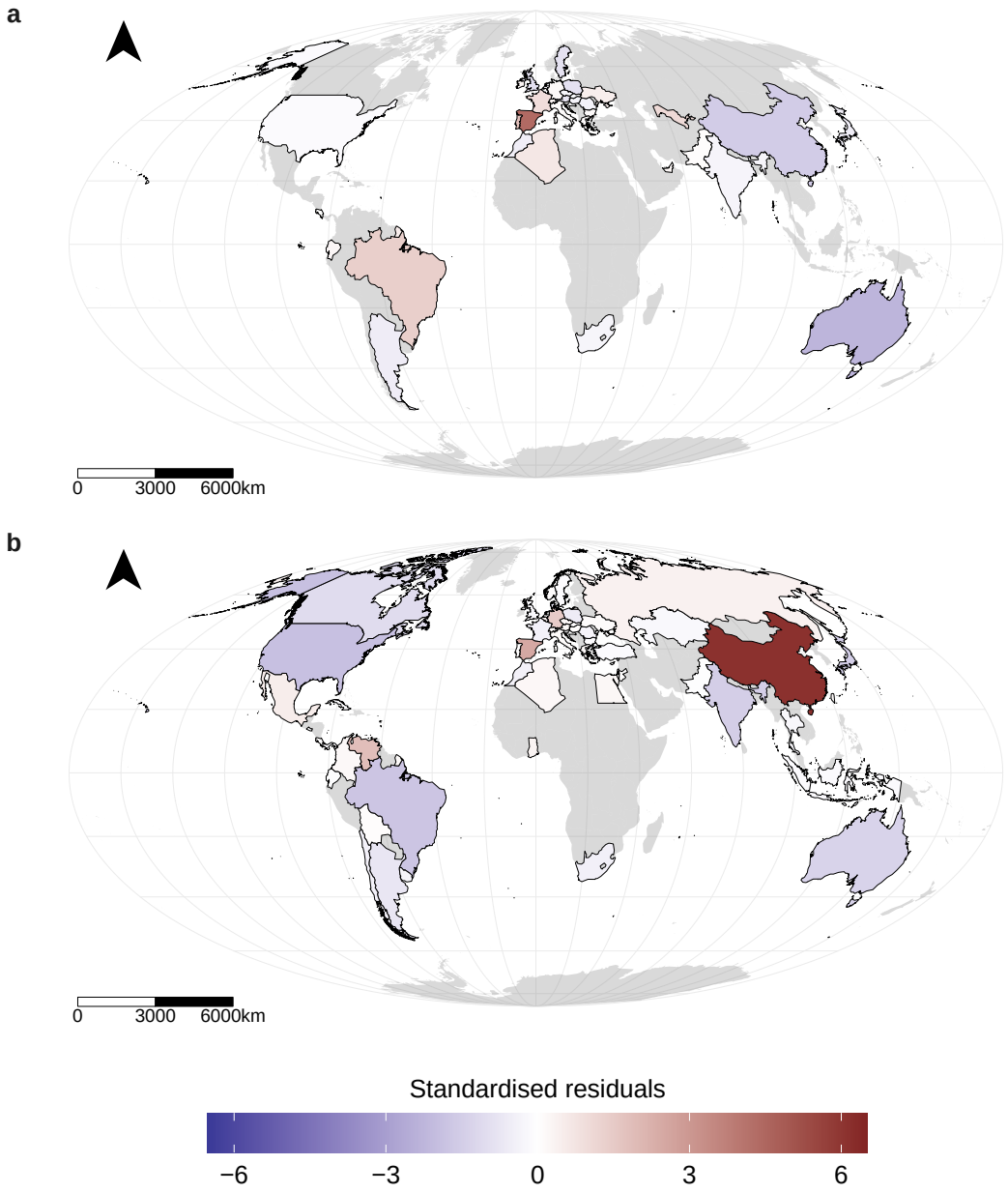

FIGURE 2.8: Standardised residuals for overlap between protected areas (a), Key Biodiversity Areas (b) and wind and solar installations. A positive residual indicates more overlap than expected, and a negative residual indicates less overlap.

Standard spatial overlaps of renewable energy and important conservation areas largely corroborate the findings of Rehbein et al. (2020): I find that 3,666 wind and solar PV installations out of a total of 24,624 (14.89%) occur within areas of conservation priority (Table A.1 in Appendix A). Protected areas and KBAs contain the majority of these overlapping installations (1,354 and 2,266), with wilderness areas containing 46 installations. The majority of overlaps occur in areas with no official IUCN designation ($n = 367$). Although the next highest number of areas containing installations are management categories V and VI, where limited development is allowed ($n = 169$), there are still overlaps in areas designated

management category I-IV ($n = 52$), where no development activity should occur (although the installations tend to be <100MW – see Table A.2 and Figure A.3 in Appendix A).

Similar to Rehbein et al. (2020), I find that when area is not considered, the vast majority of conservation areas containing renewable energy installations (820 or 76.78%) occur in Europe (Northern, Central and Southern) (Table A.3). 3 of the 7 wilderness areas containing renewable energy installations occur in North America (also the region with the largest area of wilderness globally – 8.513 million km^2).

Analysis of PADDD events and renewable energy locations led to only 8 overlapping records: 6 from validated PADDD polygons (all from the USA), and 2 from buffered point data (one from Canada and one from China). Although all instances were attributed the cause "Infrastructure", none of the records appeared to be directly linked to *renewable energy* infrastructure development. The 6 records of overlap in the USA were all examples of PADDD associated with Bill H.R. 399, *"To require the Secretary of Homeland Security to gain and maintain operational control of the international borders of the United States, and other purposes"*. Sec.13 of H.R. 399 concerns the *"Prohibition on actions that impede border security on certain Federal land"*, allowing the construction of infrastructure (roads etc.) to facilitate operation of border patrols.

The Canadian PADDD event allows various forms of research to be conducted by industry (and others) for infrastructure development, while the Chinese record does not have associated metadata elaborating the cause of the area downsizing.

2.5 Discussion

2.5.1 Inclusion of the latest global dataset of wind and solar installations improves probability surfaces

Differences in the siting of wind and solar PV installations are borne out in the results for onshore wind and solar PV probability surfaces (Figures 2.2 and 2.3). Probabilities in France display obvious geographical differences in development likelihood: wind installations are far more likely in the northwest of the country, where wind speeds are higher, whereas solar installations are much more likely in the south of the country, where the resource potential for solar irradiance is higher. However, using actual location data for infrastructure also appears to tease out differences in policy between countries: Germany is far more likely to develop solar installations irrespective of latitudinal drivers as a major renewable energy powerhouse (Eichhorn et al., 2019; Dunnett et al., 2020 and Chapter 1). This could suggest that as countries push for expansion of renewable energy technologies, siting of installations becomes less important as the market expands and economies of scale take hold.

Both Central European Random Forest models outperformed the reference models that used only the DPI values as predictors, suggesting that the inclusion of socio-economic variables, as well as actual location data, can help improve the identification of likely expansion areas. The reference solar PV model likely outperformed the wind model due to the larger number of constraints used to create the wind DPI (Section 2.3.5). This meant that a larger area of land was artificially given a value of 0 which likely increased the chances of false negatives.

The probability layers depend heavily on the assumption that historic siting of renewable energy predicts its expansion. In rapidly changing socio-ecological conditions, past predictors of land use change are unlikely to remain relevant for long (Ellis et al., 2013; Eigenbrod et al., 2020); however, as the renewable energy infrastructure estate is still arguably in its infancy, this assumption appears justified. There is also research to suggest that socio-economic drivers cause renewable energy to become clumped in "*hazard havens*", where planning permission for projects is more likely for those close to other similar developments (Blowers, 2013; Roddis et al., 2018).

The findings for Random Forest variable importance show that for wind, wind speed is by far the biggest driver of installation placement (except for Russia and the Balkans where socio-economic drivers – road and population density, accessibility – are more important). For solar PV, on the other hand, socio-economic drivers dominate, and solar irradiance appears less important for solar installation placement. It has been suggested that distance from a network connection is more important for siting solar than wind because of construction costs associated with higher land requirement per GWh (Watson & Hudson, 2015)[1]. Construction costs are, however, extremely difficult to estimate, especially at anything but an extremely localised scale, as they involve a large number of assumptions (Pogson et al., 2013). Despite this, it has been suggested that energy prices will play an important role in shaping global land use in the coming decades (Steinbuks & Hertel, 2013). These factors likely explain the increase in accuracy of the Random Forest solar model over the baseline DPI model. It may also be a result of the ease with which solar can be mounted on surfaces other than the ground. While this can also be the case for small wind turbines, it is currently not feasible to mount large wind projects in a similar way.

Livestock density also has a notable impact on placement of wind installations, although it is impossible to attribute this effect to livestock land uses attracting wind projects, or livestock being introduced to wind projects in an attempt to share land use. It has frequently been suggested that the space between wind turbines can be used for other land uses, especially livestock and farming, although more research is required to determine which land use typically drives the other (Hertwich et al., 2014; United Nations Convention to Combat Desertification, 2017).

[1]However, the authors appear to confuse the results of Fthenakis & Kim (2009), who specify wind requires *more* land per GWh than solar PV does (*"The land required for a GWh of electricity from wind turbines typically is larger than that needed for the solar-electric cycle"*, Fthenakis & Kim, 2009, p. 1469).

Clearly, solar PV and wind distributions differ on account of socio-economic variables not traditionally included in traditional calculations of development potential. It has been shown that, at least in the UK, the largest driver of an onshore wind project's planning permission being granted is the size of wind turbines: the larger the capacity of wind turbines in a project, the more likely the project is to be accepted (Harper et al., 2019). This, combined with other recent work in the UK that found *"aesthetics and visual impacts are strongly associated with planning outcomes for both onshore wind and solar farms"* (Roddis et al., 2018, p. 360), suggests that larger, more distant wind projects are more likely to become operational. More remote projects are more distant from extant electricity transmission networks, an oft-overlooked necessity for expanding renewable energy (Heard et al., 2017). Distance from transmission networks and size of project means these wind projects would seek to maximise the resource efficiency of the project, which may explain the higher DPI values for wind. Solar PV, on the other hand, has on average a much smaller spatial footprint than wind ($0.07593 < 6.728 km^2$ (Dunnett, 2020)), and is more likely to be accepted on poor quality agricultural land (Roddis et al., 2018). This allows solar PV to be sited closer to extant electricity transmission networks on poor quality land that may drive costs down so that they need not be recouped so aggressively by resource efficiency.

Numerous previous studies have attempted to identify priority areas for renewable energy expansion (Kiesecker et al., 2011; Pogson et al., 2013; Santangeli et al., 2015, 2016; Enevoldsen et al., 2019; Waldman et al., 2019). Here, I used one of the most recent studies that provides fine resolution (1-km^2) global data with a consistent methodology for 13 different sectors (Oakleaf et al., 2019). The results confirm that when using only resource potential with no socio-economic variables and limited information on current distribution, the methodology used to create the DPI layers does not adequately capture the global solar PV and wind estate (Figure 2.5 and Figure A.2 in Appendix A). Approximately 30% of wind and 12.81% of solar installations are present in cells given a DPI, despite Oakleaf et al. (2019) deliberately attempting to exclude cells with existing infrastructure in them – any cells with $\geq$ 3 turbines (Online-only Table 2). Excluding the cells these installations occupy may have had significant impacts on the ranking of cells for development potential (see Figure A.2 in Appendix A).

Existing solar PV installations were not excluded in the original analysis *"given lack of global data"* (Oakleaf et al., 2019, p. 2). This means that any solar PV installations in the novel dataset used here not given a DPI were excluded for one of the *other* constraints: slope >30% or unsuitable land cover (*ibid*, Online-only Table 2). Furthermore, only wind turbines in the United States were used for exclusions (Section 2.3.5), thus it can be assumed that wind installations outside of the United States were excluded from the analysis for other constraints as well: average wind speed $<6 ms^{-1}$, slope >30%, elevation >3,000m and unsuitable land cover. For the German case study, only 5 of 389 wind installations excluded from the Oakleaf et al. (2019) analysis possess average wind speeds of below $6 ms^{-1}$ (Figure A.2, Appendix A). Max elevation was 895.6m and max slope was 14.97%; both comfortably below constraint

levels. Unsuitable land use is left – wetlands, rock/ice and artificial areas – as the reason for exclusion. This highlights the issue with land suitability maps for predicting renewable energy expansion areas: even 1-km^2 resolution is not resolved enough to capture the intricacies of land cover for renewable energy installations. The median area for solar PV installations (over 1 hectare in panel area) is only 0.05615km^2; easily masked by a resolution of 1-km^2. As a result, large swathes of land are being excluded from feasibility analyses unnecessarily (see Pogson et al., 2013; Santangeli et al., 2015).

Wind and solar PV installations not excluded from the original Oakleaf et al. (2019) analysis allow the evaluation of the DPI surfaces for predicting "unseen" renewable energy developments globally. The results show that the DPIs for wind predict new installations more accurately than solar (Cohen's *d* |-0.8679| > |-0.5517|, Figure 2.5). Solar PV installations only demonstrate a small effect size on the DPI value over a random distribution of background points. This suggests that of the two renewable energy technologies, solar PV is less driven by purely resource potential – other than development constraints, the DPIs were calculated based on resource potential alone – and echoes the results for the Random Forest variable importances.

2.5.2 Do the novel renewable energy Random Forest layers suggest future conflict with biodiversity priority areas?

Renewable energy is consistently highlighted as a threat to areas of conservation importance (Santangeli et al., 2015, 2016; Gasparatos et al., 2017; Sutherland et al., 2017; Baruch-Mordo et al., 2019; Holland et al., 2019; Rehbein et al., 2020). However, both an expansion in renewable energy infrastructure and a concomitant expansion in areas for biodiversity conservation are crucial for the sustainable future envisioned in global agreements. Thoughtful planning of renewable energy installations may alleviate some of the pressure on lands important for biodiversity (Kiesecker et al., 2011, 2019; Baruch-Mordo et al., 2019; Oakleaf et al., 2019), but studies tend to suggest that the expansion of renewable energy is a *de facto* threat to areas of conservation importance (Santangeli et al., 2015; Gasparatos et al., 2017; Rehbein et al., 2020). Rehbein et al. (2020) quantify the threat, suggesting that *"the number of active renewable energy facilities inside important conservation areas could increase by 42% by 2028"* (p3046). However, this does not include the inevitable *expansion* of protected areas, alongside the continued expansion of renewable energy. The results here suggest, at least on a regional scale, that there is no significant association between best predictions for the expansion of protected areas (Figure 2.7 and Figure A.1 in Appendix A) and best predictions for solar PV and wind (Figures 2.2 and 2.3). Global correlation coefficients for all regions were low and suggest that there is no reason to believe, using these data, that the overlap of renewable energy and protected areas will increase markedly on the rates shown in Rehbein et al. (2020). Local correlation results for Central Europe (Figure 2.6) suggest there is no discernible regional relationship. Some measure of overlap should

be seen as inevitable as available land diminishes for varying sustainability goals (Scheidel & Sorman, 2012), and especially as a number of IUCN protected area categories explicitly allow infrastructure development (Dudley et al., 2013).

As suggested in previous sections, these results may be a result of data resolution: both wind and solar PV installations operate at spatial scales below 1-km^2; as can protected areas. However, the results here refute suggestions in Santangeli et al. (2015) that overlap between energy resource potential and species richness promote conflict between the two. Renewable energy installations operate in complex environmental *and* socio-economic envelopes that cannot be easily predicted on resource potential alone. This analysis also presents a modest expansion in protected areas from 2014 to present (659,556km^2). Policy targets emerging from the 15th meeting of the Conference of the Parties (COP 15) to the Convention on Biological Diversity and the 26th session of the Conference of the Parties (COP 26) to the UNFCCC – due to take place in 2020 but delayed due to the COVID-19 pandemic – may require a much larger protected area and renewables expansion which may drastically alter the drivers of both distributions accordingly.

As global land use continues to become squeezed between agricultural industrialisation, urbanisation, energy production, and a plethora of other uses, conservation scientists have looked to find the most efficient demarcations to preserve dwindling global biodiversity. There have been myriad studies looking to identify the 'silver bullet' for biodiversity area conservation: global species richness, endemism and threat hotspots (as discussed in Orme et al., 2005), biome hotspots (Hoekstra, Boucher, Ricketts, & Roberts, 2004), the last remaining large tracts of land free from human influence (Allan et al., 2017), areas *of* human influence (Martin et al., 2014), evolutionary distinctiveness (Safi, Armour-Marshall, Baillie, & Isaac, 2013), cost-effectiveness (Carwardine et al., 2008), or a combination of species richness, ecoregion and land use (Pouzols et al., 2014). The results here present an evaluation of how well global conservation land planners have emulated the priority areas for protected areas expansion identified by Pouzols et al. (2014) for the 1,344 sites designated in the six years since the research was conducted. Of the sampled grid cells, global rankings were consistently higher for the protected cells than the random distribution (Figure A.1 in A). This is an encouraging result: Pouzols et al. (2014) identified that if global biodiversity targets were implemented nationally, as opposed to globally, the average protection of species ranges and ecoregions would drop by two thirds.

Both global ranking scenarios were, on average, ranked higher than a random distribution of cells (Figure 2.7). All four scenarios displayed significantly different ranking distributions, but only protected cells in the two global scenarios had anything but a negligible effect size on mean ranking. This suggests that protected areas designated since June 2013 (the release date of the data used by Pouzols et al. (2014)) have been sited with an eye for species richness and ecoregion representation. Furthermore, the global 2000 land use scenario was the scenario with the potential to protect the greatest quantity of vertebrate species ranges and ecoregions, followed by global 2040, national 2040 and then national 2000.

Conservation policy practitioners have been accused historically of setting *"unrealistic and politically challenging protection targets"* (Di Minin & Toivonen, 2015, p. 637). These results show that, at least on average, increased coverage targets do not necessarily beget 'paper parks' – protected areas in only name – and that the Pouzols et al. (2014) study identified priority areas well. However, as Figures A.1 (Appendix A) and 2.7 show, there are still examples of very low ranking (e.g. <0.25) 1-km^2 grid cells being protected. This could provide evidence for poor siting of protected areas: conservation effort has been proven to be unequally distributed across the human population density spectrum (Martin et al., 2014). Alternatively, it could be an artefact of the data resolution as with the land cover exclusions in Oakleaf et al. (2019) – although I excluded protected areas < 5km^2 to attempt to limit this effect, there may well still be protected areas < 10km^2 with riverine shapes protecting slivers of suitable habitat in an otherwise unsuitable landscape.

2.5.3 Is this level of conflict reflected in recent studies looking at renewable intrusion into areas of importance for biodiversity?

These results corroborate the results of Rehbein et al. (2020) in that they show that already there is only one category of protected area currently untouched by renewable energy infrastructure globally (Category Ia – Figure A.3, Appendix A). 3,666 wind and solar PV installations out of a total of 24,624 (14.89%) occur within areas of conservation priority (Table A.1). The numbers for Table A.3 and Table A.2 are also strikingly similar to Rehbein et al. (2020).

While the exact impacts of renewable energy technologies on biodiversity are far from well-known, bird and bat mortality of wind turbines is one of the most evidenced impacts (Thaxter et al., 2017) and it is worrying to note that 1,090 utility-scale wind installations currently occur in KBAs, 79.69% of which are specifically designated as IBAs – a network of sites that are significant for the long-term viability of naturally occurring bird populations.

However, it is important to frame any overlap analysis in the context of land areas, especially when global protected areas make up 14.41% of global land area, KBAs 13.9% and wilderness areas 20.17%. The percentage areas also reveal another problem with relying on absolute overlap quantities: there is significant overlap between protected areas, KBAs and wilderness areas to the extent that some US sites are designated as all three. A country with limited land area, a large protected area network and extensive renewable energy infrastructure would find it much harder to limit the overlap than one that was land-rich. This is exemplified by the majority of absolute overlaps occurring in Southern, Northern and Central Europe – regions with large renewable energy estates and an extensive protected area network. The results for simple linear models explaining the overlap of renewable energy and areas of conservation importance (Table 2.1 and Figure 2.8) provide some nuance to the absolute overlaps shown by Rehbein et al. (2020) and emulated in Table A.3, Appendix A. Spain presents by far the largest standardised residual for the protected area overlap model, with 201 renewable

energy installations in 98 different protected areas. However, only 7 of these protected areas were not in the categories of Not Assigned, Not Applicable or Not Reported. As the IUCN emphasise, this does not mean that these areas are any less important (Dudley et al., 2013), but rather protected areas can be categorised thus for any number of reasons and would need to be investigated on a country by country basis. Brazil's inclusion in the top five standardised residuals is unfortunate: Brazil has in the past been identified as one of the world's most biodiversity-rich countries (e.g. Mittermeier, Mittermeier, & Robles Gil, 1997). It is also frequently referred to in the context of *BRICS*, or Brazil, Russia, India, China and South Africa – five major emerging economies likely to require a significant increase in energy demand over the coming decades.

In the KBAs model, China presented the highest standardised residual by a factor of 2.443, despite presenting one of the lowest in the protected areas model. This is likely an artefact of China withdrawing their national protected area data from the WDPA as identified by Rehbein et al. (2020, p. 3042). These results show that China currently operates 326 renewable energy installations in 2 different KBAs. Both this result and that from the protected area model are likely underestimations as renewable energy data for China appears more sparse than they should be (Dunnett et al., 2020). For this reason, renewable energy expansion may threaten areas of conservation importance in China, but the country needs more complete data in order to make a proper assessment. The United Kingdom, despite its relatively small size and extensive renewable energy and protected area estates, appears in the lowest standardised residuals for the protected area model, demonstrating that overlap can be avoided with strict multi-use land planning.

While the number of overlaps with wilderness areas presented here was too small to provide a useful sample for modelling, the numbers roughly correspond to the findings of Rehbein et al. (2020): 5 of the 7 wilderness overlaps occur in North America and East Asia. This is a surprisingly low figure, especially considering wilderness areas in North America alone represent 8.513 million km^2 of undeveloped land, and previous research has suggested that energy infrastructure encroachment into wilderness areas may threaten previously untouched biodiversity (Santangeli et al., 2016; Trainor et al., 2016; Laurance & Arrea, 2017; Oakleaf et al., 2019; Rehbein et al., 2020). For comparison, 2.562 million km^2 of protected areas in the USA and Canada contain 173 overlapping installations. The dearth of installations in North America's large expanse of wilderness may be a reflection of the technical difficulties of remote renewable power; previous studies have had to heavily constrain renewable suitability layers by distance to settlements to account for this (Santangeli et al., 2015, 2016), whereas others have questioned the feasibility of some renewable projections on account of weak transmission and ancillary services proposals (Heard et al., 2017).

It has also been suggested that renewable energy expansion may threaten areas of conservation importance through protected area downgrading, downsizing and degazettement (PADDD); Rehbein et al. (2020), citing Mascia & Pailler (2011) and Symes, Rao, Mascia, & Carrasco (2016), suggest that installations within strict protected areas *"strongly predict*

subsequent [PADDD], which leads to worse biodiversity outcomes" (p.3047). However, the results here, using the best available PADDD data (Golden Kroner et al., 2019), did not identify any PADDD events that were irrefutably caused by the siting of renewable energy installations. All 6 PADDD events in the United States were driven by issues of border security and unlikely to be associated with the nearby renewable energy installations. The instance in China does not have any metadata associated with it, while the Canada PADDD event allows research for infrastructure development with no concurrent change in IUCN Category. With 1,354 instances of well-established renewable energy installations in protected areas, this is a small figure (0.517%). Of course, renewable energy installations could be a contributing factor to one of the other primary causes of PADDD as described in Golden Kroner et al. (2019), but currently there is no way of providing sufficient evidence for this assertion. Regardless, best evidence suggests that renewable energy installations *per se* do not predict subsequent PADDD.

2.6 Conclusion

I have evaluated the energy and conservation literature's ability to forecast distributions, showing that although areas of conservation importance can be predicted relatively well, forecasting solar PV and onshore wind installations requires increased knowledge of the extant distribution in order to take account of complex socio-economic drivers of distribution. New data can help hone researchers' ability to forecast potential conflicts in global land use, as evidenced by the Random Forest probability layers generated here. Use of such data in this analysis suggests that although any level of overlap between infrastructure and areas specifically designated to protect biodiversity against such threats is unfortunate, there is no reason to believe that conflict between biodiversity conservation and *renewable energy* infrastructure will intensify if current moderate energy and conservation development patterns continue. I have also presented a more nuanced analysis of the current extent of overlap between the global wind and solar PV estate and areas of conservation importance, showing that the number of spatial overlaps is largely in keeping with this level of conflict. Careful land use zoning is still very much required, and it is still unclear what the effects of a much more expansive extension in required areas would be, but the evidence presented here suggests that under near-recent historical trends, there is no reason to suggest that any conflict between renewable energy and biodiversity conservation will intensify.

This page intentionally left blank.

Chapter 3

Opportunities arising from projected land change for the global expansion of renewable energy infrastructure

3.1 Abstract

Land cover and land use change remains one of the most important factors contributing to global environmental degradation. Humans have modified over half of the Earth's surface and there have been calls from some scientists to protect the other half of the Earth's surface against further modification. While technically possible, land scientists must develop a better picture of how competing demands on land may interplay and create opportunities to spatially couple development priorities. Sustainable land transitions have been achieved with sound policies and innovation. Renewable energy, required to rapidly expand to maintain global temperatures 2°C below pre-industrial levels, may be an excellent litmus test of the sustainable development concept given sufficient global data for land planning. In this study I present an updated land systems map for the year 2010 at 1-km^2 and 10-km^2 resolution that characterises human demand for urban area, livestock and food crops, and describe onshore wind and solar photovoltaic's place in these systems. Land changes are then projected to the year 2040 using the CLUMondo land use change model to identify opportunities for co-locating development of human impact. The 2010 land systems map is created in part with the aid of a novel cropland extent dataset generated from the highest resolution global data ever produced. I show that both renewable energy technologies are overwhelmingly associated with human land uses in 2010: solar photovoltaic with urban and peri-urban land systems, and onshore wind with intensively managed cropland. Both of these land systems see substantial increases in areas under a baseline scenario responding to demands for food crops, livestock and urban area for a burgeoning global population, suggesting that coupled

development of human land demands may help global ambitions to protect as much natural land as possible from modification.

3.2 Introduction

If Betty Jean Newsome were to rewrite James Brown's classic *It's a Man's Man's Man's World*, she might reference the fact that it is now undoubtedly a "*human's* world". We live on a planet predominately covered by human land uses, and since the latter half of the 20th century resource consumption and other socio-economic trends have rapidly increased in what earth system scientists refer to as "The Great Acceleration" (Steffen et al., 2015). Not only can significant human modification be demonstrated as early as 1000BC (Kaplan et al., 2009), but between 1700 and 2000, 55% of Earth's ice-free land was transformed into rangelands, croplands, villages and densely settled land uses (Ellis et al., 2010). Land use and land cover changes, hereafter referred to simply as "land change", are cumulatively a crucial driver of environmental change (Turner, Lambin, & Reenberg, 2007; B. McGill, 2015). The most important effect of this for our environmental stewardship is expansion of crop and pastoral land into undisturbed, "natural" ecosystems (Lambin & Meyfroidt, 2011). For example, during the 20 years from 1980-2000, more than half of new agricultural land came at the expense of intact forests, and another 28% from disturbed forests (Gibbs et al., 2010). The rapid takeover of the global land surface for human use has led to calls to redefine global biomes in terms of sustained and direct human interactions, often referred to as "anthromes" (Ellis & Ramankutty, 2008; Asselen & Verburg, 2012; Van Asselen & Verburg, 2013; Václavík et al., 2013). In the Ellis & Ramankutty (2008) classification, less than a quarter of ice-free land is considered "wild", with $>$36% of this classified as just "barren". This rapid expansion in human land use has taken its toll on the other inhabitants: land change and associated drivers are causing massive changes to Earth's ecological communities (Newbold, Hudson, et al., 2016a); human land uses and recovering secondary vegetation are poor at retaining species that characterise primary vegetation (Newbold, Hudson, et al., 2016b). There are hopes that land use intensification, especially with respect to agricultural systems, can be a crucial buffer that may mitigate anthropogenic impacts on undisturbed environments (Ellis et al., 2013). However, the same technology advances and globalisation lead to homogenisation of the global surface and outsourcing of impacts elsewhere (often from the developed world to the developing): for example, the electricity sector (Holland et al., 2019) and global food trade (Chaudhary & Kastner, 2016).

Within the three centuries from 1700-2000, the impact of land change on natural landscapes has increased 13-fold. However, within just one century climate change has amassed the same level of effect on natural landscapes (Ostberg et al., 2015). Worse still, climate change is itself exacerbated by land change (Kalnay & Cai, 2003). In an effort to combat what is seen as the most exigent threat to sustainable land management, multilateral environmental agreements have been signed encouraging signatories to expand the global

renewable energy estate (UNFCCC, 2016; UN, 2020). Renewable energy has significant impacts on land use, many of which are discussed in Chapter 1 and Chapter 2. By far the largest share of current global renewable energy capacity belongs to hydropower (44.7%), followed by onshore wind (23.4%) and solar photovoltaic (PV) (22.9%) (IRENA, 2019). Hydropower, while important, is excluded here because onshore wind and solar photovoltaic are consistently earmarked for immense expansion. For example, in IRENA's *Transforming Energy Scenario* for 2050 (IRENA, 2020a), hydropower is given a relatively modest increase of $\sim 66\%$ to 2,147GW global capacity whereas wind (onshore and offshore) and solar PV are given enormous increases of 1,076% and 2,118% to 6,044 and 8,519GW respectively.

Wind turbines and farms significantly impact volant species (Thaxter et al., 2017), while solar farms also pose problems for wildlife (Hernandez et al., 2014). Furthermore, renewable energy tends to exhibit much lower energy densities than conventional fuels (Smil, 2008, 2010; Trainor et al., 2016; Fritsche et al., 2017; United Nations Convention to Combat Desertification, 2017; Miller & Keith, 2018; Zalk & Behrens, 2018), and thus is at risk of exacerbating extant land change risks when increases of >2,000% are being considered. On tops of this, in order to limit carbon emissions and have some chance of keeping global temperature increases below 2°C above pre-industrial levels, bioenergy will need to represent a significant portion of global electricity generation – at the same time reducing the area of fertile land available for food production while still displaying the same negative environmental effects of mechanised agriculture (Slade et al., 2011; Fritsche et al., 2017; United Nations Convention to Combat Desertification, 2017; Donnison et al., 2020). Bioenergy area projections differ wildly (Slade et al., 2011; Fuss et al., 2018). The most optimistic of these point to large swathes of under-utilised agriculturally suitable land – crop margins and abandoned farmland – suggesting that large bioenergy increases can be achieved with little additional impact to the environment. This, however, is dependent on the optimal placement of crops: something that for other land uses is rarely the case (Chapter 2). Bioenergy, and bioenergy projections, have been extensively covered in the literature; onshore wind and solar PV, however, have not, and will be the focus of this analysis.

Despite these challenges, sustainable land use transitions can be achieved with sound policies and innovations (Lambin & Meyfroidt, 2011). Overly cautious research, following the precautionary principle, tends to warn of conflict between land uses as the baseline (Santangeli et al., 2015, 2016; Rehbein et al., 2020). However, as shown in Chapter 2, on current evidence there is no reason to suggest that conflict between renewable energy and areas of conservation importance is set to intensify with expanding commitments. There have also been suggestions that conflicts between renewable energy and natural land systems can be minimised by co-locating energy infrastructure on human land uses where productivity is minimally affected (Goetzberger & Zastrow, 1982; Marrou et al., 2013; Hassanpour Adeh, Selker, & Higgins, 2018; Barron-Gafford et al., 2019). Renewable energy is largely driven by social, not environmental, predictors (Chapter 2, Figure 2.4). As such, it is important

to know the current distribution of renewable energy with respect to predominant land systems. After this, changes in land system frequencies can be projected to see whether suitable lower-impact areas increase in frequency under baseline land change scenarios. Land change modelling is incredibly important to integrate into environmental scenarios (Titeux et al., 2016): land changes have been shown to have potentially detrimental effects on global efforts to slow biodiversity decline (Pouzols et al., 2014). There have already been efforts to investigate the role of differing environmental objectives on future land change (e.g. biodiversity conservation and carbon stock, Eitelberg, Vliet, Doelman, Stehfest, & Verburg (2016), or SDGs, Gao & Bryan (2017)), but there has been little spatially explicit analysis of how wind and solar PV might be affected by future land changes, due in part to the lack of consistent global data (Chapter 1).

Here, I address this shortcoming. Using newly-generated land systems data for the year 2010, based on the methodology used to create land systems for the year 2000 (Asselen & Verburg, 2012), I investigate the spatial association of onshore wind and solar PV with land systems and how this differs by region. I use a dynamic, spatially explicit land change model, CLUMondo, to project frequencies of the most commonly-associated land systems for the year 2040 and compare these to new regional renewable energy probability surfaces to answer the question: do projected land changes offer a continued opportunity to develop renewable energy in non-natural land systems?

3.3 Methods

3.3.1 CLUMondo

Land changes were simulated using CLUMondo (available from the Institute for Environmental Studies, Vrije Universiteit Amsterdam). CLUMondo is a spatially explicit, dynamic land change model that allocates land systems in yearly time-steps based on exogenously set demands for goods and services, spatial constraints, competition between land systems, and land system suitability. CLUMondo largely depends on the concept of land systems (Asselen & Verburg, 2012), socio-ecological systems classified using land cover composition, management intensities, and other spatially explicit socio-economic classifiers. Previously, these classifiers have been tree and bare ground cover, heads of livestock, built-up area, agricultural efficiency, and cropland cover. When defined globally, land systems vary regionally in their composition and drivers. They also produce different quantities of goods and services (e.g. tonnes of crops) regionally. Thus intensive cropland with cattle in the USA may average a much higher percentage of cropland per grid cell than the equivalent land system in Central America. All these data are required as inputs to any CLUMondo run.

The functioning of CLUMondo has been described in detail elsewhere (Van Asselen & Verburg, 2013; Pouzols et al., 2014; Eitelberg et al., 2016). At its simplest, CLUMondo induces

land intensification where available land is restricted, and land extensification where land is bountiful. This is tempered by four broad categories:

1. **Spatial restrictions**: for example, in the models presented here, conversion to agriculture is only possible in grid cells projected to be suitable for agriculture in the years 2011-2040. Cells were deemed suitable for agriculture if the cell value exceeded 0.33 (*Moderate* and *Highly suitable* as defined by the authors) (Zabel, Putzenlechner, & Mauser, 2014).
2. **Conversion resistance**: an urban land system is incredibly unlikely (short of global apocalypse) to convert to dense forest due to the capital investment required. Other land systems are more easily converted: open forest to mosaic crop and forest, for example. The presence of land systems with high conversion resistance also provides stability to the land system dynamics.
3. **Competition between land systems for provision of services**: when there is a large demand for crops, an agriculturally suitable cell is on balance more likely to convert to an agricultural land system than one that does not produce crops.
4. **Suitability**: logistic regressions produce empirical relationships between land systems and a suite of predictors (see Section 3.3.8). These produce probability maps for land systems that are used to assess the suitability of any given cell. Thus an urban land system is unlikely to crop up in cells with, for example, a prohibitively high median slope value. Suitability is also modified by neighbourhood parameters, so that peri-urban cells are more likely to appear around where peri-urban cells already are.

3.3.2 Land data

Global administrative areas were downloaded from the Database of Global Administrative Areas (available at https://gadm.org/), version 3.6. As this is primarily a *land* use assessment, I also used a water bodies mask in all conversions to raster data. I used the WWF Global Lakes and Wetlands Database (available at `https://www.worldwildlife.org/pages/global-lakes-and-wetlands-database`), Level 1. Level 1 comprises the 3,067 largest lakes (area $\geq 50\text{km}^2$) and 654 largest reservoirs (storage capacity ≥ 0.5 km^3) worldwide. The water body mask involved rasterising these polygon data to the required resolution using the `fasterize` **R** package (Ross, 2018), a high performance replacement for the standard `raster` function in the `raster` package (Hijmans, 2017). Rasterisation describes a process where data in vector format, e.g. the boundary of a country, are converted to a gridded format. Masking is a process where the mask (usually raster data as here, but not always) defines locations where a specific function is to be performed – here, cells in the water mask indicate cells where the data should be reclassified as NA/missing. This process minimised the chance of encountering missing values in some of the suitability data, where there would (correctly) be missing values where water bodies are found.

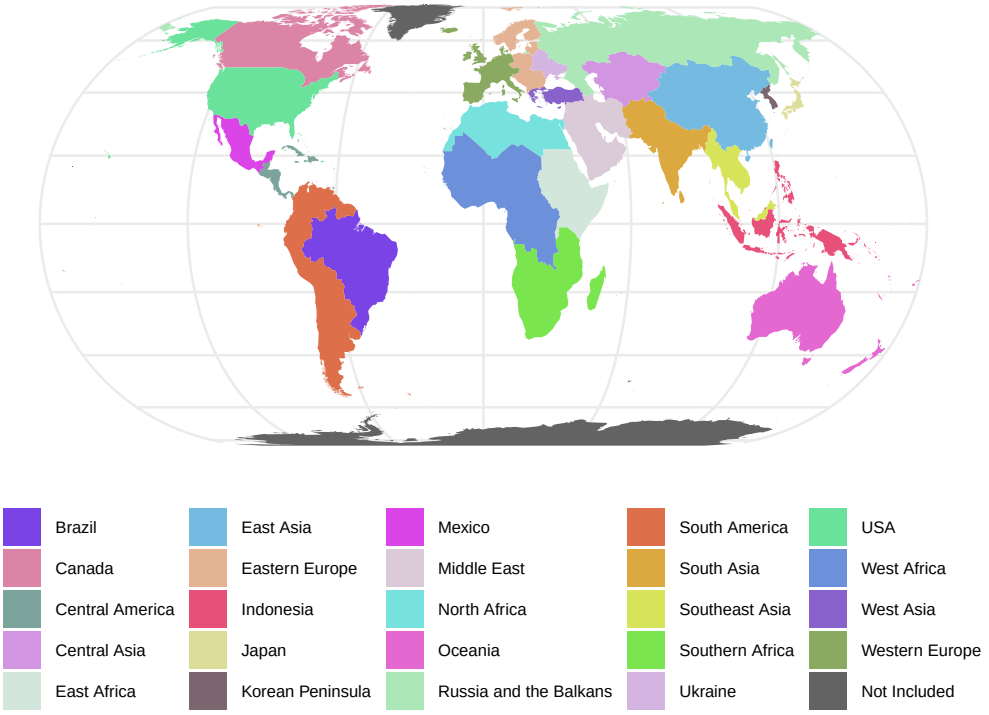

FIGURE 3.1: The 24 model regions used in this analysis. Greenland and Antarctica are excluded. Note that *Ukraine* includes Moldova and Belarus, *West Asia* comprises Turkey, Greece and Cyprus, and *Indonesia* includes the Philippines and parts of Melanesia.

The global land area was split into regions as per previous analyses in order to make use of extant data (Figure 3.1). This delineation of global regions excludes the sprawling regions of Polynesia and Micronesia, but global data deficiency forces their exclusion. This is unfortunate as land shortages are evidently extremely salient for island countries with little to no land for land use expansion. Land areas not assigned to a model region account for 0.01015% of the global land area, excluding Antarctica and Greenland.

3.3.3 Land systems

The global land systems 2010 data were generated as per methodologies from previous analyses (Asselen & Verburg, 2012; Van Asselen & Verburg, 2013; Eitelberg et al., 2016). Classification required six different inputs, all at a resolution of both 925 by 925m and 9250 by 9250m, hereafter referred to as 1 and 10-km^2 resolution for ease:

- Percentage bare ground cover
- Percentage tree cover
- Percentage urban extent
- Percentage croplands

- Agricultural efficiency index
- Number of heads of livestock (bovines, sheep and goats)

Percentage tree cover and bare ground for the year 2010 were extracted from the MODIS MOD44B Vegetation Continuous Fields (VCF - Version 6) yearly product (Dimiceli et al., 2015), which provides 250m resolution data in Sinusoidal projection. 250m tiles were mosaicked using `mosaic_rasters` from the `gdalUtils` **R** package (Greenberg & Mattiuzzi, 2018) before being reprojected and aggregated with bilinear interpolation to the targeted resolutions in Eckert IV projection using `gdalwarp` from the same package.

Urban extent percentage data were downloaded from the Global Human Built-up And Settlement Extent (HBASE) dataset from Landsat (Wang, Huang, Brown de Colstoun, Tilton, & Tan, 2017). Data are provided in WGS 1984 geographic projection at 0.008333 resolution and were reprojected as above.

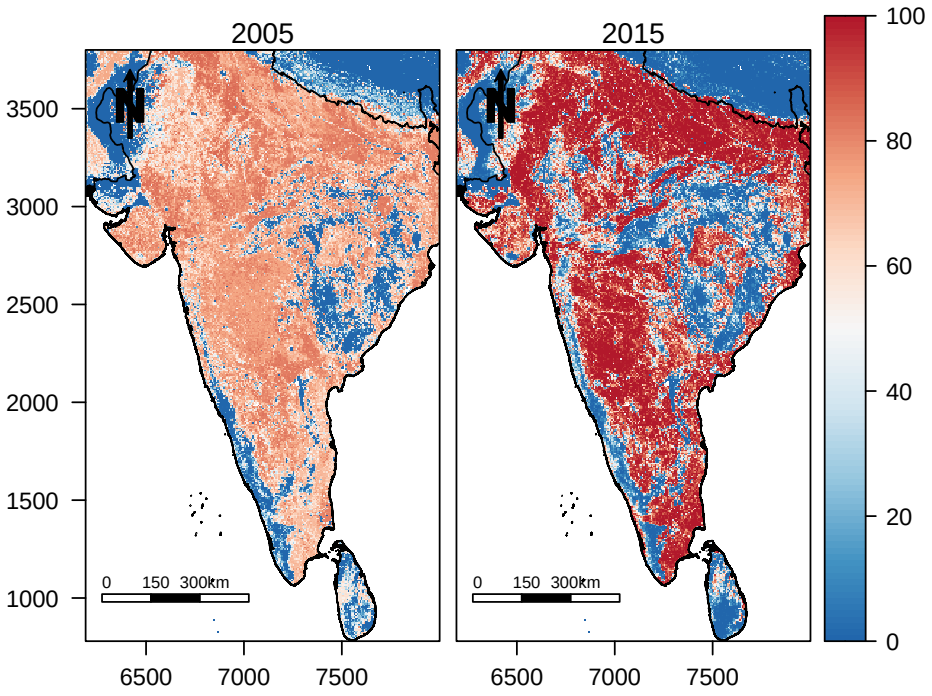

FIGURE 3.2: Percentage cropland at 1-km^2 resolution for South Asia. 2005 represents data produced by Fritz et al. (2015); 2015 data generated as described here, using 30m cropland extent data (Oliphant et al., 2017).

Percentage croplands per 1-km^2 involved use of a novel global cropland extent dataset at 30m resolution for the year 2015 (Oliphant et al., 2017). Data were downloaded as 10 by 10 degree 30m resolution tiles in WGS 1984, and reclassified from their native coding (0 for water, 1 for non-cropland, 2 for cropland) to custom coding for easy aggregation (NA for water, 0 for non-cropland, 1 for cropland). This allowed straight aggregation using an

average resampling algorithm and reprojection to produce cropland percentage at 1 and 10-km^2 Eckert IV resolution. As displayed in Figure 3.2, the newly created data appears much more heterogeneously distributed than previous efforts, especially Fritz et al. (2015) – to date the only study to describe global croplands at 1-km^2 resolution. Despite the evident visual difference in their distributions, the difference between their mean values is only 4.44 (%, absolute).

An agricultural efficiency index was used for classifying agricultural intensity for the same reasons as those detailed in Asselen & Verburg (2012) and Van Asselen & Verburg (2013): the index is a proxy for land management independent of local crop suitability. If yield were used, regions with high agricultural output despite low effort (e.g. extremely fertile lands) may be classified as intensive agriculture. The index was calculated for the year 2000 based on stochastic frontier production functions for rice, wheat and maize for a selection of 10 x 10km grid cells globally (Neumann, Verburg, Stehfest, & Müller, 2010). Indices compare the agricultural output for a grid cell in comparison to the maximum agricultural output given the same biophysical conditions, and range from 0 to 1. As with Asselen & Verburg (2012), I produced global gridded data using inverse distance weighted interpolation with ArcMap defaults: power of 2, and a minimum number of search points of 12. The wheat, maize and rice global maps were combined in such a way that the crop map of the most productive crop per region (using 2010 SPAM crop data (HarvestChoice, 2014)) was used for that region, e.g. rice for East Asia, maize for the USA.

Finally, heads of livestock utilised FAO's Gridded Livestock of the World 0.008333-resolution map for 2006 (2010 0.08333-resolution data for 10-km^2). Outright densities for cattle, sheep and goats were combined and reprojected from WGS 1984 to Eckert IV to create overall livestock densities (Robinson et al., 2014) at 1 and 10-km^2 resolution.

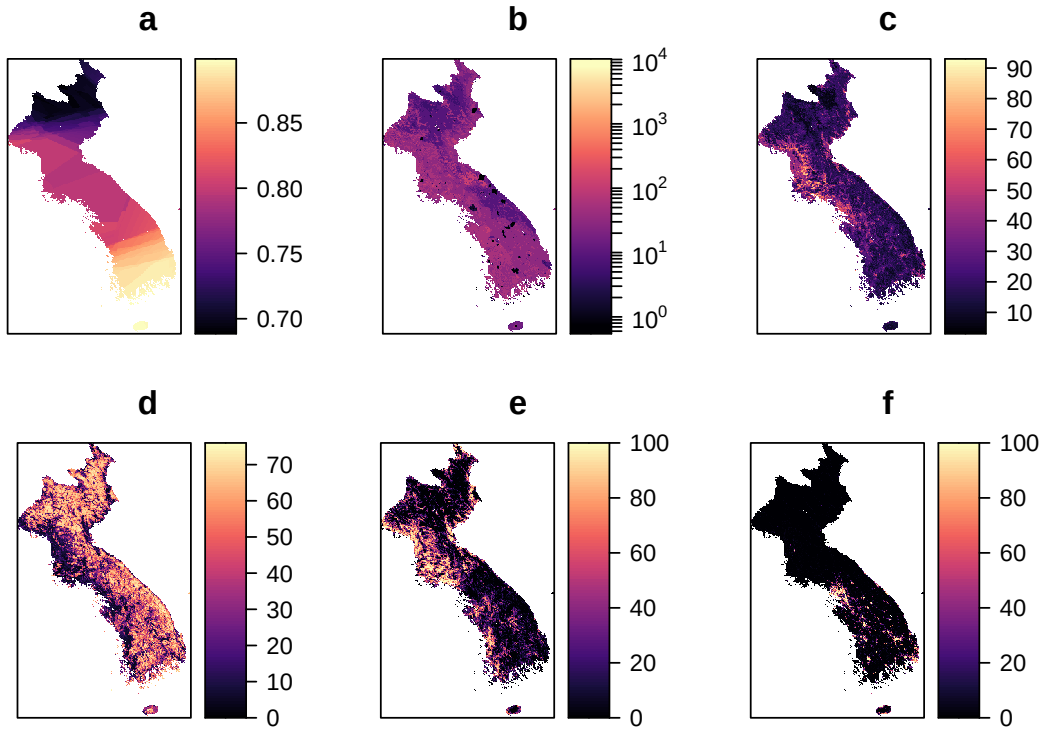

FIGURE 3.3: Six input data layers for land systems on the Korean peninsula at 1-km^2 resolution: (a) agricultural efficiency index, (b) heads of livestock (log(x+1) scale), (c) bare ground %, (d) tree cover %, (e) croplands %, (f) urban cover %.

The six land system data inputs (Figure 3.3) were then used to classify land systems in a simple threshold hierarchical classification (Eitelberg et al. (2016), Supplementary Information) such that a grid cell would be classified *Mosaic grass & forest* if urban extent $<5\%$, bare ground $<25\%$, cropland extent $\leq 20\%$, and tree cover is between 15 and 40%.

Land system classes are further split into management intensities, with two main distinctions:

1. *Low ls* or *high ls*, representing low and high intensity livestock systems; and
2. *Extensive*, *medium*, and *intensive* crops, representing low, medium and high intensity respectively. So *intensive* crop land systems are intensively managed crop production systems (e.g. high fertiliser use, mechanisation, etc.).

3.3.4 Suitability factors

Independent of the data required to classify land systems, a suite of datasets were selected and prepared as probable local predictors of land systems. These were selected based on previous usage (Asselen & Verburg, 2012), likelihood of influencing land system dynamics, and availability at 10-km^2 (and 1-km^2) global resolution. All were reprojected to the appropriate Eckert IV resolution, with bilinear resampling for continuous data and nearest neighbour resampling for categorical data. The suitability factors considered were:

Variable	1-km^2	10-km^2
Silt content	SoilGrids, available at `https://soilgrids.org/`	ISRIC-WISE (v1.2), available at `https://www.isric.org/explore/wise-databases`
Sand content	"	"
Clay content	"	"
Aqueous pH	"	"
Soil organic carbon	"	"
Cation exchange capacity	"	"
Temperature (mean of monthly mean)	WorldClim	WorldClim
Rainfall (total annual)	"	"
FAO soil drainage	ISRIC, available at `https://www.isric.org/`	ISRIC, available at `https://www.isric.org/`
Accessibility to cities	Weiss et al. (2018)	Verburg, Ellis, & Letourneau (2011)
Population density 2010	Gridded Population of the World v4	Gridded Population of the World v4
Gridded distance to freshwater	Kummu, Moel, Ward, & Varis (2011)	Kummu et al. (2011)
Gridded distance to coast	Available from `https://oceancolor.gsfc.nasa.gov/docs/distfromcoast/`	Available from `https://oceancolor.gsfc.nasa.gov/docs/distfromcoast/`
Elevation and slope	SRTM	SRTM
Gridded roadless areas	Ibisch et al. (2016)	Ibisch et al. (2016)
Gridded GDP 2010	No 1-km^2 data	Kummu, Taka, & Guillaume (2018)

Notes

- " marks represent repeated data sources vertically.
- FAO drainage classes were converted to binary maps using `layerize` from the `raster` **R** package (Hijmans, 2017) for each of five classes: very poorly and poorly drained, imperfectly drained, moderately drained, well drained, and excessively and somewhat excessively drained.
- Elevation (and slope – calculated with the `terrain` function from the **R** `raster` package) from SRTM and processed as per `http://viewfinderpanoramas.org/dem3.html`.

- Gridded roadless areas rasterised from original polygons provided by Ibisch et al. (2016).

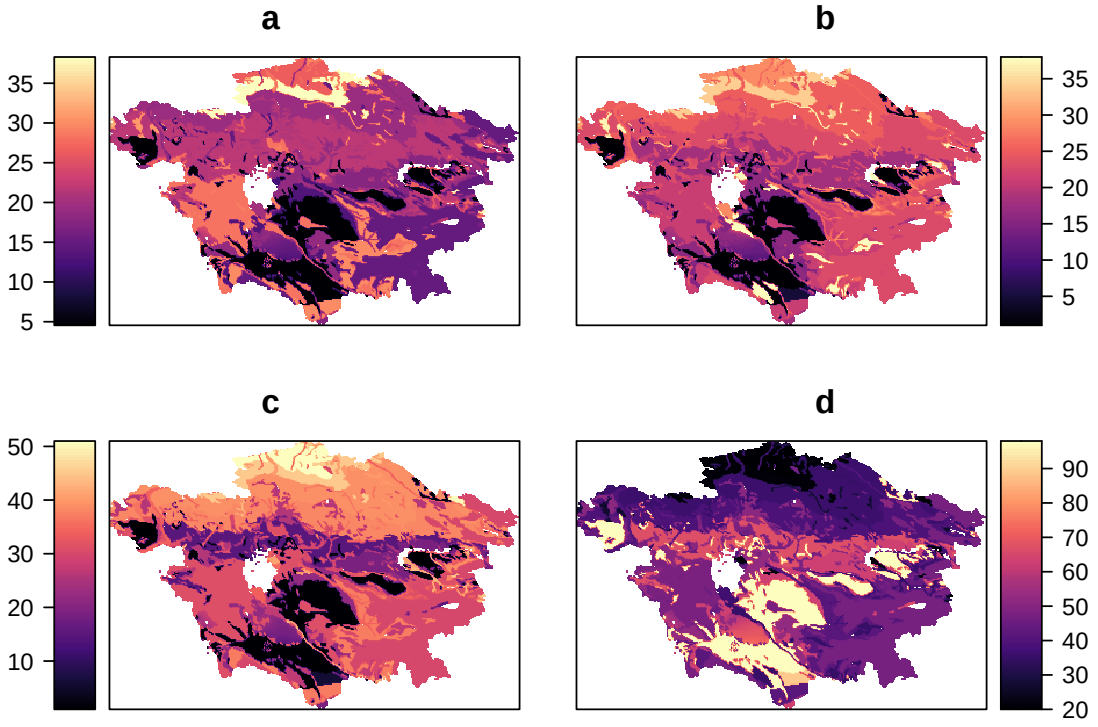

FIGURE 3.4: Four soil suitability layers for land systems in Central Asia at 10-km^2 resolution: (a) cation exchange capacity mmol(c)kg^{-1}, (b) clay content gkg^{-1}, (c) silt content gkg^{-1}, (d) sand content gkg^{-1}.

3.3.5 Filling missing data

The current implementation of CLUMondo does not allow for missing values in any of the input data. To counter this, I replaced missing values in data using a custom function based on the `focal` function from the **R** `raster` package. This function computed the mean (for continuous data) or mode (for categorical data) for missing cells using a neighbourhood area of 15 by 15 cells around the missing cell. This function was iterated until the number of missing data in the input data matched the number of missing cells in a target reference raster for the region.

To validate use of this technique, I took one such input raster, bare ground percentage for Central Asia, and randomly introduced 10,000 missing values to the raster, ran the fill function, and compared predicted values to the observed percentages. Predicted values correlated well with observed values (R^2 (Pearson's) $= 0.8874$, $N = 10{,}000$).

Larger regions of missing values presented problems with this technique mostly in terms of computational processing time when at 1-km^2 resolution. The global soil data provided by

SoilGrids is excellent in its coverage, with the exception of South Georgia and the Sandwich Islands, US-owned islands off the Eastern coast of Russia, and some Russian islands in the Arctic Circle. For these regions, gaps in the data were filled using inverse distance weighted interpolation.

3.3.6 Demand scenarios

CLUMondo requires an exogenously set demand for goods and services per year of the simulation. I used the same demand scenarios as those used by Eitelberg et al. (2016) (Supplementary Information Table S1) for crop production, livestock, and urban area. These demand scenarios were for the years 2000-2040, so in order to derive a start point of 2010 I simply interpolated values for each demand. Crop yield and changes in livestock densities were also used as in Eitelberg et al. (2016) to simulate expected increases in crop and livestock technology.

3.3.7 Crop production, livestock and urban area per land system

To produce crop production quantities per land system, I used data from the Spatial Production Allocation Model (SPAM) (HarvestChoice, 2014). SPAM produces spatially explicit production, yield and harvested area maps using national and sub-national data, disaggregated using cross-entropy techniques. I only used data explicitly identified as a food crop, as opposed to non-food crops such as cotton. The production quantities for all such food crops were then summed per 10-km^2 grid cell. Due to the mismatch in the resolution of the SPAM data (the finest resolution crop production data available) and the 1-km^2 data, crop production per land system for this was calculated initially using 10-km^2 land system data, and then downscaled with the assumption that a 1-km^2 grid cell produces 1% of the output of a 10-km^2 cell of the same land system. This is evidently problematic for naturally heterogeneous mosaic land systems where crop production is highly likely to vary significantly from cell to cell at 1-km^2 resolution, but this was unavoidable given data limitations. Livestock numbers were calculated simply from overlaying the livestock data (Robinson et al., 2014) onto land systems. Urban area was calculated using mean urban percentages and allocating the urban area demand for the year 2010 proportionally to each land system. In order to match the calculated yearly production demands, the quantity of each service available per land system was scaled to match the exogenous regional demand.

3.3.8 Land system suitability models

Logit link binomial regression models were constructed for each land system in each of the 24 CLUMondo regions. Firstly, the model region was made into a binary surface for all land systems present in the land system using the `layerize` function from the **R** `raster`

package (Hijmans, 2017). Each binary land system surface was stacked atop all suitability factors before being made into a data frame where each observation contains a response for presence of the land system (0 or 1) and a suite of suitability factors for the given cell. As the primary aim of these models is prediction and not explanation, and that CLUMondo limits the number of suitability factors, the function `stepAIC` from the `MASS` **R** package (Venables & Ripley, 2002) was used to select the most parsimonious models in a stepwise manner to arrive at a model with 5 explanatory factors.

The probability layers garnered from this process (for each land system in each region) represent a suitability surface for that land system in that specific region. Most model datasets were heavily imbalanced in favour of negative cases (absence of the land system); in normal circumstances this would usually necessitate the use of evaluation metrics specifically targeting the positive class (e.g. sensitivity, positive prediction value, etc.). However, in this use case, I am more interested in accurately predicting socio-environmental niches for each land system – i.e. accurately predicting where land systems are *unlikely* to be found. Thus, especially with on average an imbalance in favour of absences, standard metrics (AUC, accuracy) are appropriate.

However, not all model regions contained every instance of the 24 land system classes. To counter this, two solutions were implemented: firstly, if the land system in question were present in the wider region (e.g. in Europe as opposed to Western Europe), a suitability surface was generated using data from the entire region and cropped to the region without the land system. Secondly, if the land system were not present in the wider region, the suitability model from the most similar land system was used. For example, *Natural grassland* is incredibly rare globally in 2010 (most likely due to overestimation of the distribution of livestock in the FAO dataset), leaving a large number of regions without this land system. For these, *Grassland, low livestock* suitability models were used instead. I did not calculate global land suitability models for this use because it has been previously shown that the drivers of land systems change significantly at this scale (Van Asselen & Verburg, 2013).

The results of these land system suitability models can be seen in Appendix A Figure A.4.

3.3.9 Renewable energy

The spatially explicit wind and solar data represent 12,581 and 12,043 installations worldwide in 153 countries, totalling 322.8 and 125.6GW of capacity respectively (Dunnett et al., 2020). They currently represent the best available data for wind and solar infrastructure globally. These datasets were created by extracting features from OpenStreetMap, an open-source collaborative global mapping project. Data were extracted from OpenStreetMap that were tagged in a manner representing either a wind turbine or solar PV. Data were then spatially aggregated to approximate utility-scale installations. Power estimates were provided based on prediction models trained on independent data. For full methodology please see either

Chapter 1 or the accompanying paper (Dunnett et al., 2020). As suggested by the authors, these data were filtered to remove any wind installations with fewer than 5 turbines and not in cells identified as water or urban, and any solar installations with less than 1 hectare ($0.01km^2$) in panel area and in water or urban cells.

Random Forest probability surfaces for both onshore wind and solar PV were generated using these spatially explicit renewable data and a suite of global environmental and socio-economic predictors: accessibility, livestock density, percentage cropland, elevation and slope, population density, distance from protected areas, road density, wind speed, and global horizontal irradiance (see Chapter 2 for full methodology). Random Forest 10-fold, 5-repeat models were performed on world regions with more than 100 wind or solar PV observations: Middle East, Southern Europe, South America, South Asia, North America, Russia and the Balkans, East Asia, Northern Europe, and Central Europe. The onshore wind models had a mean accuracy of 0.8976; the solar PV models had a mean accuracy of 0.8735. While these layers were generated from installation locations at a single point in time, the probabilities are assumed to be good indicators of future development.

3.4 Results

Figure 3.5 shows the newly generated 2010 data for global land systems at 10-km^2 resolution. The general patterns present in previous data (Asselen & Verburg, 2012) can still be seen – dense forests largely confined to the tropics, with more open boreal forests at high latitudes. Europe, North America and India are still regions largely dominated by human land uses (urban and cropland systems). A detailed comparison of the 2000 and 2010 land systems is shown in Figure A.5 in Appendix A for India and its surroundings. Figure 3.2 suggests that increased homogeneity of the data could lead to a reduction in mosaic land systems. However globally in the 2000 data, mosaic land systems occupied 43.44 million km^2, and 43.47 million km^2 in the 2010 data. In fact, many of the largest differences in land system class frequencies appear to be driven by the latest iteration of the Gridded Livestock of the World (Robinson et al., 2014). The area of *Natural grassland* decreased by 3.887 million km^2 globally, with a concomitant increase in *Grassland, low livestock* of 2.757 million km^2 – the classification difference between these land systems is predicated on livestock density. Similarly, *Bare, no livestock* land systems decreased by 3.552 million km^2, with an increase in *Bare, low livestock* land systems of 4.498 million km^2.

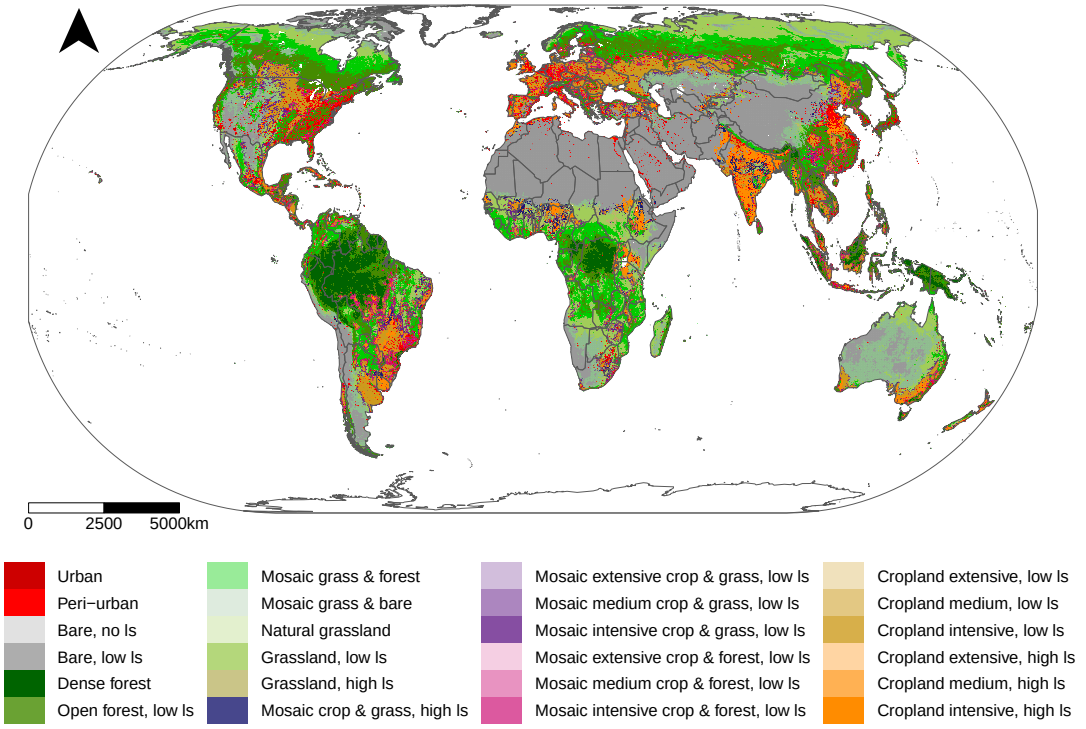

FIGURE 3.5: Global land systems 2010, Eckert IV equal area projection. Note Greenland and Antarctica are excluded from the analysis.

Figure 3.6 shows the impact of a higher resolution on the classification of land systems, and its importance for smaller regions like Japan. It is also important to note that the increase in resolution does not drastically change the general trend of land systems – in both Figure 3.6a and Figure 3.6b Japan consists largely of forested land systems, with pockets of cropland land systems in the North and heavily urbanised land systems in the South and Southeast. However, the higher resolution land system data are able to identify more specialised land systems (in Japan's case, *Dense forest*). This happens to also be the case globally for *Dense forest*, which represents 1.514% more (absolute) of global land systems at 1-km^2 than at 10-km^2 – a relative increase of 33.61%, and also *Natural grassland* (1.264% more absolute, 434.5% relative increase). The way *Natural grassland* is classified is heavily dependent on zero human impact – the land system requires a value of 0 for percentage cropland, built area, and livestock; this becomes increasingly unlikely at lower resolutions.

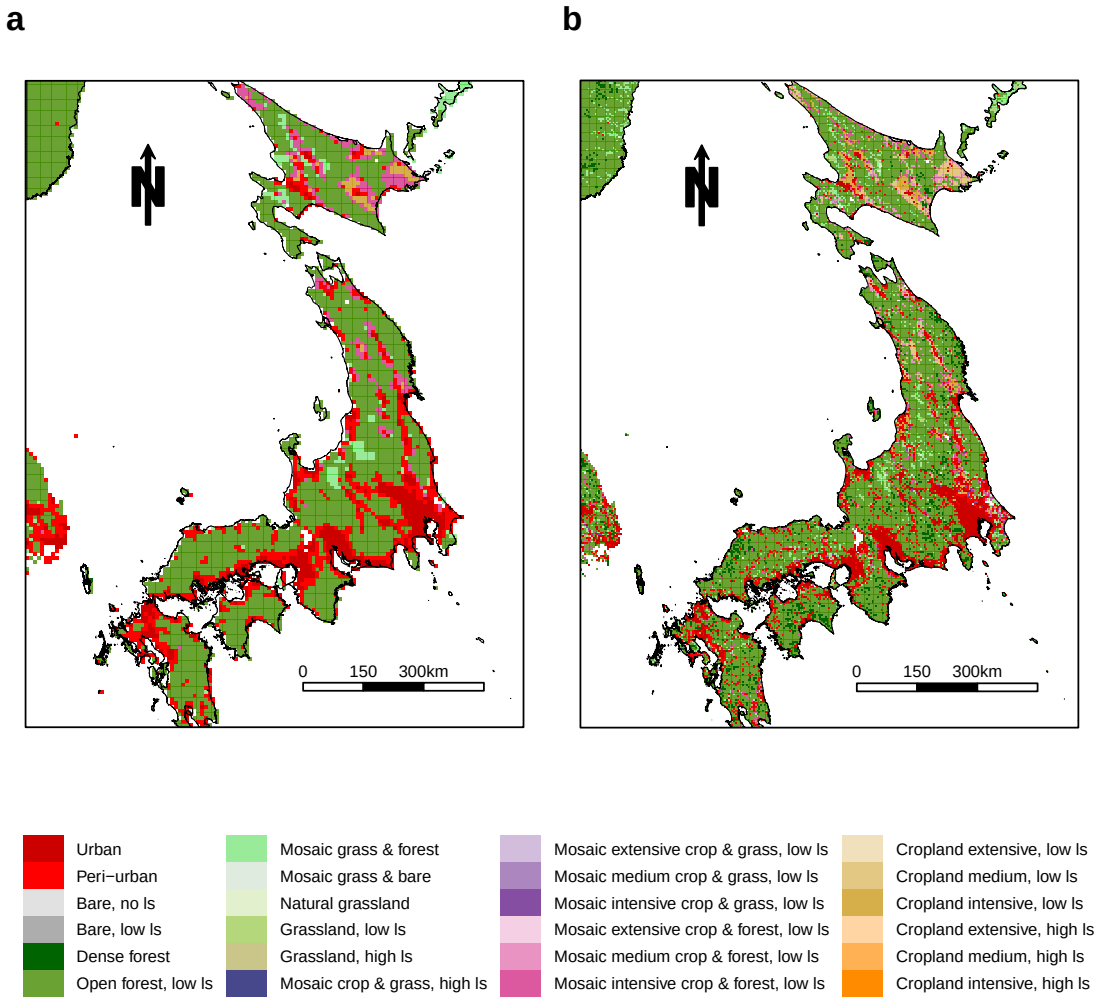

FIGURE 3.6: A comparison of 2010 land systems at 10-km^2 resolution (a) and 1-km^2 (b) for Japan.

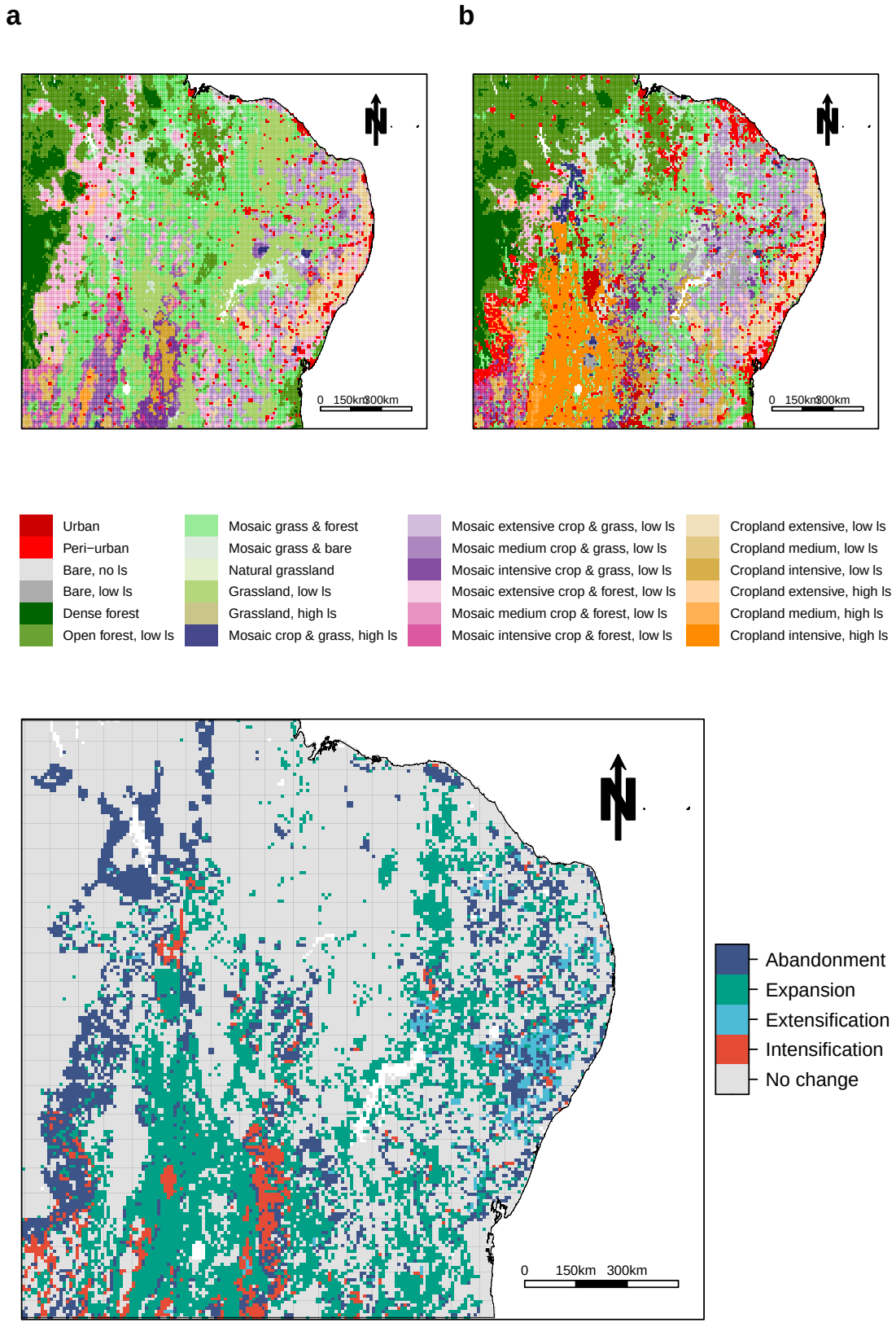

FIGURE 3.7: CLUMondo results for east Brazil, showing projected land changes between 2010 (a) and 2040 (b). Intensification describes an increase in management of extant cropland; extensification is a decrease in management. Expansion describes the appearance of mosaic or cropland land systems where previously absent; abandonment is the opposite.

Figure 3.7 shows the output of CLUMondo for eastern Brazil. As perhaps expected, there is a large increase in land systems in 2040 capable of providing important contributions to the significant demand for heads of livestock in the region (*Cropland intensive, high livestock* and *Mosaic crop & grass, high livestock*) while also providing a large increase in supply of food crops (also seen in Table A.4). This comes largely at the expense of grassland and mosaic grass and crop land systems; something echoed globally as *Grassland, low livestock* land systems reduce in size by 6.377 million km^2, with a concomitant increase in *Cropland intensive, high livestock* of 1.426 million km^2. Area increases in intensive cropland systems tend to outstrip extensive systems: globally, *Intensive cropland* increases by 2.378 million km^2 compared to 0.4617 million km^2 for *Extensive cropland*. This picture is of course more varied at the region level – for example, Mexico, West Africa, and Western Europe all have larger increases in area for *Extensive cropland* over *Intensive cropland*. *Urban* and *Peri-urban* land systems also both increase to accommodate growing human populations (increases of 1.69 and 3.549 million km^2 respectively).

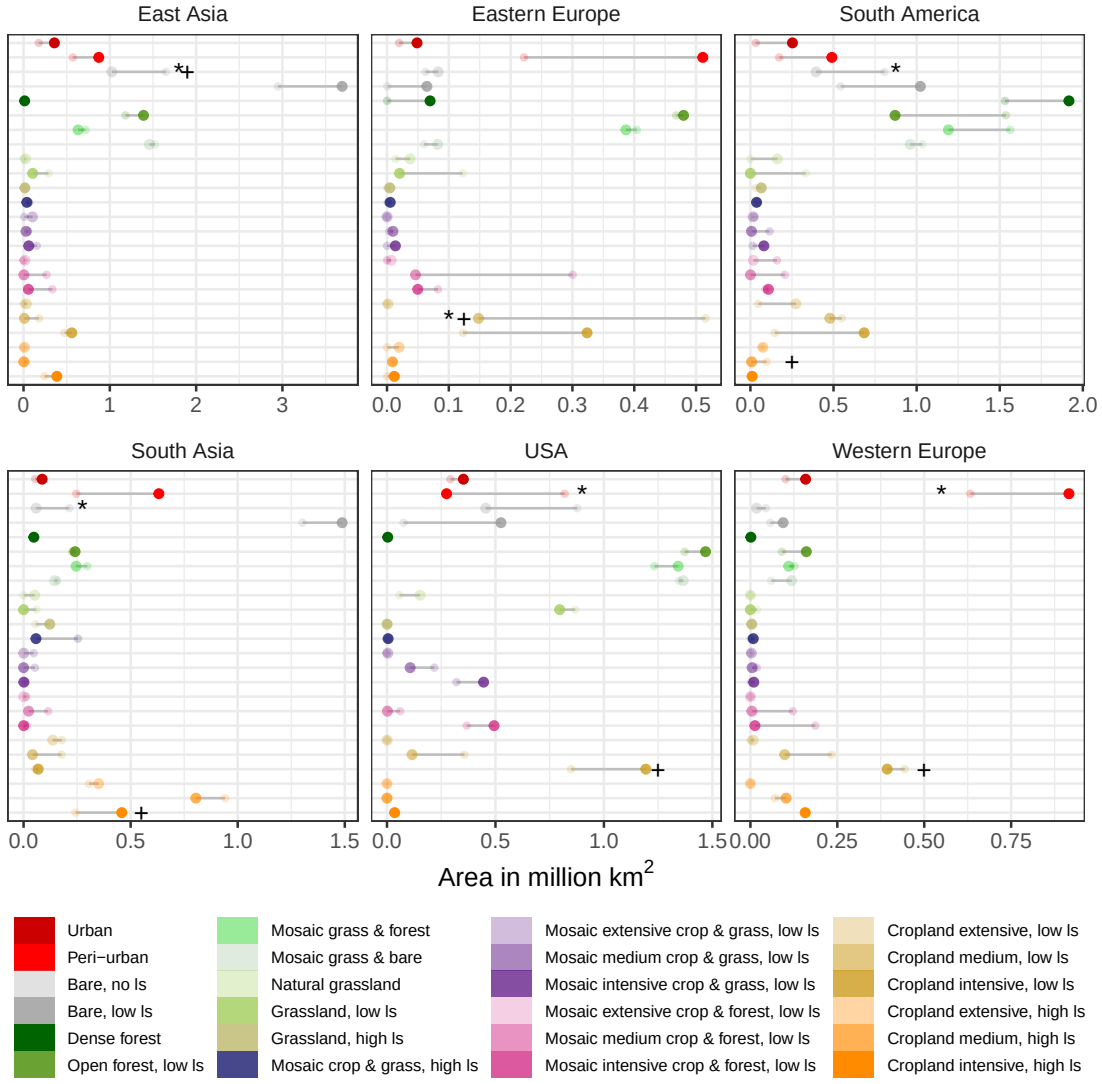

FIGURE 3.8: Changes in land system area between 2010 and 2040 for selected regions. The land system in a region with the most solar PV installations in 2010 is marked with *; wind with +. Larger, darker points represent 2040; smaller, lighter points 2010.

Figure 3.8 presents the difference in area between all land systems in 2010 and in 2040 for selected regions, as well as the land systems in which onshore wind installations and utility-scale solar panels are most commonly found in 2010 (see Table A.4 in Appendix A for more details). I used the same criteria as Chapter 2 for inclusion in Figure 3.8 – model regions with >100 wind or solar observations – in order to get a reliable impression of distributions with respect to land systems. However, Russia and the Balkans and the Middle East were excluded from figures to help legibility.

Bare, no livestock, *Bare, low livestock* and *Peri-urban* are the most commonly associated land system for 7 of the 10 qualifying regions for solar PV; for wind installations, cropland systems dominate (7 of 10 qualifying regions). For solar PV, the area of *Peri-urban* land systems available for utility-scale solar installations increase substantially in Western Europe,

West Asia and Brazil as these regions respond to growing demand for human populations – 247.7, 70.15, 44.79% respectively. Brazil also displays a large increase in area for its most commonly associated wind installation land system – *Mosaic crop extensive & grass, low livestock* – with an increase of 40.47%.

Eastern Europe sees a significant decrease in *Cropland medium, low livestock* – the most commonly associated land system for both renewable technologies – with a decrease of 71.26%. However, this is partly offset by a large increase in *Cropland intensive, low livestock* and *Peri-urban*: in 2010, 33.66% of wind installations and 38.14% of solar installations were found in *Cropland medium, low livestock* (the highest proportion), but 8.661% and 14.42% were found in *Cropland intensive, low livestock* and 11.81% and 30.88% in *Peri-urban* respectively. For this reason, land area changes by land system (Table A.4) could over or under-estimate the amount of land systems if it is assumed that renewable energy associations with land systems occur at a broader level – i.e. installations are associated with a certain land system class grouping, irrespective of management intensity. Aggregations of land systems into groups independent of land management intensity can be found in Table A.5, Appendix A, where for example *Cropland, low livestock* presents the aggregated area and percentage change for three land systems between 2010 and 2040: *Cropland extensive, low livestock*, *Cropland medium, low livestock*, and *Cropland intensive, low livestock*. Grouping land systems serves to moderate some of the increases (for example Brazil, USA and South Asia's 40.47, 88.73, 40.63% increases become 9.814, 8.333, 8.661% respectively), but the general pattern of land availability appears similar.

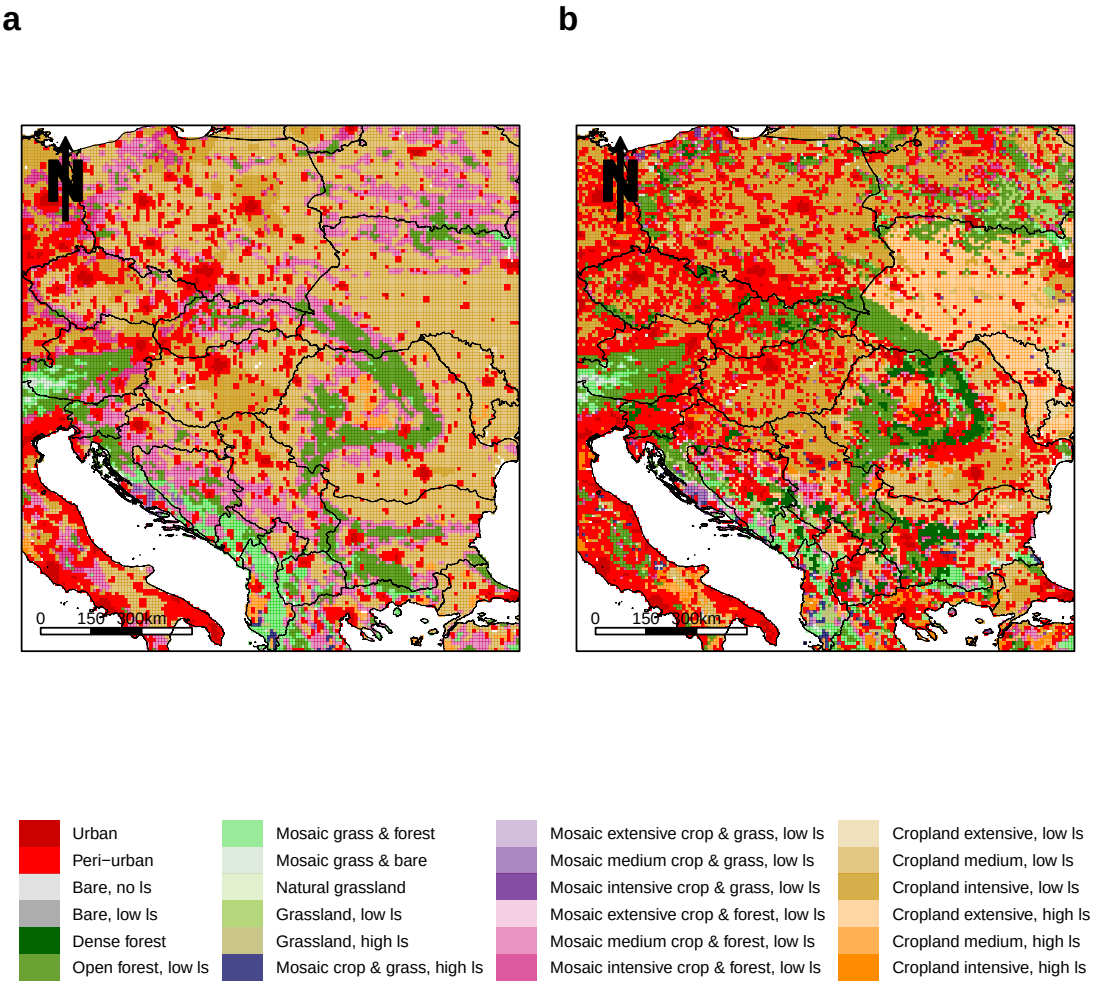

FIGURE 3.9: Land systems in 2010 (a) and 2040 (b) for Eastern Europe.

Figure 3.10 shows, using wind energy in Eastern Europe as a case study, effects of land changes on the land system in which Eastern European wind installations are most commonly found: *Medium cropland, low livestock* (for reference, Figure 3.9 shows land changes for the same region – see also Tables A.4 and A.5 for more information on wind and solar associations with land systems by region). Areas of abandoned cropland represented lower likelihoods of wind development, whereas areas of extensification or intensification in the North – which include land transitioning from *Cropland medium, low livestock* to *Cropland intensive, low livestock* – present high probabilities of development. *Cropland, low livestock* land systems (extensive, medium and intensive) in Eastern Europe in 2040 retain relatively high mean wind development probabilities of 0.3812 to 0.5191.

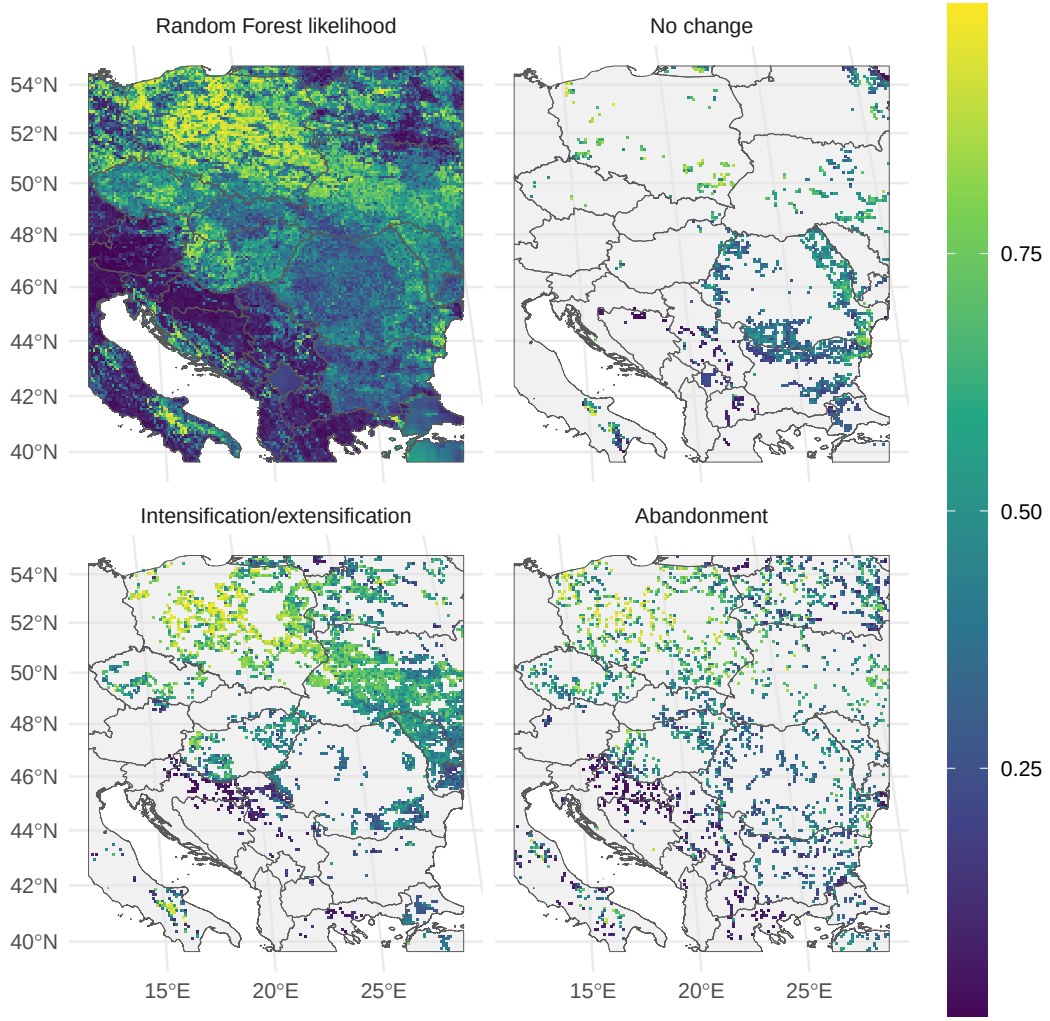

FIGURE 3.10: RF probability layer for wind energy in Eastern Europe. Panels highlight changes in the land system with the highest density of wind installations in the region in 2010, *Medium cropland, low ls*, showing (clockwise from top left) the raw wind RF probability layer; cells with no change in this land system; cells that have converted from this land system to mosaic, natural, or urban land systems; and cells that have changed intensity within cropland land systems.

The most commonly associated land systems also change at a higher resolution, especially solar PV: whereas at 10-km^2 resolution (for regions with >100 observations) *Peri-urban* and bare land systems dominate, at 1-km^2 resolution, *Cropland intensive, low livestock* accounts for 5 of the 10 regions. Wind, however, remains dominated by medium to high intensity cropland. In total, 55.43% and 61.95% of wind and solar installations respectively changed land systems between resolutions. For onshore wind, the most common transition was *Peri-urban* to *Cropland extensive, low livestock*, which made up 13.6% of the wind installations changing land system between resolutions. The latter was already one of the more common land systems in which wind installations are found (Table A.4 in Appendix A). The next three most common transitions were changes between the intensity of cropland, but changes from *Peri-urban* to cropland systems generally comprises 19.16% of the changes. For solar PV, the most common transition was also *Peri-urban* to *Cropland extensive, low livestock*

(18.59%). The second most common transition was *Peri-urban* to *Urban* (10.56%). 26.35% of changes between the resolutions again were *Peri-urban* to cropland systems.

3.5 Discussion

Renewable energy expansion has in the past been highlighted as a potential threat to areas of conservation importance and wild places (Santangeli et al., 2015; Gasparatos et al., 2017; Rehbein et al., 2020). If utility-scale solar PV and wind installations also turn out to be land use *exclusive*, i.e. prevent land from contributing to other goods and services, then renewable energy could be considered a threat to other human needs and require its own place in a mosaic of specialised land systems each producing a large amount of one good or service.

The aim of this study was to investigate whether projected land change offers a continued opportunity to develop renewable energy in non-natural systems. Figure 3.8 (and Tables A.4 and A.5 in Appendix A) show that under the current distribution, renewable energy is overwhelmingly associated with human land uses: peri-urban areas and intensively managed cropland systems. Both of these land systems are projected to increase substantially in area globally by 2040 – 3.549 million km^2 for *Peri-urban* and 1.578 million km^2 for croplands.

This relationship with human land uses is perhaps to be expected: the majority of utility solar and wind occurs in the USA, Europe and China (Chapter 1, Figure 1.5): regions with high proportions of converted land use (Václavík et al. (2013); also Figure 3.5). The USA in 2010 contained 36.25% urban and cropland land systems, Western Europe 21.58%, and East Asia (including China) 27.2%. For comparison, urban and cropland land systems in all four African model regions account for 12.81%. However, these same land systems are projected to increase by 2.429 million km^2 by 2040.

The distributions of solar PV and onshore wind have already been shown to be heavily influenced by socio-economic, as well as biophysical, factors (Chapter 2), and should the continent of Africa follow the same trajectory as more established renewable energy national capacities, there is no reason to suggest that onshore wind and solar PV will drive *more* land change than is already projected to meet food and housing requirements due to the association of renewable energy installations and human-orientated land systems. This association could also be a symptom of the transmission constraints of current renewable energy technologies, as highlighted in Heard et al. (2017) – changes in transmission requirements could shift infrastructure to more remote, natural land systems.

Interestingly for the inclusion of renewable energy installations in land change models, their siting appears to be independent of management intensity – solar PV and onshore wind are found in both extensive and highly intensive croplands. There is a slight increase in likelihood of both solar PV and wind installations in higher intensity cropland (projected 2040) (e.g. $0.3797 > 0.3011$ for solar PV in *Cropland intensive, low livestock* and *Cropland*

extensive, low livestock; 0.3706 > 0.2622 for wind in *Cropland intensive, high livestock* and *Cropland extensive, high livestock*). However, largely, the 2040 land system distributions do not affect the development likelihoods of renewable energy installations, especially when the land systems are considered in the broader extensification/intensification and abandonment/expansion dynamics (Figure 3.10).

One assumption with this study is that the yields of goods and services remain unaffected by the presence of wind or solar installations. Complete global data for crop production is already sparse: spatially disaggregated crop production has been produced in 5-year intervals since 2005 (HarvestChoice, 2014), but the methodology focuses on sub-national crop production statistics and low resolution cropland extent and crop suitability (10-km^2) inputs. Furthermore, the lack of operational lifespan attributes in the data generated in Chapter 1 negates the possibility of investigating how the presence of such installations affect yield. Some research suggests that *agrivoltaic* systems – food crops under solar PV panels – require little adaptation from traditional food crops (Marrou et al., 2013), while other authors even suggest production can increase under such systems (Barron-Gafford et al., 2019; Marrou, 2019). Analysis of land cover microclimates highlights cropland as having the greatest median solar potential of approximately 28Wm^{-2} (Adeh, Good, Calaf, & Higgins, 2019).

Despite assumptions here, thoughtfully planned utility-scale solar can actually benefit multiple goods and services: some UK solar installations have been shown to increase vegetation diversity and butterfly abundance (Randle-Boggis et al., 2020), while a techno–ecological synergy (TES) framework has been proposed to specifically engineer mutually beneficial relationships between solar energy and "competing" land uses (Hernandez et al., 2019). However, the evidence is not sufficient to include in land change models at global scale. This is especially the case with wind installations, where despite suggestions that wind turbines can significantly alter their immediate ground-level climate, raising night air temperatures by 0.18°C and absolute humidity by 0.03 gm^{-3} (Armstrong et al., 2016), there is a dearth in studies investigating any impact on crop yield. As such, I was unable to modify land use when co-located with renewable energy installations. However, the fact that there is such a strong association between cropland and wind installations in the Northern Hemisphere suggests that at least with the current scale of deployment, there is unlikely a significant effect.

Bioenergy crops are frequently maligned as a potentially large future occupier of agriculturally suitable land (Slade et al., 2011; Alexander et al., 2015; Fritsche et al., 2017; United Nations Convention to Combat Desertification, 2017; Fuss et al., 2018), and policies promoting bioenergy have proved to be successful in rapid expansions in cultivated area (Thornley & Cooper, 2008). Policies can also have a direct effect on the type of land converted for bioenergy – many studies eschew prime arable land for area calculations based on potential marginal lands (Slade et al., 2011; Fuss et al., 2018). However, aggressive subsidy policies could overcome the opportunity cost of traditional food crops and open up much more of agriculturally suitable land. For this reason it is extremely hard to include bioenergy crops in

global land change scenarios as deployment is likely to vary hugely between model regions. Better data are needed describing *where* current bioenergy crops are located beyond simple suitability maps largely assuming the drivers behind bioenergy crops are superficially the same as agriculture (Oakleaf et al., 2019). With better data, researchers could evaluate interactions between bioenergy crops and other land uses, including onshore wind and solar PV. With the current base of evidence it might be assumed that onshore wind and solar PV can co-exist with high intensity bioenergy crops as they are shown to here with cropland land systems. As such, bioenergy expansion, and agricultural expansion driven by bioenergy, may provide *more* location opportunities for renewable energy outside natural land systems.

The differences in data distribution between 2000 and 2010 and 1-km^2 and 10-km^2 emphasise the difficulty in characterising distribution of phenomena at global scale, and in many ways corroborate the conclusions of Chapter 2 with respect to the spatial scale that renewable energy installations operate at. The cropland data presented here were generated using the highest resolution croplands datset ever produced (Oliphant et al., 2017), producing 1-km^2 and 10-km^2 resolution maps of percentage crops per pixel with 30m resolution extent data. Figure 3.2 shows for India and its surroundings the increase in homogeneity of the new data – echoed globally – where cropland percentages for the new dataset are $\sim 20\%$ greater than the highest cropland percentages in the Fritz et al. (2015) data. However, the distribution of land systems at 1-km^2 resolution remains similar to land systems at 10-km^2 and suggests that previous land system delineations (Asselen & Verburg, 2012; Van Asselen & Verburg, 2013; Václavík et al., 2013) were more driven by global data availability at the correct resolution, as opposed to anything inherently sacrosanct about classifying human land uses at 10-km^2. The utility of higher resolution data is also important for renewable energy: as discussed in Chapter 2, renewable energy installations likely operate at smaller spatial scales than even 1-km^2. This may explain how utility-scale solar installations can, and most frequently, exist in *Peri-urban* land systems at 10-km^2 resolution; at 1-km^2 resolution this largely shifts to cropland. Pixel limits hard coded into the CLUMondo model prevented running land change scenarios for model regions at 1-km^2.

In this implementation of CLUMondo, there were limited restrictions on land change, including no land policy restrictions other than restricting cropland to agriculturally suitable cells. There is evidence to suggest that protected areas are not able to stem the tide of land change, even within strict reserves (Bailey, McCleery, Binford, & Zweig, 2016; Golden Kroner et al., 2019). As such, protected area land change exemptions were not included in this analysis. Ambitious conservation protection targets may well alter land change trajectories but slow progress towards the 17% land protection mandated by the Aichi Targets suggests that the renewal of the targets may be nowhere near the 50% target that some conservation scientists are calling for (Dinerstein et al., 2017, 2019). The association between renewable energy and human-orientated land uses, all of which significantly increase in area when projected to 2040, may suggest an avoidance of conflict with natural land systems (and by assumption, biodiversity). However, it is important to note that the current protected area

network is heavily biased towards more densely populated anthromes (Martin et al., 2014) and renewable energy's dependence on these types of land systems should not be read as absence of impact on the environment, especially when considered cumulatively.

3.6 Conclusion

Current onshore wind and solar PV installations are mostly associated with human-dominated urban and cropland land systems. Under a baseline scenario of land change to the year 2040, these categories of land system markedly increase in area, presenting an excellent opportunity to co-locate renewable energy infrastructure impacts in areas likely to shift independently in response to more salient human demands: food and housing. These projected areas of urban and cropland systems maintain high likelihoods of renewable energy infrastructure development, as measured by Random Forest probability layers generated from current onshore wind and solar PV distributions. I also presented a global map of land systems for the year 2010 at 1-km^2 and 10-km^2 resolution, showing that in the ten year period since the first iteration of global land systems, human land systems – mainly urban and peri-urban – display a striking increase. The characterisation of global land systems at 1-km^2 show a superficially similar distribution to land systems at 10-km^2. Quality data is the foundation of any land management plan and the land systems data presented here allows land scientists to characterise human land use globally at a much higher resolution than previously possible in order to inform more sustainable land transitions needed for decarbonising economies.

Conclusion

"It's not the end of the world. It is the end of the wild." – Karl Ammann

The aim of this thesis was to assess the potential for significant trade-offs between two crucial pillars of a sustainable future: our ability to supply and markedly expand renewable energy, and our ability to protect global biodiversity. I describe the extent of onshore wind and solar PV deployment worldwide and show that while any overlap of infrastructure with areas of conservation importance is unfortunate, there is no evidence to suggest that expansion of renewable energy disproportionately affects more speciose areas. I show that current siting of renewable energy is overwhelmingly associated with human-dominated land uses – even at 10-km^2 resolution, and that expansion of human impact in response to other (arguably more important) demands – food, fibre, housing – provides ample space in which to co-locate renewable infrastructure without unnecessarily impacting natural land systems. The following sections reflect on the main conclusions of each analysis, and offer up avenues for further work.

Increasing the accountability of renewable energy expansion

Chapter 1 (Dunnett et al., 2020) presents a first attempt at leveraging global open access data to pinpoint the global onshore wind and solar PV estate. The analysis was designed in as rigorous and replicable a way as possible in order to combat metadata inaccuracies with the sheer weight of global observations. The data allow environmental scientists to better interrogate renewable energy siting and cumulative impacts that might otherwise have escaped scrutiny. Data availability has allowed myriad studies assessing the global protected area estate thanks to the quality and relevance of the World Database on Protected Areas (WDPA) (UNEP-WCMC & IUCN, 2020). Up to date data has the ability to inform key policy makers of progress towards global sustainability goals: for example, one of the most recognisable Aichi Biodiversity Targets is Target 11:

> By 2020, at least 17 per cent of terrestrial and inland water, and 10 per cent of coastal and marine areas, especially areas of particular importance for biodiversity and ecosystem services, are conserved through effectively and equitably

> managed, ecologically representative and well connected systems of protected areas and other effective area-based conservation measures, and integrated into the wider landscapes and seascapes.

Quality spatial data for protected areas has meant that progress towards Aichi Target 11, at least in terms of area coverage, can be easily assessed (Tittensor et al., 2014; Mace et al., 2018; UNEP-WCMC, IUCN, & NGS, 2018). This has allowed research to focus on more important aspects of achieving the target, namely what does it mean for protected areas to be *effectively and equitably managed*, *ecologically representative*, and *well connected*. Renewable energy spatial data, like those presented here, have the potential to serve a similar purpose supporting measurement of the SDGs, especially Goal 7 – *Ensure access to affordable, reliable, sustainable and modern energy for all* – Target 7.1 and 7.2 (UN, 2020):

- Target 7.1: By 2030, ensure universal access to affordable, reliable and modern energy services.
- Target 7.2: By 2030, increase substantially the share of renewable energy in the global energy mix.

Currently progress towards Target 7.1 is tracked by indicators measuring the proportion of the population with access to electricity and with primary reliance on clean fuels and technology. Target 7.2 is tracked by the renewable energy share in the total final energy consumption. The wind and solar data presented here could provide a significant insight into traditionally data-poor regions when used in conjunction with other high resolution global data, e.g. the Gridded Population of the World (Doxsey-Whitfield et al., 2015) or even newer spatially disaggregated census data (Lloyd et al., 2019). Furthermore, the data could contribute to new indicators assessing the *quality* of data for the other indicators. The wind and solar data correlated strongly with official renewable energy capacities provided by IRENA (and much more so than the raw observations from OpenStreetMap): the data clearly represent a good proxy of actual renewable energy distribution.

There is undoubtedly more to be done: researchers would likely appreciate the explicit delineation of solar photovoltaic panels, where solar energy is directly converted to electricity *in situ* through the photovoltaic effect, and concentrating solar power (CSP), where mirrors or lenses concentrate a large area of sunlight onto a receiver to generate electricity either through a steam turbine or thermochemical reaction. While the two technologies are superficially similar in their energy source and area requirement, there are differences in their environmental impacts (Hernandez et al., 2014). Similarly, discerning the difference between traditional horizontal axis wind turbines and newer *vertical* axis wind turbines – the subject of a 2015 call for the evaluation of their opportunities and risks (Santangeli & Katzner, 2015) – would help clarify the cumulative impact of global wind. Despite the 2015 call, by 2018 there had still been no controlled study of the impact of vertical axis wind turbines on volant species (Hui, Cain, & Dabiri, 2018). Given that impact mortality of volant species remains

one of the most cited environmental risks of wind turbines, and the potential of vertical axis wind to vastly reduce the risk, this is an evidence gap that needs urgently addressing.

The data methodology laid out in Chapter 1 could also easily be extended to *offshore* wind installations to aid with marine spatial planning, and is not restricted to renewable technologies. As discussed in the data [Usage Notes], there is nothing preventing the methodology being extended to conventional fuels to support regional environmental impact assessments. Previous global assessments of conventional fuel impact, as with renewable energy, focused on implied impacts using resource availability maps, e.g. the biodiversity risk from global fossil fuel extraction (Butt et al., 2013) and potential threats to areas of biodiversity importance from oil and gas activities in Africa (Leach et al., 2016). The latter highlights the potential for different ministries to "double book" resources when there is no central spatial data repository – e.g. when both the energy and environment ministries claim the same parcel of land unaware of the other's claim to the same land – something unfortunately not fixed by generating higher and higher quality data. Harfoot et al. (2018) improved substantially on the analysis of Butt et al. (2013), but the spatially explicit oil and gas data they used are not open access.

The focus on replicability utilises OpenStreetMap's (and the global renewable energy estate's) constant state of flux. The ability to update the data at any time cements their utility for global progress assessments, but also allows the methodology to be tightened as more independent data become available. For example, post-publication, we were made aware of Swedish national wind data (available at `https://vbk.lansstyrelsen.se/sv`) that describe estimated annual production for wind installations in Sweden. These data can be easily included in the power estimations to further hone the capacity figures calculated for the OpenStreetMap data. Furthermore, the open access nature of the research gives the data further reach: scientists from the Open Energy Modelling Initiative have already started validating the wind data against one of the largest proprietary wind datasets, The Wind Power (available at `https://www.thewindpower.net`), and found the data to be as comprehensive (see analysis on GitHub – `https://github.com/JanFrederickUnnewehr/wind_dataset_comparison/blob/master/main.ipynb`) (Jan Frederick Unnewehr 2020, pers. comm., 5 June). The data were generated in such a way as to provide the simplest possible approximation of the global renewable energy estate and we welcome future validations of the methodology and data.

One of the most useful additions to the data for further research would, without a doubt, be the addition of operational dates, as with the renewable energy data used by Rehbein et al. (2020). Future snapshot updates of the dataset may achieve this, but the 2020 snapshot published does not describe the age of the installations presented. Estimates of the age could be achieved using the power densities of the wind installations, assuming that installations are optimally spaced (~ 10 turbine diameters apart). This could estimate the power capacities of the individual turbines, which in turn could estimate the year the installation was built as turbine capacities have been increasing year on year with newer models.

Operational dates could facilitate incredibly important global scale *local* biodiversity analyses, as done for land use (Newbold, Hudson, et al., 2016a), and could tie in with land change datasets to further isolate the relationship between land change and renewable energy development. It might also facilitate spatial analysis of the impact of various renewable policies. Figure 2.2 in Chapter 2 shows a clear *spatial* difference in solar PV policy between France and Germany; operational dates would allow assessment of *temporal* differences.

Whilst these analyses focused on specifically *utility*-scale renewable energy installations, there is much research to be done on built infrastructure and variable mounting of installations. Effort was made to include solar PV thought to be in an urban environment in the data despite not being used in the subsequent analysis in Chapter 3 – data coded as `urban=1`, classified by the 2015 Global Human Settlement Layer as *City*, *Dense town*, *Semi-dense town* or *Suburbs* (Pesaresi et al., 2019). We hope that these data can inform assessments of roof-mounted solar PV panels and small wind turbines, as well as providing a potential starting point for pinpointing an extremely dispersed (by definition) network of off-grid infrastructure.

Onshore wind and solar PV are two of the fastest growing renewable energy technologies, together comprising 90% of new renewable capacity built in 2019 (IRENA, 2019, 2020b). IRENA's *Transforming Energy Scenario* for 2050 (IRENA, 2020a) estimates wind (onshore and offshore) and solar PV will show enormous increases of 1,076% and 2,118% respectively. While this justifies this thesis' focus on these technologies, other renewable technologies will still be present in energy mixes. Hydropower currently comprises 47% of the global total installed renewable capacity; however, the technology has been excluded from previous studies as "*most of the potential sites have already been exploited*" (Santangeli et al., 2015, p. 943). Hydropower installation locations are already well documented (e.g. Lehner et al., 2011), as well as their impacts on biodiversity (Scherer & Pfister, 2016; Winemiller et al., 2016; Latrubesse et al., 2017). Hydropower was excluded from this thesis on this basis, as well as hydropower's somewhat limited terrestrial impact and obvious restriction to riverine sites. Other technologies (e.g. geothermal and marine – tidal and wave – energy) were excluded on the basis of their expected small contribution to renewable targets (IRENA, 2020a), although simple siting assessments with respect to biodiversity are evidently desirable given limited knowledge of their environmental impacts.

Finally, advancements in artificial intelligence and machine learning have the potential to revolutionise the identification of energy infrastructure, and updates made to the dataset presented in Chapter 1, made easy by the code supplied with the data, could take advantage of these improvements. For example, analysis for Dunnett et al. (2020) highlighted a number of extremely remote PV "panels" in rural Uganda that on random inspection appeared more likely to be corrugated iron roofs – this could be evidence for machine learning data already being present in the OpenStreetMap renewable infrastructure data. Research projects like the United Kingdom Research and Innovation (UKRI) funded solar 'nowcasting' project run by the Alan Turing Institute (available at `https://www.turing.ac.uk/research/research-projects/solar-nowcasting-machine-vision`) show the potential for such

data. The technology would not be restricted to energy infrastructure; improved classification of food and fuel crops at the field level (such as OneSoil – `https://onesoil.ai/en/`) would open up research into the fine-scale drivers of energy crops and develop a better understanding of how bioenergy expansion interacts with global food production.

Data for the foundations of sustainable land planning

Chapter 2 highlights the utility of higher quality spatial data for predicting human impact on the terrestrial surface. Even the most recent attempt at predicting areas of the Earth most likely to exhibit certain types of development (Oakleaf et al., 2019) falls short due to data limitations: the authors exclude 32.23% of the Earth's terrestrial area as unsuitable for solar PV, and as much as 76.86% for wind. However, the data generated here suggests there are a vast number of renewable energy installations present in these excluded areas. The data generated in this thesis are thus incredibly important for this application and others in refining our understanding of spatial dynamics that underpin sustainable land management.

Conservation scientists have long battled an emergent epidemic of alarmism. It appears to have grown root in the laudable sanctity of the precautionary principle, which "*counters the presumption that activities should proceed until and unless there is clear evidence that they are harmful, and supports action to anticipate and avert environmental harm in advance of, or without, a clear demonstration that such action is necessary*" (Cooney & Dickson (2012), 4-5; also Cooney (2004)). A recent paper that garnered international interest reflects this well – the study concluded that "*unless we change our ways of producing food, insects as a whole will go down the path of extinction in a few decades*" (Sánchez-Bayo & Wyckhuys, 2019, p. 22). Subsequent responses suggested that the study was "*alarmist by bad design*" (Komonen, Halme, & Kotiaho, 2019, p. 17) and called for "*more robust data and rigorous analyses*" (Thomas, Jones, & Hartley, 2019, p. 1891). Similarly, landscape ecologists have recently taken umbrage at the oft-repeated claim that habitat fragmentation *per se* is detrimental to biodiversity, when evidence reviews consistently prove its insignificance (Fahrig, 2019; Fahrig et al., 2019); "*Even patterns that seem well established, like the global decline in biodiversity ($\alpha - G$), have never been directly measured and rely on models to estimate the changes*", leading to calls for conservation scientists to better communicate the "*currently very large error bars in estimates of biodiversity trends*" (B. J. McGill et al., 2015, pp. 110–111).

The expansion of renewable energy, or even the shadow of it, has provided a similar environment for precautionary claims: Santangeli et al. (2015) highlight Central America as a "*single distinct hotspot of conflict*" between renewable energy and biodiversity (p. 949), whereas the work of Santangeli et al. (2016) "*suggests an impending threat to biodiversity, as the most densely populated countries have highest [renewable energy] potential concentrated within the top 30% biodiversity priority areas*" (p. 1198). The latter study even describes renewable energy as "*perhaps one of the major drivers of future land-use change*"

(p. 1199). Gasparatos et al. (2017) provide an excellently balanced view of renewable energy impact pathways on biodiversity, concluding that impacts may "*vary between technologies, locations and species; adopting the avoid-minimize-restore-compensate mitigation hierarchy would seem appropriate on a case-by-case basis*" (p. 175). The Rehbein et al. (2020) study was the first study to specifically interrogate the spatially explicit global relationship between areas of conservation importance and renewable energy. The study presents absolute and relative overlaps between the two land uses, concluding that "*overlaps are numerous, and are potentially compromising the goals of biodiversity conservation*" (p. 3048). However, the approach here provides some context to the absolute figures – overlaps are more numerous in Europe where there are more areas of conservation importance and renewable energy installations competing for space (Table A.3).

The global estate of areas of conservation importance (protected areas, KBAs, and wilderness areas) occupy a significant portion of the terrestrial surface despite overlapping significantly. While the spatial manipulation of finding the intersection of 61,091 multipolygon records (some with well over 100 constituent parts) proved too computationally prohibitive, rasterising the polygons to a resolution of 1-km^2 globally suggests that they could occupy a total of up to 30.8% of the terrestrial surface. As a result, zero overlap of the two land uses seems unrealistic, especially as many protected areas worldwide already contain housing infrastructure and cropland. Addition of a correction for area allowed the highlighting of regions where there are more or fewer overlaps than would be expected given the areas of both conservation importance and renewable energy (Figure 2.8, Chapter 2). Rehbein et al. (2020) go on to conclude that "*many important conservation areas contain renewable energy resources that could potentially be exploited to produce electricity in the future, and will likely face increased pressure from developments as the demand for renewable energy inevitably grows*" (pp. 3046-3047), something not borne out in the analyses here: although resource potential is one of a number of factors that drive the distribution of wind installations, it is not a factor that currently drives the distribution of solar PV installations (Figure 2.4, Chapter 2). Pressure from solar PV development should perhaps be considered more as an ancillary impact of urban area creep.

The new RF development probability layers were generated for a subset of global regions that contained sufficient renewable observations. The technique could be expanded to investigate potential renewable expansion sites in countries without significant extant renewable capacity. World regions have already been shown to exhibit different (and sometimes completely antithetical) effects of land drivers (Asselen & Verburg, 2012; Van Asselen & Verburg, 2013) which likely prevents simply adding excluded regions to previously analysed regions, and is also the reason why global RF maps were not produced. However, one way to approach such an analysis would be to use the land system archetypes (LSAs) described by Václavík et al. (2013). LSAs span continents and represent land systems with similar socio-economic and biophysical drivers. For example, East Asia comprises large expanses of LSA7 (*Extensive cropping systems*) and LSA8 (*Pastoral systems*) – both LSAs also commonly found in Africa.

East Asia contains many renewable energy installation observations, so may provide a good opportunity to predict likely renewable energy expansion areas in these LSAs in Africa.

One potential future avenue for research is alluded to briefly in Chapter 2: the association of high livestock densities with wind installations (see Figure 2.4). This is corroborated in Chapter 3 with wind's common association with *Cropland, high ls* land systems, especially in South Asia, Oceania and South America. One of the main proposed benefits of *marine* renewable energy infrastructure (MREI – currently largely referring to offshore wind) is the ability to shelter vulnerable fish life stages in *de facto* protected areas safe from mechanised fishing (Inger et al., 2009; Schuster et al., 2015); onshore wind farms could ameliorate biodiversity through a different mechanism – by co-locating intensive livestock systems within the installations. It is as yet unclear whether intensive livestock systems beget wind installations or vice versa; further research could identify the correct direction of effect. Operational dates, as suggested in Section 3.6, would greatly assist this endeavour.

Although local correlation analysis suggested there were no *regional* scale relationships between renewable energy development likelihood and conservation importance (Figure 2.6), there are still *sub*regional examples of high correlation: for example in the Central Europe case study, there is an area of 2,486km^2 that has a correlation value of $>$0.9. In regions with small viable terrestrial estates to work with, e.g. the Middle East, the RF probability surfaces can highlight potential conflict at a practical resolution for land planners. While evidence for the localised impacts of renewable energy structures is still being gathered (Gasparatos et al., 2017), the evidence base for impacts on, for example, soaring birds, is robust enough to utilise analyses like those presented here to direct wind deployment to areas of conservation importance for species other than threatened bird species (Thaxter et al., 2017; Santangeli et al., 2018).

Taking advantage of baseline land change to minimise the impact of renewables expansion

In Chapter 3 I generate a new, updated global map of land systems at 1 and 10-km^2 resolutions to seed a baseline land change scenario to the year 2040. I demonstrate that at 10-km^2 resolution onshore wind and solar PV are most commonly found in cropland and peri-urban land systems respectively, and that at a higher resolution of 1-km^2, the association with cropland becomes even more pronounced. At 10-km^2 resolution, urban, peri-urban and cropland land system areas increase under a baseline scenario of increasing food, urban housing, and livestock demand to 2040, revealing a potential opportunity to minimise developmental impacts of renewable energy by co-locating with projected cropland and peri-urban land systems.

In the CLUMondo analysis, I chose not to characterise renewable energy systems as their own land systems as there is little evidence that installations affect the management intensity or use of land systems even at 1-km^2 resolution. Large wind installations are found in intensive cropland with both low and high densities of livestock, and there are global examples of both technologies in every land system, including dense forest. As discussed in Chapter 3, there is also little evidence evaluating the impact of installations on crop yield, necessary for the land system competition component of CLUMondo to function.

Solar PV and its interaction with cropland is already a growing area of research (Marrou, 2019), with one recent study even suggesting that cropland microclimate provides the highest median solar energy potential of any land cover (Adeh et al., 2019) and another suggesting that food production could even increase under agrivoltaics (Barron-Gafford et al., 2019). This is encouraging for global solar PV deployment: the land change analysis presented here (and others) confirm that croplands are set to increase in area, especially in regions likely to benefit from renewable energy – e.g. West and East Africa, and Brazil (see Figure A.6 in Appendix A), providing plenty of land cover with high solar potential.

Bioenergy, or energy crops, represent an important unknown for global achievement of sustainability goals. As a negative emissions technology (NET), bioenergy represents a potentially huge opportunity to contribute to an increase in energy demand while at the same time removing CO_2 from the atmosphere. However, there is huge variability in the assumed placement and area of energy crops globally (a recent review – Smith et al. (2016) – suggested 380 to 700Mha, equivalent to 7-25% of agricultural land), as well as the yield that could be achieved (Slade et al., 2011; Fuss et al., 2018). There are also concerns that global bioenergy projections do not adequately take into account regional social and environmental dynamics (Donnison et al., 2020), and risk exacerbating overspill of planetary boundaries (Heck, Gerten, Lucht, & Popp, 2018).

As a result of the uncertainty in global deployment of bioenergy, I chose not to include energy crops in the baseline land change scenario. However, as some of the traditional crops considered for energy (e.g. *Miscanthus*) largely have the same biophysical requirements as food crops (except short rotation coppiced bioenergy, favoured for its tolerance of marginal agricultural land), it can be presumed that introducing bioenergy into land change models will almost inevitably lead to increased cropland; bioenergy's conflict with food production is well known (Donnison et al., 2020). As such, this dynamic is likely to increase further the land available for potential co-location of renewable energy.

The CLUMondo analysis includes regional year-on-year changes in crop yield and livestock stocking densities (Eitelberg et al. (2016), Supplementary Information) representing technological advances in farming. Any discussion on renewable energy installations and their association with land systems should at some point acknowledge the rapid development of renewable technologies. Onshore wind turbines are now manufactured with 4.8MW nameplate capacity, whereas offshore turbines are now manufactured with 10MW capacities –

a far cry from the first 100kW turbines. One of the driving factors of reductions in solar PV unit costs over the period 2005-2015 has been a linear increase in light-to-electricity conversion efficiency (Pillai, 2015).

Research must hold pace with technological improvements in installations, and how efficiency gains change spatial interactions – larger wind turbines may not be as compatible with cropland land systems, whereas increases in the solar conversion efficiency of PV inevitably removes solar energy from any agrivoltaic food system. Furthermore, improvements in ancillary energy services – transmission and storage – could also have important effects on renewable energy siting. Ancillary services are an area oft-overlooked in decarbonisation scenarios (Heard et al., 2017). I hypothesise in Chapter 3 that the difference in distributions of solar PV and onshore wind could be down to economics, and this would be an important avenue of research as both continually improve in efficiency to characterise how their associations with land systems differ, if at all. Currently there is little evidence to suggest, as Rehbein et al. (2020) do, that wilderness areas are under threat from utility-scale installations, but this may change as transmission improves and national grids become accustomed to the intermittent nature of renewable electricity generation.

The addition of operational dates to the data generated in Chapter 1 would allow further scrutiny of this effect. For example, Smith, Kern, Raven, & Verhees (2014) documented the subsequent stark increase in UK solar capacity from 26.5MWp in 2009 to 594MWp in 2011 in response to aggressive government feed-in tariffs. It may be the case that renewable installations built during this period, stripped of much of the economic burden of high development costs, were sited with much less of an eye for high resource potential. Increased knowledge of what affects siting of installations with respect to resource availability will allow researchers to make more use of the abundant literature on land suitability for renewable energy infrastructure.

The importance of place

For spatial analyses, especially those at the largest scales, the importance of the spatial context should always be considered. There exists with biodiversity conservation and renewable energy deployment, as with any other sustainability issue, a largely irreconcilable disconnect between analyses at the global scale and those at the local scale. For renewable energy, this is perfectly represented by the development potential indices generated by Oakleaf et al. (2019): the most recent, highest resolution representation of resource suitability layers. They generated data at 1-km^2 resolution globally, applying sensible spatial constraints backed by an extensive literature search, and this approach still misclassified 21.56% of installations worldwide. The appropriate spatial scale has long been a difficult concept to address in global sustainability studies (Eigenbrod et al., 2015), and it is clear that available independent variables have not yet caught up with the scale that renewable installations

clearly operate at. Global analyses will therefore rely on the assumption that fluctuations in the relationship will average out over the study region to provide a general perspective; this was the approach followed in Chapter 1, with the assumption that the sheer weight of the OpenStreetMap data would approximate a good general understanding of the global distribution of renewable energy. This assumption appeared to be justified by the results for simple correlations between the processed data and reported national capacities.

This was also one of the primary reasons I used the concept of land *systems* for Chapter 3; land systems "*serve as an efficient platform for integrating different perspectives and dimensions of land use research*" (Václavík et al., 2016, p. 14; citing Verburg et al., 2015). This use of land *systems* over land *cover* meant that for my analyses the influence of scale was tempered: not only did the distribution of land systems remain relatively stable (e.g. Figure 3.6) between spatial resolutions, but also the association of renewable energy with land systems (see Table A.4 and Table A.5 in Appendix A). Research by Václavík et al. (2016) sought to use a land systems approach to address this fundamental problem of transferability in place-based research. They used socio-economic systems described in previous work (Václavík et al., 2013) to estimate the *transferability* of place-based land projects to similar socio-economic systems. Although there was predictably a tendency for high transferability scores to cluster around the project site, there were many instances of high scores geographically distant. In Chapter 2, I aggregated results simply by regions delineated in the `maptools` **R** package with no real socio-economic justification; the approach provided by Václavík et al. (2016) provides a better evidenced framework for grouping regional environmental data. Moreover, this approach could have mitigated some of the concerns already mentioned and allowed me to extend the renewable energy probability surfaces beyond regions containing installations to regions with similar socio-economic profiles.

The generation of the cropland extent data used in Chapter 3 functions as an example of how extant data can be repurposed to answer questions at disparate scales from those originally intended. The GFSAD 30m data layer details cropland extent globally at an incredibly high resolution, intended mainly for food security analysis at a regional scale at most. Aggregation of these data using cell averages to a larger spatial scale allows the use of these data as percentage extent at the global scale seen here.

The importance of place is a fundamental disconnect emphasised by Allison et al. (2014) (and Yohe (2014)): that the costs to biodiversity of renewable energy construction and operation are accrued locally, but their benefits are dispersed regionally, if not globally. As such, it is incredibly hard to sensibly balance the environmental costs, and remains why this thesis focused largely on land change: land change is one of the most important drivers of biodiversity change locally, and scales much more predictably to larger scales than climate change.

The impacts of renewable energy on biodiversity also suffers from not only scale-dependent interactions, but also life cycle *and* scale-dependence. For example, impacts of the *construction* of solar panels may be restricted to the immediate locality, but the *operational* impacts, e.g. ecotoxicity of panel cleaning (Hernandez et al., 2014; Gasparatos et al., 2017), may be extended to the installation's immediate watershed. Again, I believe the focus of this analysis on the land change impacts of renewable infrastructure avoids many of these potential pitfalls. However, one area where the inclusion of context would greatly aid the interpretation of the data generated in Chapter 2 is the *ecological* context, especially the ecological fragility or resilience of the local environment. Although there were no significant regional trends in renewable energy and protected area placement (Figure 2.6), there may well be cells that contain especially fragile ecosystems that are more susceptible to developmental impacts; for these cells, any suggested positive correlation may reflect a need to suggest other cells be exploited first.

Data availability and open data

A common thread of this thesis quickly became the assimilation and use of data from a wide variety of sources. Chapter 1 evolved from my urgent need for spatially explicit data of renewable energy infrastructure with which to conduct the succeeding analyses in Chapters 2 and 3. The global data community is now exceedingly rich with high quality, high resolution datasets, e.g. a 30m crop mask (Oliphant et al., 2017), or 250m global soil data (`https://www.isric.org/explore/soilgrids`). While this means that analyses like those presented in this thesis can be conducted with a vast array of data, it also means that it becomes prohibitive to reliably assess the merits of each individual dataset. Data for one variable will have been collected and analysed very differently to other variables, and even within the same data theme, changing techniques over time may have a large effect on the output. This seemed to be the case with the Gridded Livestock of the World data for cattle, sheep and goats (Robinson et al., 2014). There appeared to be a substantial difference between the original 2005 data published in 2007, and the updated dataset for 2010, released in 2014. This produced some purportedly unnatural variation in the land system data generated in Chapter 3 (see, for example, changes in livestock land systems between Figure A.5a and A.5b in Appendix A), as well as seemingly removing the majority of global natural grassland (zero heads of livestock is one of the key thresholds for natural grassland) – most of which shifted to *Grassland, low ls*.

Continuity of data is something that is garnering more attention in land system science: while the land systems generated in Chapter 3 sought to emulate the Asselen & Verburg (2012) land systems as much as possible, only the percentage tree cover and percentage bare ground variables were time series data generated using the same methodology (Dimiceli et al. (2015)); livestock, as already mentioned, updated its methodology between 2005 and 2010. Updated urban and cropland extents were not available from the same source, and the

Neumann et al. (2010) data used for agricultural efficiency was so novel in its spatial nature and extent that the same data (for the year 2000) had to be used. New time series data, e.g. the European Space Agency Climate Change Initiative (ESA CCI) land cover data, have the potential to alleviate methodological inconsistencies and inspire exciting new research (e.g. analysis by Eigenbrod et al. (2020) of frontier crop expansion). Van Asselen & Verburg (2013) suggest that the availability of these sorts of data would greatly aid in the setting of land change model parameters.

One important caveat to the wealth of data currently available is that data tends to exist in data 'ecosystems'. This is most obvious when trying to amalgamate separate data sources; for example, crop extent and production data in Chapter 3. In the original land systems land change analysis by Van Asselen & Verburg (2013), crop production and extent were from the same data 'ecosystem': the 2008 *Farming the planet* report (Monfreda, Ramankutty, & Foley, 2008; Ramankutty, Evan, Monfreda, & Foley, 2008). For my updated analysis, I was forced to use crop extent data as generated from Oliphant et al. (2017), paired with spatially disaggregated production statistics from SPAM (HarvestChoice, 2014). As such, there was additional processing necessary in order to map the two datasets onto each other, as well as assumptions as to what food crops were analagous between them. This decision was made, despite the HarvestChoice (2014) data providing estimated crop production extents, to take advantage of the detail of the highly advanced Oliphant et al. (2017) data. One approach, beyond simply acknowledging the disparity between data 'ecosystems', is to ensure comparison of novel data with previous standards: Fritz et al. (2015) do this excellently, comparing their novel cropland data with the previous EarthStat data (Ramankutty et al., 2008).

Finally, this thesis has striven to follow an open data philosophy: I chose to publish Chapter 1 in an open access journal to ensure its freedom of use (Dunnett et al., 2020); as aforementioned, this has led to members of the Open Energy Modelling Initiative interrogating the data and validating it against similar, proprietary data (e.g. The Wind Power). The **R** code used to generate the data is also freely available, allowing users with geospatial (and **R** programming) experience to update the data for their own use as more information becomes available. Feedback from users has already resulted in an update to the data: they are now available in WGS 1984, as well as Eckert IV, as many users were not familiar with equal-area projections (Dunnett, 2020). This emphasis on openness has allowed feedback from the user community but unfortunately likely precludes the data from official use, for example as indicators of progress towards SDGs. Although suggested, it is more likely that these data facilitate civil society holding authorities to account for their climate ambitions, as well as more *reproducible* science.

Reproducible science and evaluating previous research

Reproducible science is arguably at risk as data and modelling complexity spirals. Houlahan et al. (2016) warn that ecology, for example, has "*abandoned prediction as a central focus and faces its own crisis of reproducibility*", and that "*ecologists rarely test to assess whether new models have made advances*" (p. 1); in a similar manner I would argue that the renewable energy and biodiversity conservation literatures are more balanced towards identifying new priority areas to target than assessing which approach land managers are appearing to take. For this reason, a large part of this thesis involved the assessment of prior work in order to get perspective on the current land management trajectory. The data generated in Chapter 1 allowed the assessment of the most recent, comprehensive assessment of likely development pressure from renewable energy (Oakleaf et al., 2019), which vastly improves upon previous work (e.g. Pogson et al., 2013). However, *post hoc* evaluation of the analysis, as Houlahan et al. (2016) suggest, identifies new variables of importance (e.g. the inclusion of socio-economic data), as well as improving parameter estimates (e.g. tempering the weight of slope and elevation in land constraints).

Analysis of the priority expansion areas produced by Pouzols et al. (2014) somewhat unexpectedly showed reasons to be encouraged with the growing global protected area estate. Although this analysis focused on Pouzols et al. (2014), the methodology is potentially transferable to other priority delineations identified in Chapter 2 (Hoekstra et al., 2004; Orme et al., 2005; Carwardine et al., 2008; Safi et al., 2013; Martin et al., 2014; Allan et al., 2017). Some measures of priority biodiversity areas have been shown not to be spatially congruent (Orme et al., 2005), but it would be useful to know where this is, and is not, the case.

The same can be said of land change projections. The global presentation of land system change by Van Asselen & Verburg (2013) is now ten years into its forty year projection. An initial idea for Chapter 3 involved collating data for 2010, and rerunning land change projections from the 2000 land systems to validate with empirical (as far as possible) data – while the data for 2000 and 2040 (i.e. start and end of run) land systems are freely available, mid-run projections (e.g. 2010) are not. This intended rerun was unfortunately precluded by the complexity of the CLUMondo land change model. The complexity greatly aids the scope of the model, but it also adds a high degree of variability to its functioning – Van Asselen & Verburg (2013) explain that, in the absence of quality global time series of land cover, "*for the moment, model calibration, therefore, relies on expert judgement or regional level time series of land cover data*" (p. 3661).

Uncertainty propagation

Just as uncertainty can perforate global analyses with the inclusion of too many datasets to adequately vet, uncertainty can also propagate through analyses *series*, like those presented in this thesis: i.e. when each subsequent analysis is built on the previous work. While I have made every effort to account for and address bias within each analysis, the potential stacking and accumulation of these uncertainties needs to be addressed. Data pertaining to China are an obvious and stark example. As highlighted in Chapter 1 (Technical Validation), China appears to have few data in OpenStreetMap generally, and this extends to renewable energy data. In my correlative models between reported renewables capacity and OpenStreetMap data, China has few data in comparison to its expected capacity. Although processing did improve the correlation considerably, we have to remain under the assumption that installation data for China are very uncertain.

Thus, when Chapter 2 sought to generate a Random Forest probability layer for East Asia, which includes China, the model was fed presumed incomplete data. As China, despite being incomplete, comprises the majority of the data for the region, this is likely to have affected the weighting of variables and the corresponding maps. For Chapter 2, this uncertainty was confounded by a detail identified by Rehbein et al. (2020): that China has removed a large portion of their national protected area data from the WDPA. This was the reason I proffered for the strong disparity between the protected area and KBA overlap models (Figure 2.8 and Table 2.1). As a result, overlap results for China suffer from two sources of potential bias: incomplete data for both renewable installations and protected areas.

For the land change data and models, there are similar uncertainties that are at risk of stacking. All cropland data are known to incorporate considerable error (Pérez-Hoyos, Rembold, Kerdiles, & Gallego, 2017); estimates of cropland availability have been shown to vary from 1,552 to 5,131 Mha (Eitelberg et al., 2015). The same could be true of vegetation or urban extent. As such, the results in Chapter 3 are presented with this knowledge; as mentioned for the difficulty of *place* in global analyses, this research was conducted with the assumption that these uncertainties would largely average out at global scale. However, it could also be the case, as with data for China, that there are regional hotspots of uncertainty. Although this would be undoubtedly useful to present, it was not investigated here. This thesis worked with the best possible data currently available and intended to provide an insight into general trends at global scale; I very much welcome data advancements that allow further interrogation of the approaches presented here.

The implications for global biodiversity of a transition to low carbon economies

The aim of this thesis represented an adaptation of the fourth grand challenge for biodiversity conservation in the face of renewable energy expansion set out by Katzner et al. (2013):

> A central assumption of renewable energy is that over the short term (<100yrs), the impacts of deployment are lesser than the business as usual scenario of continuing fossil fuel generation. Renewable energy may have an impact lessening climate change but they may also convert more habitat than fossil fuels so there is a need to explicitly define which implementation scenarios this central assumption is and is not met.

The approach here explored the global distribution of renewable energy with respect to areas of conservation importance, human and natural land systems. From the evidence presented here, renewable expansion is most likely to occur in tandem with, and masked by, more important drivers of land change like urbananisation and agricultural expansion. This research presents a global scale analysis of the spatial relationship between renewable energy deployment and biodiversity conservation. Importantly, it provides a framework within which to include the local impacts of onshore wind and solar PV when they are better known, or when higher resolution environmental data become available.

While many large-scale global assessments, e.g. the most recent IPBES Global Assessment, conclude that global biodiversity is declining, concrete (i.e. non-modelled) evidence of this decline eludes us (McGill et al., 2015). This uncertainty in the reaction of biodiversity to novel pressures drives conservationists' caution when assessing renewable energy. However, this thesis suggests that the contributions of renewable energy to land change, one of the most exigent threats to global biodiversity, are minimal. The potential benefits, on the other hand, of decarbonising economies and lessening the impact of climate change, are far from minimal. The work presented here provides evidence to continue targeting climate change as the greater of two evils. The road to energy sustainability is paved with good evidence, and I hope that the data generated in this thesis can help further interrogation of the spatial interplays between biodiversity conservation and renewable energy. While it may well be "*the end of the wild*", renewable energy is not the driving force.

This page intentionally left blank.

Appendix A

Supplementary Information

TABLE A.1: Summary statistics for renewable installations in areas of conservation priority.

	n	variable	mean	min	max	sd	sum	pct
Protected areas								
solar								
	305	power	16.04	0.85	695.13	67.11	4891.64	3.89
		landscape area	0.51	0.01	29.32	2.72	156.07	4.09
		panel area	0.46	0.01	29.32	2.71	141.51	4.58
		installations	1.91	1.00	20.00	2.23	583.00	4.84
wind								
	283	power	56.77	4.73	1159.43	116.29	16064.54	4.98
		landscape area	19.68	2.41	570.85	46.23	5569.68	4.42
		turbines	41.11	5.00	644.00	73.99	11633.00	4.91
		installations	2.72	1.00	63.00	4.90	771.00	6.13
Key Biodiversity Areas								
solar								
	327	power	48.31	0.85	3052.64	230.27	15798.63	12.57
		landscape area	1.59	0.01	155.68	9.93	519.58	13.61
		panel area	1.46	0.01	155.68	9.58	476.16	15.40
		installations	3.60	1.00	52.00	5.99	1176.00	9.77
wind								
	281	power	75.23	1.60	2702.35	196.27	21140.42	6.55
		landscape area	27.40	2.33	1156.68	81.15	7699.90	6.11
		turbines	54.75	5.00	1827.00	146.33	15386.00	6.50
		installations	3.88	1.00	52.00	6.18	1090.00	8.66
Wilderness areas								
solar								
	1	power	3.52	3.52	3.52	NA	3.52	0.00
		landscape area	0.06	0.06	0.06	NA	0.06	0.00
		panel area	0.06	0.06	0.06	NA	0.06	0.00
		installations	1.00	1.00	1.00	NA	1.00	0.01
wind								
	6	power	164.38	8.92	491.81	187.56	986.25	0.31
		landscape area	76.18	3.58	234.46	87.34	457.07	0.36
		turbines	93.67	19.00	275.00	102.41	562.00	0.24
		installations	7.50	1.00	20.00	7.97	45.00	0.36

TABLE A.2: Summary statistics for renewable installations in IUCN Category protected areas.

	n	variable	mean	min	max	sd	sum	pct
I-IV								
solar								
	27	power	9.14	0.89	80.64	16.74	246.71	0.20
		landscape area	0.29	0.01	2.28	0.49	7.77	0.20
		panel area	0.19	0.01	2.00	0.42	5.20	0.17
		installations	1.70	1.00	6.00	1.49	46.00	0.38
wind								
	25	power	90.80	8.71	1159.43	234.52	2270.07	0.70
		landscape area	38.42	3.01	570.85	114.48	960.51	0.76
		turbines	55.96	5.00	644.00	129.87	1399.00	0.59
		installations	4.80	1.00	63.00	12.50	120.00	0.95
V-VI								
solar								
	93	power	14.12	0.85	247.28	36.08	1313.38	1.05
		landscape area	0.38	0.01	8.60	1.15	35.77	0.94
		panel area	0.31	0.01	8.60	1.03	28.75	0.93
		installations	2.47	1.00	20.00	3.08	230.00	1.91
wind								
	76	power	58.42	4.73	1111.42	144.47	4440.27	1.38
		landscape area	20.78	2.48	380.57	50.90	1579.14	1.25
		turbines	41.29	5.00	624.00	84.44	3138.00	1.33
		installations	3.09	1.00	34.00	5.04	235.00	1.87
None								
solar								
	185	power	18.01	0.87	695.13	82.08	3331.54	2.65
		landscape area	0.61	0.01	29.32	3.40	112.53	2.95
		panel area	0.58	0.01	29.32	3.40	107.57	3.48
		installations	1.66	1.00	14.00	1.70	307.00	2.55
wind								
	182	power	51.40	6.09	517.21	70.27	9354.20	2.90
		landscape area	16.65	2.41	135.64	21.47	3030.02	2.40
		turbines	38.99	5.00	450.00	57.49	7096.00	3.00

TABLE A.3: Summary statistics for renewable installation overlaps with areas of conservation priority by region.

Area	Region	n
Protected areas	Southern Europe	228
	Central Europe	189
	Russia and the Balkans	86
	Northern Europe	27
	East Asia	22
Key Biodiversity Areas	Southern Europe	222
	Central Europe	154
	East Asia	51
	Russia and the Balkans	44
	Middle East	38
Wilderness areas	North America	3
	East Asia	2
	North Africa	1
	South Asia	1

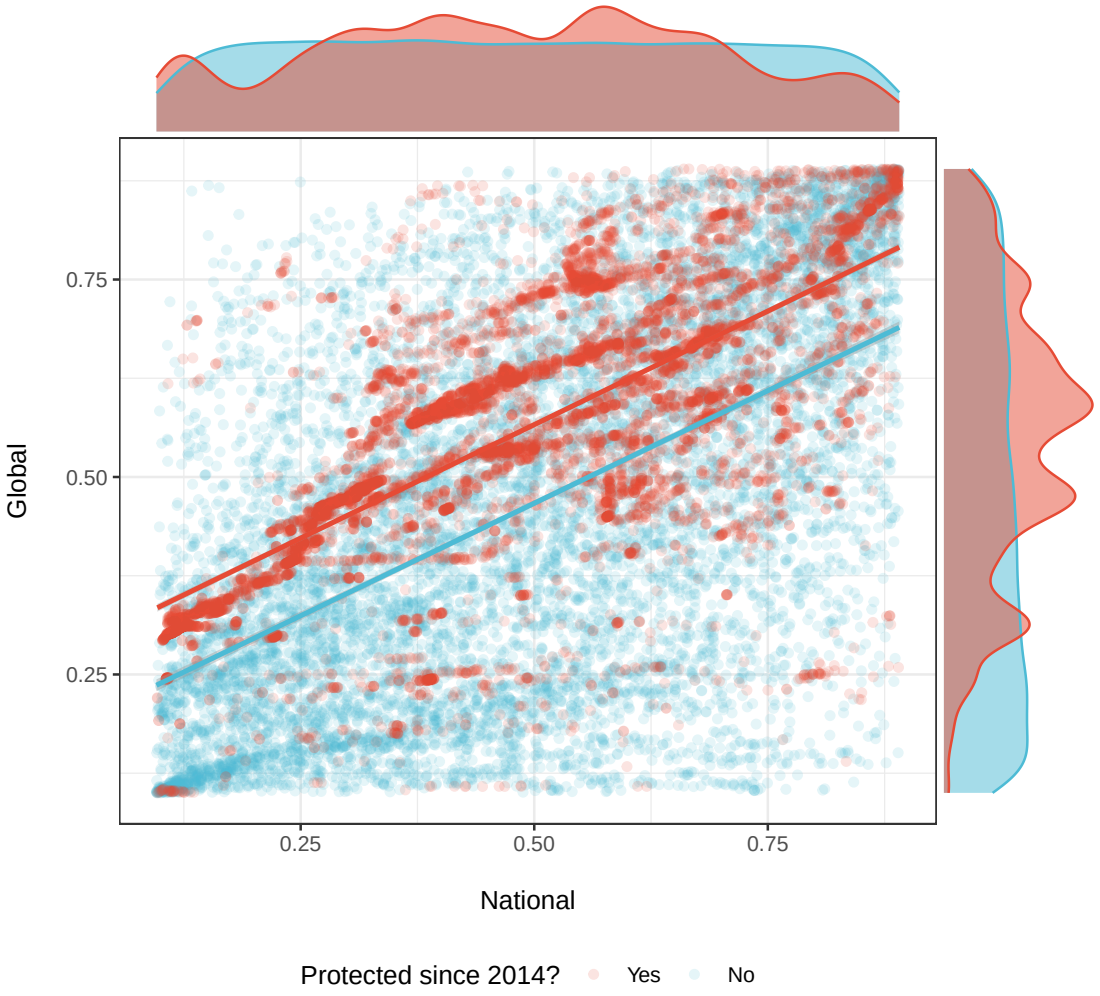

FIGURE A.1: Scatterplot showing biodiversity conservation rankings for 20,000 randomly selected 1-km^2 cells that were protected (n = 10,000) or not (n = 10,000) since 2014. The x axis shows national rankings, i.e. cells ranked per country, whereas the y axis shows global rankings, i.e. cells ranked globally irrespective of countries. Both scenarios are with 2040 land use. For full details, see Pouzols et al. (2014).

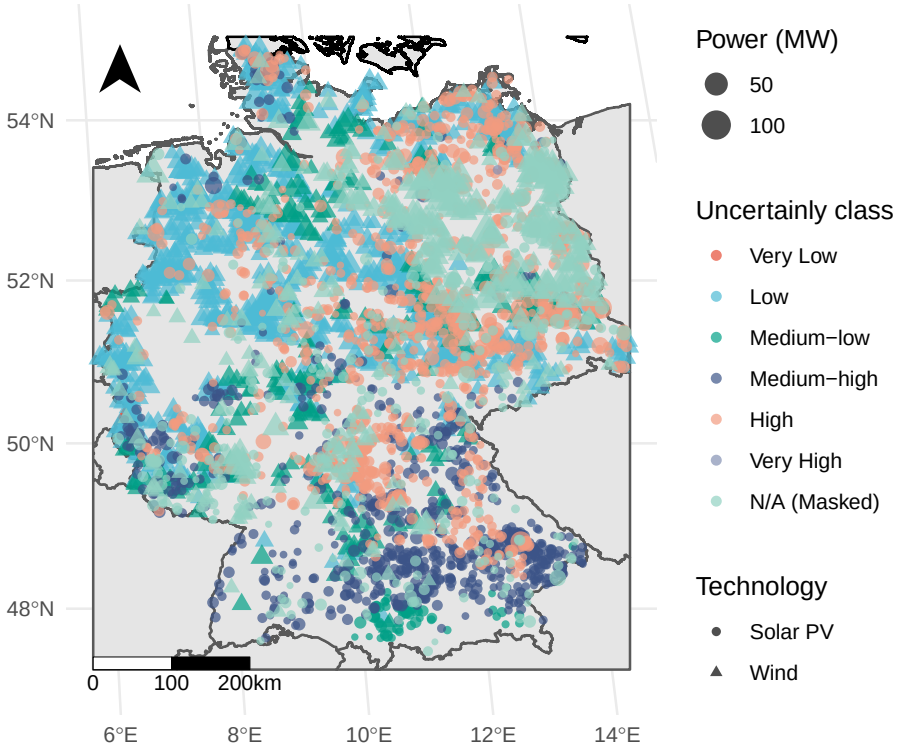

FIGURE A.2: Comparing a new spatially explicit wind and solar PV dataset with development potential indices using Germany as a case study. Map shows, for wind and solar respectively, installation location and power capacity (Dunnett, 2020) as well as the uncertainty class for DPI values, as described in Oakleaf et al. (2019). An uncertainty class of "N/A (Masked)" denotes an installation in a 1-km^2 cell that was masked with one of the constraints.

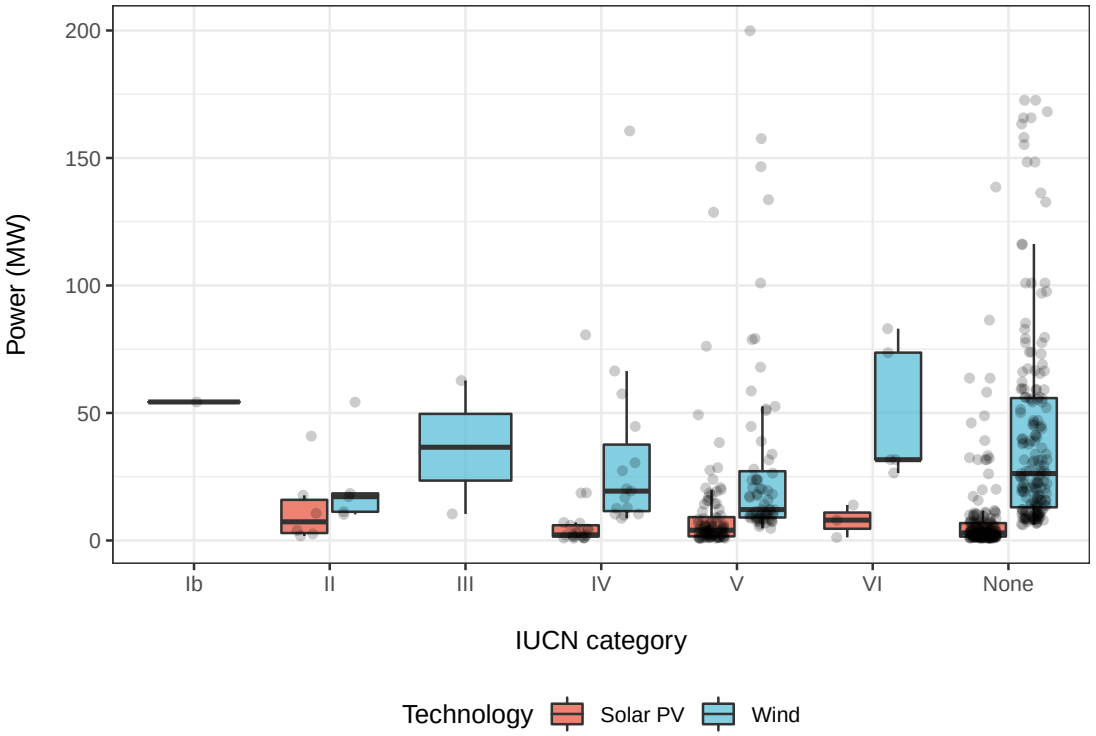

FIGURE A.3: Power distributions for onshore wind and solar PV in each IUCN protected area category (note Category Ia is absent as there were no overlaps with these areas).

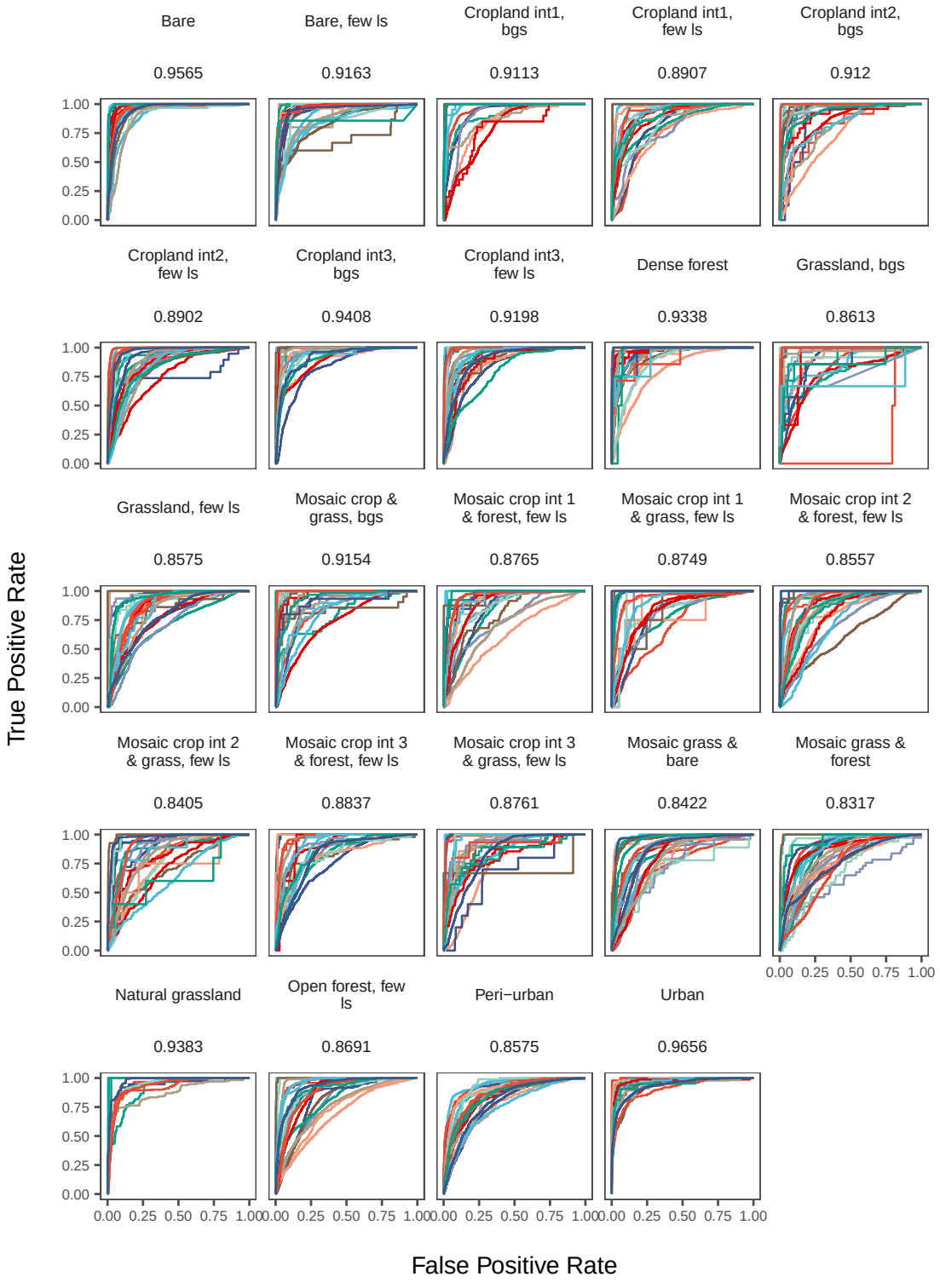

FIGURE A.4: ROC curves and mean AUC values for each land system class' land suitability model. Colours represent different model regions.

TABLE A.4: Differences in land area between 2010 and 2040 of the land systems with the highest renewable density per region.

	Model Region	Land System	Area	Percentage
Solar PV				
	Brazil	Peri-urban	533,910	247.7
	Canada	Mosaic intensive crop & forest, low ls	-31,744	-61.02
	East Asia	Bare, low ls	744,993	25.28
	Eastern Europe	Cropland medium, low ls	-367,234	-71.26
	Oceania	Mosaic grass & bare	-21,220	-0.5728
	South America	Bare, no ls	-411,128	-50.97
	South Asia	Bare, low ls	184,729	14.18
	USA	Peri-urban	-544,263	-66.45
	West Asia	Peri-urban	60,322	70.15
	Western Europe	Peri-urban	283,469	44.79
Wind				
	Brazil	Mosaic extensive crop & grass, low ls	82,482	40.47
	Canada	Cropland intensive, low ls	21,305	22.31
	East Asia	Bare, low ls	744,993	25.28
	Eastern Europe	Cropland medium, low ls	-367,234	-71.26
	Oceania	Cropland medium, high ls	-140,237	-56.93
	South America	Cropland medium, high ls	-89,584	-92
	South Asia	Cropland intensive, high ls	215,618	88.73
	USA	Cropland intensive, low ls	344,731	40.63
	West Asia	Mosaic medium crop & forest, low ls	-65,626	-79.07
	Western Europe	Cropland intensive, low ls	-50,482	-11.37

Note:
Areas in square kilometres.

TABLE A.5: Differences in land area between 2010 and 2040 of the land systems with the highest renewable density per region, irrespective of cropland intensity.

	Model Region	Land System	Area	Percentage
Solar PV				
	Brazil	Peri-urban	533,910	247.7
	Canada	Mosaic crop & forest	-77,177	-64.38
	East Asia	Bare, low ls	744,993	25.28
	Eastern Europe	Cropland, low ls	-164,879	-25.83
	Oceania	Mosaic grass & bare	-21,220	-0.5728
	South America	Bare, no ls	-411,128	-50.97
	South Asia	Bare, low ls	184,729	14.18
	USA	Peri-urban	-544,263	-66.45
	West Asia	Peri-urban	60,322	70.15
	Western Europe	Peri-urban	283,469	44.79
Wind				
	Brazil	Mosaic crop & grass	45,947	9.814
	Canada	Cropland, low ls	-44,321	-11.25
	East Asia	Bare, low ls	744,993	25.28
	Eastern Europe	Cropland, low ls	-164,879	-25.83
	Oceania	Cropland, high ls	22,674	8.604
	South America	Cropland, high ls	-81,969	-46.62
	South Asia	Cropland, high ls	124,151	8.333
	USA	Cropland, low ls	104,386	8.661
	West Asia	Mosaic crop & forest	-55,188	-65.02
	Western Europe	Cropland, low ls	-177,884	-26.23

Note:
Areas in square kilometres.

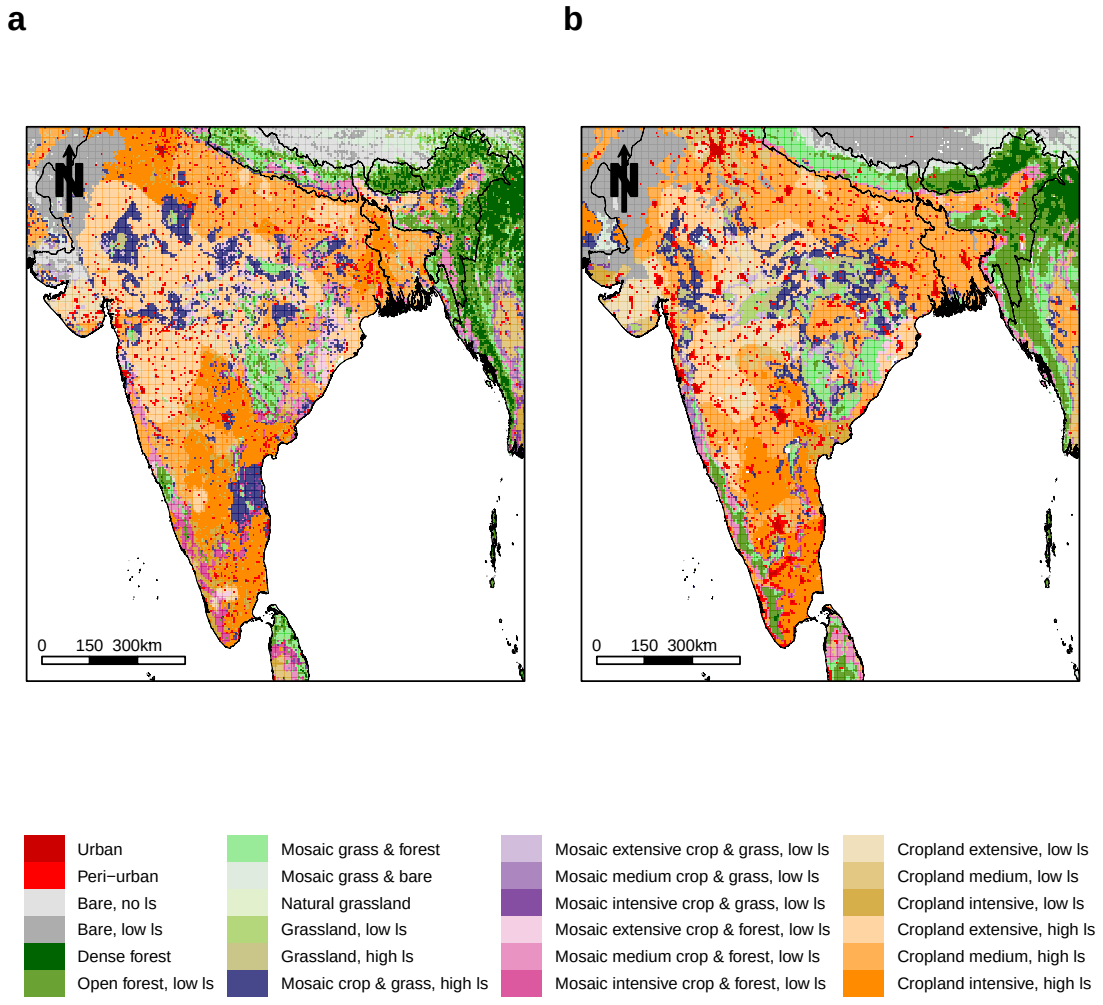

FIGURE A.5: A comparison of (a) land systems in 2000 (described in Asselen & Verburg (2012)) and (b) land systems in 2010, generated here, for India and its surroundings.

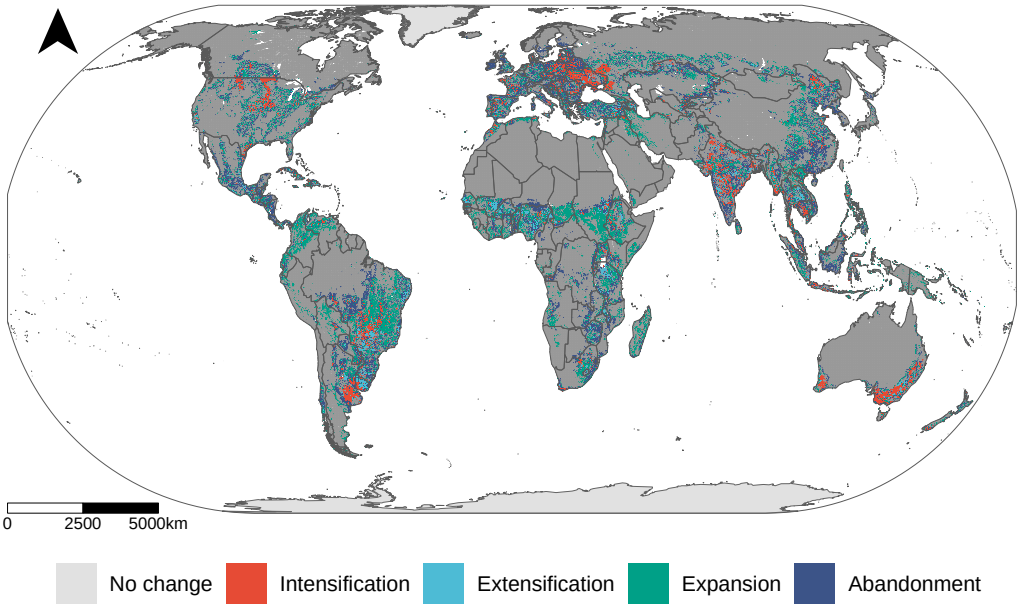

FIGURE A.6: Global cropland land system change between 2010 and 2040. Intensification describes an increase in management of extant cropland; extensification is a decrease in management. Expansion describes the appearance of mosaic or cropland land systems where previously absent; abandonment is the opposite.

References

Adeh, E. H., Good, S. P., Calaf, M., & Higgins, C. W. (2019). Solar PV Power Potential is Greatest Over Croplands. *Scientific Reports*, *9*(1), 11442. http://doi.org/10.1038/s41598-019-47803-3

Akçakaya, H. R., Butchart, S. H. M., Watson, J. E. M., & Pearson, R. G. (2014). Preventing species extinctions resulting from climate change. *Nature Climate Change*, *4*(12), 1048–1049. http://doi.org/10.1038/nclimate2455

Alexander, P., Rounsevell, M. D. A., Dislich, C., Dodson, J. R., Engström, K., & Moran, D. (2015). Drivers for global agricultural land use change: The nexus of diet, population, yield and bioenergy. *Global Environmental Change*, *35*, 138–147. http://doi.org/10.1016/j.gloenvcha.2015.08.011

Allan, J. R., Venter, O., & Watson, J. E. M. (2017). Temporally inter-comparable maps of terrestrial wilderness and the Last of the Wild. *Scientific Data*, *4*(1), 170187. http://doi.org/10.1038/sdata.2017.187

Allison, T. D., Root, T. L., & Frumhoff, P. C. (2014). Thinking globally and siting locally – renewable energy and biodiversity in a rapidly warming world. *Climatic Change*, *126*(1), 1–6. http://doi.org/10.1007/s10584-014-1127-y

Araújo, M. B., & Peterson, A. T. (2012). Uses and misuses of bioclimatic envelope modeling. *Ecology*, *93*(7), 1527–1539. http://doi.org/10.1890/11-1930.1

Armstrong, A., Burton, R. R., Lee, S. E., Mobbs, S., Ostle, N., Smith, V., ... Whitaker, J. (2016). Ground-level climate at a peatland wind farm in Scotland is affected by wind turbine operation. *Environmental Research Letters*, *11*(4), 044024. http://doi.org/10.1088/1748-9326/11/4/044024

Asselen, S. van, & Verburg, P. H. (2012). A Land System representation for global assessments and land-use modeling. *Global Change Biology*, *18*(10), 3125–3148. http://doi.org/10.1111/j.1365-2486.2012.02759.x

Bailey, K. M., McCleery, R. A., Binford, M. W., & Zweig, C. (2016). Land-cover change within and around protected areas in a biodiversity hotspot. *Journal of Land Use Science*,

11(2), 154–176. http://doi.org/10.1080/1747423X.2015.1086905

Barbet-Massin, M., Jiguet, F., Albert, C. H., & Thuiller, W. (2012). Selecting pseudo-absences for species distribution models: how, where and how many? *Methods in Ecology and Evolution*, *3*(2), 327–338. http://doi.org/10.1111/j.2041-210X.2011.00172.x

Barbosa, F. G., & Schneck, F. (2015). Characteristics of the top-cited papers in species distribution predictive models. *Ecological Modelling*, *313*, 77–83. http://doi.org/10.1016/j.ecolmodel.2015.06.014

Barrington-Leigh, C., & Millard-Ball, A. (2017). The world's user-generated road map is more than 80% complete. *PLOS ONE*, *12*(8), e0180698. http://doi.org/10.1371/journal.pone.0180698

Barron-Gafford, G. A., Pavao-Zuckerman, M. A., Minor, R. L., Sutter, L. F., Barnett-Moreno, I., Blackett, D. T., ... Macknick, J. E. (2019). Agrivoltaics provide mutual benefits across the food–energy–water nexus in drylands. *Nature Sustainability*, *2*(9), 848–855. http://doi.org/10.1038/s41893-019-0364-5

Baruch-Mordo, S., Kiesecker, J. M., Kennedy, C. M., Oakleaf, J. R., & Opperman, J. J. (2019). From Paris to practice: sustainable implementation of renewable energy goals. *Environmental Research Letters*, *14*(2), 024013. http://doi.org/10.1088/1748-9326/aaf6e0

BEIS. (2019). Renewable Energy Planning Database (REPD). Retrieved from https://data.gov.uk/dataset/a5b0ed13-c960-49ce-b1f6-3a6bbe0db1b7/renewable-energy-planning-database-repd

Bingham, H. C., Deguignet, M., Lewis, E., Stewart, J., Juffe-Bignoli, D., MacSharry, B., ... Kingston, N. (2019). *User Manual for the World Database on Protected Areas and world database on other effective area-based conservation measures: 1.6*. Cambridge, UK: UNEP-WCMC.

BirdLife International. (2019). Digital boundaries of Key Biodiversity Areas from the World Database of Key Biodiversity Areas. September 2019 Version. Retrieved from http://www.keybiodiversityareas.org/site/requestgis

Bivand, R., & Lewin-Koh, N. (2019). maptools: Tools for Handling Spatial Objects. Retrieved from https://cran.r-project.org/package=maptools

Blowers, A. (2013). *Planning for a sustainable environment.* Routledge.

Breiman, L. (2001). Random Forests. *Machine Learning*, *45*, 5–32. Retrieved from https://doi.org/10.1023/A:1010933404324

Brook, B. W., & Bradshaw, C. J. A. (2015). Key role for nuclear energy in global biodiversity conservation. *Conservation Biology*, *29*(3), 702–712. http://doi.org/10.1111/

cobi.12433

Brooks, T. M., Akçakaya, H. R., Burgess, N. D., Butchart, S. H. M., Hilton-Taylor, C., Hoffmann, M., ... Young, B. E. (2016). Analysing biodiversity and conservation knowledge products to support regional environmental assessments. *Scientific Data*, *3*, 160007. http://doi.org/10.1038/sdata.2016.7

Butt, N., Beyer, H. L., Bennett, J. R., Biggs, D., Maggini, R., Mills, M., ... Possingham, H. P. (2013). Biodiversity Risks from Fossil Fuel Extraction. *Science*, *342*(6157), 425–6. http://doi.org/10.1126/science.1237261

Carwardine, J., Wilson, K. A., Ceballos, G., Ehrlich, P. R., Naidoo, R., Iwamura, T., ... Possingham, H. P. (2008). Cost-effective priorities for global mammal conservation. *Proceedings of the National Academy of Sciences*, *105*(32), 11446–11450. http://doi.org/10.1073/pnas.0707157105

Chaudhary, A., & Kastner, T. (2016). Land use biodiversity impacts embodied in international food trade. *Global Environmental Change*, *38*, 195–204. http://doi.org/10.1016/j.gloenvcha.2016.03.013

Cohen, J. (1992). A power primer. *Psychological Bulletin*, *112*(1), 155.

Cooney, R. (2004). *The precautionary principle in biodiversity conservation and natural resource management: an issues paper for policy-makers, researchers and practitioners. No. 2*. IUCN.

Cooney, R., & Dickson, B. (2012). *Biodiversity and the precautionary principle: risk, uncertainty and practice in conservation and sustainable use.* Routledge.

Dimiceli, C., Carroll, M., Sohlberg, R., Kim, D. H., Kelly, M., & Townshend, J. R. G. (2015). MOD44B MODIS/Terra Vegetation Continuous Fields Yearly L3 Global 250m SIN Grid V006. http://doi.org/10.5067/MODIS/MOD44B.006

Di Minin, E., & Toivonen, T. (2015). Global Protected Area Expansion: Creating More than Paper Parks. *BioScience*, *65*(7), 637–638. http://doi.org/10.1093/biosci/biv064

Dinerstein, E., Olson, D., Joshi, A., Vynne, C., Burgess, N. D., Wikramanayake, E., ... Saleem, M. (2017). An Ecoregion-Based Approach to Protecting Half the Terrestrial Realm. *BioScience*, *67*(6), 534–545. http://doi.org/10.1093/biosci/bix014

Dinerstein, E., Vynne, C., Sala, E., Joshi, A. R., Fernando, S., Lovejoy, T. E., ... Wikramanayake, E. (2019). A Global Deal For Nature: Guiding principles, milestones, and targets. *Science Advances*, *5*(4), eaaw2869. http://doi.org/10.1126/sciadv.aaw2869

Donnison, C., Holland, R. A., Hastings, A., Armstrong, L., Eigenbrod, F., & Taylor, G. (2020). Bioenergy with Carbon Capture and Storage (BECCS): Finding the win-wins for energy, negative emissions and ecosystem services - size matters. *GCB Bioenergy*, gcbb.12695. http://doi.org/10.1111/gcbb.12695

Doxsey-Whitfield, E., MacManus, K., Adamo, S. B., Pistolesi, L., Squires, J., Borkovska, O., & Baptista, S. R. (2015). Taking Advantage of the Improved Availability of Census Data: A First Look at the Gridded Population of the World, Version 4. *Papers in Applied Geography*, *1*(3), 226–234. http://doi.org/10.1080/23754931.2015.1014272

Dudley, N., Shadie, P., & Stolton, S. (2013). *Guidelines for Applying Protected Area Management Categories*. (N. Dudley, Ed.) (pp. x, 86p.+ iv, 31p.: ill). Gland, Switzerland: IUCN. Retrieved from https://portals.iucn.org/library/node/30018

Dunnett, S. (2020). Harmonised global datasets of wind and solar farm locations and power. *Figshare*. http://doi.org/https://doi.org/10.6084/m9.figshare.11310269

Dunnett, S., Sorichetta, A., Taylor, G., & Eigenbrod, F. (2020). Harmonised global datasets of wind and solar farm locations and power. *Scientific Data*, *7*(130). http://doi.org/10.1038/s41597-020-0469-8

Eichhorn, M., Scheftelowitz, M., Reichmuth, M., Lorenz, C., Louca, K., Schiffler, A., ... Thrän, D. (2019). Spatial Distribution of Wind Turbines, Photovoltaic Field Systems, Bioenergy, and River Hydro Power Plants in Germany. *Data*, *4*(1), 29. http://doi.org/10.3390/data4010029

Eigenbrod, F., Beckmann, M., Dunnett, S., Graham, L., Holland, R. A., Meyfroidt, P., ... Verburg, P. H. (2020). Identifying frontiers of global cropland expansion. *One Earth*, (In press).

Eigenbrod, F., Gonzalez, P., Dash, J., & Steyl, I. (2015). Vulnerability of ecosystems to climate change moderated by habitat intactness. *Global Change Biology*, *21*(1), 275–286. http://doi.org/10.1111/gcb.12669

Eisner, R., Seabrook, L. M., & McAlpine, C. A. (2016). Are changes in global oil production influencing the rate of deforestation and biodiversity loss? *Biological Conservation*, *196*, 147–155. http://doi.org/10.1016/j.biocon.2016.02.017

Eitelberg, D. A., Vliet, J. van, Doelman, J. C., Stehfest, E., & Verburg, P. H. (2016). Demand for biodiversity protection and carbon storage as drivers of global land change scenarios. *Global Environmental Change*, *40*, 101–111. http://doi.org/10.1016/j.gloenvcha.2016.06.014

Eitelberg, D. A., Vliet, J. van, & Verburg, P. H. (2015). A review of global potentially available cropland estimates and their consequences for model-based assessments. *Global Change Biology*, *21*(3), 1236–1248. http://doi.org/10.1111/gcb.12733

Elith, J., H. Graham, C., P. Anderson, R., Dudík, M., Ferrier, S., Guisan, A., ... E. Zimmermann, N. (2006). Novel methods improve prediction of species' distributions from occurrence data. *Ecography*, *29*(2), 129–151. http://doi.org/10.1111/j.2006.0906-7590.04596.x

Ellis, E. C., Goldewijk, K. K., Siebert, S., Lightman, D., & Ramankutty, N. (2010). Anthropogenic transformation of the biomes, 1700 to 2000. *Global Ecology and Biogeography*, *19*(5), 589–606. http://doi.org/10.1111/j.1466-8238.2010.00540.x

Ellis, E. C., Kaplan, J. O., Fuller, D. Q., Vavrus, S., Klein Goldewijk, K., & Verburg, P. H. (2013). Used planet: A global history. *Proceedings of the National Academy of Sciences*, *110*(20), 7978–7985. http://doi.org/10.1073/pnas.1217241110

Ellis, E. C., & Ramankutty, N. (2008). Putting people in the map: anthropogenic biomes of the world. *Frontiers in Ecology and the Environment*, *6*(8), 439–447. http://doi.org/10.1890/070062

Enevoldsen, P., Permien, F.-H., Bakhtaoui, I., Krauland, A.-K. von, Jacobson, M. Z., Xydis, G., ... Oxley, G. (2019). How much wind power potential does Europe have? Examining European wind power potential with an enhanced socio-technical atlas. *Energy Policy*, *132*, 1092–1100. http://doi.org/10.1016/j.enpol.2019.06.064

Enevoldsen, P., & Valentine, S. V. (2016). Do onshore and offshore wind farm development patterns differ? *Energy for Sustainable Development*, *35*, 41–51. http://doi.org/10.1016/j.esd.2016.10.002

Ester, M., Kriegel, H.-P., Sander, J., & Xu, X. (1996). A Density-based Algorithm for Discovering Clusters a Density-based Algorithm for Discovering Clusters in Large Spatial Databases with Noise. In *Proceedings of the second international conference on knowledge discovery and data mining* (pp. 226–231). AAAI Press. Retrieved from http://dl.acm.org/citation.cfm?id=3001460.3001507

Evans, J. S., & Kiesecker, J. M. (2014). Shale Gas, Wind and Water: Assessing the Potential Cumulative Impacts of Energy Development on Ecosystem Services within the Marcellus Play. *PLoS ONE*, *9*(2), e89210. http://doi.org/10.1371/journal.pone.0089210

Fahrig, L. (2019). Habitat fragmentation: A long and tangled tale. *Global Ecology and Biogeography*, *28*(1), 33–41. http://doi.org/10.1111/geb.12839

Fahrig, L., Arroyo-Rodríguez, V., Bennett, J. R., Boucher-Lalonde, V., Cazetta, E., Currie, D. J., ... Watling, J. I. (2019). Is habitat fragmentation bad for biodiversity? *Biological Conservation*, *230*, 179–186. http://doi.org/10.1016/j.biocon.2018.12.026

Finer, M., Jenkins, C. N., Pimm, S. L., Keane, B., & Ross, C. (2008). Oil and gas projects in the Western Amazon: Threats to wilderness, biodiversity, and indigenous peoples. *PLoS ONE*, *3*(8). http://doi.org/10.1371/journal.pone.0002932

Fritsche, U. R., Berndes, G., Cowie, A. L., Dale, V. H., Kline, K. L., Johnson, F. X., ... Woods, J. (2017). *Energy and Land Use - Global Land Outlook Working Paper*. UNCCD; IRENA. http://doi.org/10.13140/RG.2.2.24905.44648

Fritz, S., See, L., McCallum, I., You, L., Bun, A., Moltchanova, E., ... Obersteiner, M.

(2015). Mapping global cropland and field size. *Global Change Biology*, *21*(5), 1980–1992. http://doi.org/10.1111/gcb.12838

Fthenakis, V., & Kim, H. C. (2009). Land use and electricity generation: A life-cycle analysis. *Renewable and Sustainable Energy Reviews*, *13*(6-7), 1465–1474. http://doi.org/10.1016/j.rser.2008.09.017

Fuss, S., Lamb, W. F., Callaghan, M. W., Hilaire, J., Creutzig, F., Amann, T., ... Minx, J. C. (2018). Negative emissions—Part 2: Costs, potentials and side effects. *Environmental Research Letters*, *13*(6), 063002. http://doi.org/10.1088/1748-9326/aabf9f

Gao, L., & Bryan, B. A. (2017). Finding pathways to national-scale land-sector sustainability. *Nature*, *544*(7649), 217–222. http://doi.org/10.1038/nature21694

García-Callejas, D., & Araújo, M. B. (2016). The effects of model and data complexity on predictions from species distributions models. *Ecological Modelling*, *326*, 4–12. http://doi.org/10.1016/j.ecolmodel.2015.06.002

Gasparatos, A., Doll, C. N. H., Esteban, M., Ahmed, A., & Olang, T. A. (2017). Renewable energy and biodiversity: Implications for transitioning to a Green Economy. *Renewable and Sustainable Energy Reviews*, *70*, 161–184. http://doi.org/10.1016/j.rser.2016.08.030

Gibbs, H. K., Ruesch, A. S., Achard, F., Clayton, M. K., Holmgren, P., Ramankutty, N., & Foley, J. A. (2010). Tropical forests were the primary sources of new agricultural land in the 1980s and 1990s. *Proceedings of the National Academy of Sciences*, *107*(38), 16732–16737. http://doi.org/10.1073/pnas.0910275107

Gibson, L., Wilman, E. N., & Laurance, W. F. (2017). How Green is 'Green' Energy? *Trends in Ecology & Evolution*. http://doi.org/10.1016/j.tree.2017.09.007

Goetzberger, A., & Zastrow, A. (1982). On the Coexistence of Solar-Energy Conversion and Plant Cultivation. *International Journal of Solar Energy*, *1*(1), 55–69. http://doi.org/10.1080/01425918208909875

Golden Kroner, R. E., Qin, S., Cook, C. N., Krithivasan, R., Pack, S. M., Bonilla, O. D., ... Mascia, M. B. (2019). The uncertain future of protected lands and waters. *Science*, *364*(6443), 881–886. http://doi.org/10.1126/science.aau5525

Golding, N., August, T. A., Lucas, T. C. D., Gavaghan, D. J., Loon, E. E., & McInerny, G. (2018). The zoon r package for reproducible and shareable species distribution modelling. *Methods in Ecology and Evolution*, *9*(2), 260–268. http://doi.org/10.1111/2041-210X.12858

Gonzalez, P., Neilson, R. P., Lenihan, J. M., & Drapek, R. J. (2010). Global patterns in the vulnerability of ecosystems to vegetation shifts due to climate change. *Global Ecology and Biogeography*, *19*(6), 755–768. http://doi.org/10.1111/j.1466-8238.2010.

00558.x

Gove, B., Williams, L. J., Beresford, A. E., Roddis, P., Campbell, C., Teuten, E., ... Bradbury, R. B. (2016). Reconciling Biodiversity Conservation and Widespread Deployment of Renewable Energy Technologies in the UK. *Plos One*, *11*(5), e0150956. http://doi.org/10.1371/journal.pone.0150956

Grassini, P., Eskridge, K. M., & Cassman, K. G. (2013). Distinguishing between yield advances and yield plateaus in historical crop production trends. *Nature Communications*, *4*(1), 2918. http://doi.org/10.1038/ncomms3918

Gray, C. L., Hill, S. L. L., Newbold, T., Hudson, L. N., Börger, L., Contu, S., ... Scharlemann, J. P. W. (2016). Local biodiversity is higher inside than outside terrestrial protected areas worldwide. *Nature Communications*, *7*(May), 12306. http://doi.org/10.1038/ncomms12306

Greenberg, J. A., & Mattiuzzi, M. (2018). gdalUtils: Wrappers for the Geospatial Data Abstraction Library (GDAL) Utilities. R package version 2.0.1.14. Retrieved from https://cran.r-project.org/package=gdalUtils

Harfoot, M. B. J., Tittensor, D. P., Knight, S., Arnell, A. P., Blyth, S., Brooks, S., ... Burgess, N. D. (2018). Present and future biodiversity risks from fossil fuel exploitation. *Conservation Letters*, e12448. http://doi.org/10.1111/conl.12448

Harper, M., Anderson, B., James, P. A. B., & Bahaj, A. S. (2019). Onshore wind and the likelihood of planning acceptance: Learning from a Great Britain context. *Energy Policy*, *128*, 954–966. http://doi.org/10.1016/J.ENPOL.2019.01.002

HarvestChoice. (2014). Crop Production: SPAM. International Food Policy Research Institute, Washington, DC.,; University of Minnesota, St. Paul, MN. Retrieved from http://harvestchoice.org/node/9716

Hassanpour Adeh, E., Selker, J. S., & Higgins, C. W. (2018). Remarkable agrivoltaic influence on soil moisture, micrometeorology and water-use efficiency. *PLOS ONE*, *13*(11), e0203256. http://doi.org/10.1371/journal.pone.0203256

Heard, B. P., Brook, B. W., Wigley, T. M. L., & Bradshaw, C. J. A. (2017). Burden of proof: A comprehensive review of the feasibility of 100% renewable-electricity systems. *Renewable and Sustainable Energy Reviews*, *76*, 1122–1133. http://doi.org/10.1016/j.rser.2017.03.114

Heck, V., Gerten, D., Lucht, W., & Popp, A. (2018). Biomass-based negative emissions difficult to reconcile with planetary boundaries. *Nature Climate Change*, *8*(2), 151–155. http://doi.org/10.1038/s41558-017-0064-y

Hernandez, R. R., Armstrong, A., Burney, J., Ryan, G., Moore-O'Leary, K., Diédhiou, I.,

... Kammen, D. M. (2019). Techno–ecological synergies of solar energy for global sustainability. *Nature Sustainability*, *2*(7), 560–568. http://doi.org/10.1038/s41893-019-0309-z

Hernandez, R. R., Easter, S. B., Murphy-Mariscal, M. L., Maestre, F. T., Tavassoli, M., Allen, E. B., ... Allen, M. F. (2014). Environmental impacts of utility-scale solar energy. *Renewable and Sustainable Energy Reviews*, *29*, 766–779. http://doi.org/10.1016/j.rser.2013.08.041

Hernandez, R. R., Hoffacker, M. K., Murphy-Mariscal, M. L., Wu, G. C., & Allen, M. F. (2015). Solar energy development impacts on land cover change and protected areas. *Proceedings of the National Academy of Sciences*, *112*(44), 13579–13584. http://doi.org/10.1073/pnas.1517656112

Hertwich, E. G., Gibon, T., Bouman, E. A., Arvesen, A., Suh, S., Heath, G. A., ... Shi, L. (2014). Integrated life-cycle assessment of electricity-supply scenarios confirms global environmental benefit of low-carbon technologies. *Proceedings of the National Academy of Sciences of the United States of America*, *112*(20), 6277–6282. http://doi.org/10.1073/pnas.1312753111

Hijmans, R. J. (2017). raster: Geographic Data Analysis and Modeling. R package version 2.6-7. Retrieved from https://cran.r-project.org/package=raster

Hodas, D. R. (2008). Biodiversity and Climate Change Laws: A Failure to Communicate? In M. I. Jeffery, J. Firestone, & K. Buna-Litic (Eds.), *Biodiversity conservation, law and livelihoods: Bridging the north-south divide* (pp. 383–399). Cambridge University Press. http://doi.org/10.1017/CBO9780511551161.023

Hoekstra, J. M., Boucher, T. M., Ricketts, T. H., & Roberts, C. (2004). Confronting a biome crisis: global disparities of habitat loss and protection. *Ecology Letters*, *8*(1), 23–29. http://doi.org/10.1111/j.1461-0248.2004.00686.x

Hoen, B., Diffendorfer, J., Rand, J., Kramer, L., Garrity, C., & Hunt, H. (2019). United States Wind Turbine Database. U.S. Geological Survey, American Wind Energy Association, and Lawrence Berkeley National Laboratory data release: USWTDB V2.2. http://doi.org/10.5066/F7TX3DN0

Hole, D. G., Willis, S. G., Pain, D. J., Fishpool, L. D., Butchart, S. H. M., Collingham, Y. C., ... Huntley, B. (2009). Projected impacts of climate change on a continent-wide protected area network. *Ecology Letters*, *12*(5), 420–431. http://doi.org/10.1111/j.1461-0248.2009.01297.x

Holland, R. A., Beaumont, N., Hooper, T., Austen, M., Gross, R. J. K., Heptonstall, P. J., ... Taylor, G. (2018). Incorporating ecosystem services into the design of future energy systems. *Applied Energy*, *222*, 812–822. http://doi.org/10.1016/j.apenergy.2018.04.022

Holland, R. A., Scott, K. A., Flörke, M., Brown, G., Ewers, R. M., Farmer, E., ... Eigenbrod, F. (2015). Global impacts of energy demand on the freshwater resources of nations. *Proceedings of the National Academy of Sciences*, *112*(48), E6707–E6716. http://doi.org/10.1073/pnas.1507701112

Holland, R. A., Scott, K., Agnolucci, P., Rapti, C., Eigenbrod, F., & Taylor, G. (2019). The influence of the global electric power system on terrestrial biodiversity. *Proceedings of the National Academy of Sciences*, *116*(51), 26078–26084. http://doi.org/10.1073/pnas.1909269116

Holland, R. A., Scott, K., Hinton, E. D., Austen, M. C., Barrett, J., Beaumont, N., ... Taylor, G. (2016). Bridging the gap between energy and the environment. *Energy Policy*, *92*, 181–189. http://doi.org/10.1016/j.enpol.2016.01.037

Houlahan, J. E., Mckinney, S. T., Anderson, T. M., & Mcgill, B. J. (2016). The priority of prediction in ecological understanding. *Oikos*, (August), 1–7. http://doi.org/10.1111/oik.03726

Howard, D. C., Burgess, P. J., Butler, S. J., Carver, S. J., Cockerill, T., Coleby, A. M., ... Scholefield, P. (2013). Energyscapes: Linking the energy system and ecosystem services in real landscapes. *Biomass and Bioenergy*, *55*, 17–26. http://doi.org/10.1016/j.biombioe.2012.05.025

Hudson, L. N., Newbold, T., Contu, S., Hill, S. L. L., Lysenko, I., De Palma, A., ... Purvis, A. (2016). The database of the PREDICTS (Projecting Responses of Ecological Diversity In Changing Terrestrial Systems) project. *Ecology and Evolution*, (September 2016), 145–188. http://doi.org/10.1002/ece3.2579

Hui, I., Cain, B. E., & Dabiri, J. O. (2018). Public receptiveness of vertical axis wind turbines. *Energy Policy*, *112*, 258–271. http://doi.org/10.1016/j.enpol.2017.10.028

Ibisch, P. L., Hoffmann, M. T., Kreft, S., Pe'er, G., Kati, V., Biber-Freudenberger, L., ... Selva, N. (2016). A global map of roadless areas and their conservation status. *Science*, *354*(6318), 1423–1427. http://doi.org/10.1126/science.aaf7166

IEA. (2019). *Renewables 2019*. Paris: IEA. Retrieved from https://www.iea.org/reports/renewables-2019

Inger, R., Attrill, M. J., Bearhop, S., Broderick, A. C., James Grecian, W., Hodgson, D. J., ... Godley, B. J. (2009). Marine renewable energy: Potential benefits to biodiversity? An urgent call for research. *Journal of Applied Ecology*, *46*(6), 1145–1153. http://doi.org/10.1111/j.1365-2664.2009.01697.x

IRENA. (2019). *Renewable energy highlights*. Abu Dhabi: The International Renewable Energy Agency.

IRENA. (2020a). *Global Renewables Outlook: Energy transformation 2050*. Abu Dhabi: International Renewable Energy Agency.

IRENA. (2020b). *Renewable energy highlights*. Abu Dhabi: The International Renewable Energy Agency.

Jackson, A. L. R. (2011). Renewable energy vs. biodiversity: Policy conflicts and the future of nature conservation. *Global Environmental Change*, *21*(4), 1195–1208. http://doi.org/10.1016/j.gloenvcha.2011.07.001

Jensen, C. U., Panduro, T. E., Lundhede, T. H., Nielsen, A. S. E., Dalsgaard, M., & Thorsen, B. J. (2018). The impact of on-shore and off-shore wind turbine farms on property prices. *Energy Policy*, *116*, 50–59. http://doi.org/10.1016/j.enpol.2018.01.046

Jetz, W., Wilcove, D. S., & Dobson, A. P. (2007). Projected impacts of climate and land-use change on the global diversity of birds. *PLoS Biology*, *5*(6), 1211–1219. http://doi.org/10.1371/journal.pbio.0050157

Kalnay, E., & Cai, M. (2003). Impact of urbanization and land-use change on climate. *Nature*, *423*(6939), 528–531. http://doi.org/10.1038/nature01675

Kaplan, J. O., Krumhardt, K. M., & Zimmermann, N. (2009). The prehistoric and preindustrial deforestation of Europe. *Quaternary Science Reviews*, *28*(27-28), 3016–3034. http://doi.org/10.1016/j.quascirev.2009.09.028

Katzner, T., Johnson, J. A., Evans, D. M., Garner, T. W. J., Gompper, M. E., Altwegg, R., ... Pettorelli, N. (2013). Challenges and opportunities for animal conservation from renewable energy development. *Animal Conservation*, *16*(4), 367–369. http://doi.org/10.1111/acv.12067

Kiesecker, J., Baruch-Mordo, S., Kennedy, C. M., Oakleaf, J. R., Baccini, A., & Griscom, B. W. (2019). Hitting the Target but Missing the Mark: Unintended Environmental Consequences of the Paris Climate Agreement. *Frontiers in Environmental Science*, *7*. http://doi.org/10.3389/fenvs.2019.00151

Kiesecker, J. M., Evans, J. S., Fargione, J., Doherty, K., Foresman, K. R., Kunz, T. H., ... Niemuth, N. D. (2011). Win-Win for Wind and Wildlife: A Vision to Facilitate Sustainable Development. *PLoS ONE*, *6*(4), e17566. http://doi.org/10.1371/journal.pone.0017566

Komonen, A., Halme, P., & Kotiaho, J. S. (2019). Alarmist by bad design: Strongly popularized unsubstantiated claims undermine credibility of conservation science. *Rethinking Ecology*, *4*, 17–19. http://doi.org/10.3897/rethinkingecology.4.34440

Köppel, J., Dahmen, M., Helfrich, J., Schuster, E., & Bulling, L. (2014). Cautious but Committed: Moving Toward Adaptive Planning and Operation Strategies for Renewable Energy's Wildlife Implications. *Environmental Management*, *54*(4), 744–755. http:

//doi.org/10.1007/s00267-014-0333-8

Kriegel, H., Kröger, P., Sander, J., & Zimek, A. (2011). Density-based clustering. *WIREs Data Mining and Knowledge Discovery*, *1*(3), 231–240. http://doi.org/10.1002/widm.30

Kuhn, M. (2020). caret: Classification and Regression Training. Retrieved from https://cran.r-project.org/package=caret

Kummu, M., Moel, H. de, Ward, P. J., & Varis, O. (2011). How Close Do We Live to Water? A Global Analysis of Population Distance to Freshwater Bodies. *PLoS ONE*, *6*(6), e20578. http://doi.org/10.1371/journal.pone.0020578

Kummu, M., Taka, M., & Guillaume, J. H. A. (2018). Gridded global datasets for Gross Domestic Product and Human Development Index over 1990–2015. *Scientific Data*, *5*(1), 180004. http://doi.org/10.1038/sdata.2018.4

Lamb, A., Green, R., Bateman, I., Broadmeadow, M., Bruce, T., Burney, J., ... Balmford, A. (2016). The potential for land sparing to offset greenhouse gas emissions from agriculture. *Nature Clim. Change*, *6*(5), 488–492. Retrieved from http://dx.doi.org/10.1038/nclimate2910%20http://10.0.4.14/nclimate2910%20http://www.nature.com/nclimate/journal/v6/n5/abs/nclimate2910.html%7B/#%7Dsupplementary-information

Lambin, E. F., & Meyfroidt, P. (2011). Global land use change, economic globalization, and the looming land scarcity. *Proceedings of the National Academy of Sciences*, *108*(9), 3465–3472. http://doi.org/10.1073/pnas.1100480108

Landis, J. R., & Koch, G. G. (1977). The Measurement of Observer Agreement for Categorical Data. *Biometrics*, *33*(1), 159. http://doi.org/10.2307/2529310

Lanz, B., Dietz, S., & Swanson, T. (2018). The Expansion of Modern Agriculture and Global Biodiversity Decline: An Integrated Assessment. *Ecological Economics*, *144*, 260–277. http://doi.org/10.1016/j.ecolecon.2017.07.018

Latrubesse, E. M., Arima, E. Y., Dunne, T., Park, E., Baker, V. R., D'Horta, F. M., ... Stevaux, J. C. (2017). Damming the rivers of the Amazon basin. *Nature*, *546*(7658), 363–369. http://doi.org/10.1038/nature22333

Laurance, W. F., & Arrea, I. B. (2017). Roads to riches or ruin? *Science*, *358*(6362), 442–444. http://doi.org/10.1126/science.aao0312

Leach, K., Brooks, S. E., & Blyth, S. (2016). *Potential threat to areas of biodiversity importance from current and emerging oil and gas activities in Africa* (No. June) (p. 41). Cambridge, UK: UNEP-WCMC.

Leadley, P. W., Pereira, H. W., Alkemade, R., Fernandez-Manjarrés, J. F., Proença, V., Scharlemann, J. P. W., & Walpole, M. (2010). *Projections of 21st Century Change in*

Biodiversity and Associated Ecosystem Services. Montreal, Canada: Secretariat of the Convention on Biological Diversity.

Lehner, B., Liermann, C. R., Revenga, C., Vörömsmarty, C., Fekete, B., Crouzet, P., ... Wisser, D. (2011). High-resolution mapping of the world's reservoirs and dams for sustainable river-flow management. *Frontiers in Ecology and the Environment*, *9*(9), 494–502. http://doi.org/10.1890/100125

Lennon, J. J. (2000). Red-shifts and red herrings in geographical ecology. *Ecography*, *23*(1), 101–113. http://doi.org/10.1111/j.1600-0587.2000.tb00265.x

Lenzen, M., Moran, D., Kanemoto, K., Foran, B., Lobefaro, L., & Geschke, A. (2012). International trade drives biodiversity threats in developing nations. *Nature*, *486*, 109–112. http://doi.org/10.1038/nature11145

Liu, C., Newell, G., & White, M. (2019). The effect of sample size on the accuracy of species distribution models: considering both presences and pseudo-absences or background sites. *Ecography*, *42*(3), 535–548. http://doi.org/10.1111/ecog.03188

Lloyd, C. T., Chamberlain, H., Kerr, D., Yetman, G., Pistolesi, L., Stevens, F. R., ... Tatem, A. J. (2019). Global spatio-temporally harmonised datasets for producing high-resolution gridded population distribution datasets. *Big Earth Data*, *3*(2), 108–139. http://doi.org/10.1080/20964471.2019.1625151

Lovich, J. E., & Ennen, J. R. (2013). Assessing the state of knowledge of utility-scale wind energy development and operation on non-volant terrestrial and marine wildlife. *Applied Energy*, *103*, 52–60. http://doi.org/10.1016/j.apenergy.2012.10.001

Mace, G. M., Barrett, M., Burgess, N. D., Cornell, S. E., Freeman, R., Grooten, M., & Purvis, A. (2018). Aiming higher to bend the curve of biodiversity loss. *Nature Sustainability*, *1*(9), 448–451. http://doi.org/10.1038/s41893-018-0130-0

Marmion, M., Luoto, M., Heikkinen, R. K., & Thuiller, W. (2009). The performance of state-of-the-art modelling techniques depends on geographical distribution of species. *Ecological Modelling*, *220*(24), 3512–3520. http://doi.org/10.1016/j.ecolmodel.2008.10.019

Marrou, H. (2019). Co-locating food and energy. *Nature Sustainability*, *2*(9), 793–794. http://doi.org/10.1038/s41893-019-0377-0

Marrou, H., Guilioni, L., Dufour, L., Dupraz, C., & Wery, J. (2013). Microclimate under agrivoltaic systems: Is crop growth rate affected in the partial shade of solar panels? *Agricultural and Forest Meteorology*, *177*, 117–132. http://doi.org/10.1016/j.agrformet.2013.04.012

Martin, L. J., Quinn, J. E., Ellis, E. C., Shaw, M. R., Dorning, M. A., Hallett, L. M., ... Wiederholt, R. (2014). Conservation opportunities across the world's anthromes.

Diversity and Distributions, *20*(7), 745–755. http://doi.org/10.1111/ddi.12220

Mascia, M. B., & Pailler, S. (2011). Protected area downgrading, downsizing, and degazettement (PADDD) and its conservation implications. *Conservation Letters*, *4*(1), 9–20. http://doi.org/10.1111/j.1755-263X.2010.00147.x

May, R., Nygård, T., Falkdalen, U., Åström, J., Hamre, Ø., & Stokke, B. G. (2020). Paint it black: Efficacy of increased wind turbine rotor blade visibility to reduce avian fatalities. *Ecology and Evolution*, *10*(16), 8927–8935. http://doi.org/10.1002/ece3.6592

McGill, B. (2015). Land use matters. *Nature*, *520*(7545), 38–39. http://doi.org/10.1038/520038a

McGill, B. J., Dornelas, M., Gotelli, N. J., & Magurran, A. E. (2015). Fifteen forms of biodiversity trend in the Anthropocene. *Trends in Ecology & Evolution*, *30*(2), 104–113. http://doi.org/10.1016/j.tree.2014.11.006

McGlade, C., & Ekins, P. (2015). The geographical distribution of fossil fuels unused when limiting global warming to 2 °C. *Nature*, *517*(7533), 187–190. http://doi.org/10.1038/nature14016

Meijer, J. R., Huijbregts, M. A. J., Schotten, K. C. G. J., & Schipper, A. M. (2018). Global patterns of current and future road infrastructure. *Environmental Research Letters*, *13*(6), 064006. http://doi.org/10.1088/1748-9326/aabd42

Meyers, J., & Meneveau, C. (2012). Optimal turbine spacing in fully developed wind farm boundary layers. *Wind Energy*, *15*(2), 305–317. http://doi.org/10.1002/we.469

Miao, R., Ghosh, P. N., Khanna, M., Wang, W., & Rong, J. (2019). Effect of wind turbines on bird abundance: A national scale analysis based on fixed effects models. *Energy Policy*, *132*, 357–366. http://doi.org/10.1016/j.enpol.2019.04.040

Miller, L. M., & Keith, D. W. (2018). Observation-based solar and wind power capacity factors and power densities. *Environmental Research Letters*, *13*(10), 104008. http://doi.org/10.1088/1748-9326/aae102

Mittermeier, R. A., Mittermeier, C. G., & Robles Gil, P. (1997). *Megadiversity : earth's biologically wealthiest nations* (1st Englis, p. 501). Mexico, D.F.: CEMEX.

Monfreda, C., Ramankutty, N., & Foley, J. A. (2008). Farming the planet: 2. Geographic distribution of crop areas, yields, physiological types, and net primary production in the year 2000. *Global Biogeochemical Cycles*, *22*(1), n/a–n/a. http://doi.org/10.1029/2007GB002947

Montoya, J. M., Donohue, I., & Pimm, S. L. (2018). Planetary Boundaries for Biodiversity: Implausible Science, Pernicious Policies. *Trends in Ecology & Evolution*, *33*(2), 71–73. http://doi.org/10.1016/j.tree.2017.10.004

Moore-O'Leary, K. A., Hernandez, R. R., Johnston, D. S., Abella, S. R., Tanner, K. E., Swanson, A. C., ... Lovich, J. E. (2017). Sustainability of utility-scale solar energy - critical ecological concepts. *Frontiers in Ecology and the Environment*, *15*(7), 385–394. http://doi.org/10.1002/fee.1517

Neumann, K., Verburg, P. H., Stehfest, E., & Müller, C. (2010). The yield gap of global grain production: A spatial analysis. *Agricultural Systems*, *103*(5), 316–326. http://doi.org/10.1016/j.agsy.2010.02.004

Newbold, T., Hudson, L. N., Arnell, A. P., Contu, S., Palma, A. D., Ferrier, S., ... Zhang, H. (2016a). Has land use pushed terrestrial biodiversity beyond the planetary boundary? A global assessment. *Science*, *353*(6296), 288–291. Retrieved from http://science.sciencemag.org/content/sci/353/6296/288.full.pdf

Newbold, T., Hudson, L. N., Hill, S. L. L., Contu, S., Gray, C. L., Scharlemann, J. P. W., ... Purvis, A. (2016b). Global patterns of terrestrial assemblage turnover within and among land uses. *Ecography*, *39*(12), 1151–1163. http://doi.org/10.1111/ecog.01932

Newbold, T., Hudson, L. N., Hill, S. L. L., Contu, S., Lysenko, I., Senior, R. A., ... Purvis, A. (2015). Global effects of land use on local terrestrial biodiversity. *Nature*, *520*(7545), 45–50. http://doi.org/10.1038/nature14324

Nogués-Bravo, D., Rodríguez-Sánchez, F., Orsini, L., Boer, E. de, Jansson, R., Morlon, H., ... Jackson, S. T. (2018). Cracking the Code of Biodiversity Responses to Past Climate Change. *Trends in Ecology & Evolution*, *33*(10), 765–776. http://doi.org/10.1016/j.tree.2018.07.005

Norris, K., Terry, A., Hansford, J. P., & Turvey, S. T. (2020). Biodiversity Conservation and the Earth System: Mind the Gap. *Trends in Ecology & Evolution*. http://doi.org/10.1016/j.tree.2020.06.010

Northrup, J. M., & Wittemyer, G. (2013). Characterising the impacts of emerging energy development on wildlife, with an eye towards mitigation. *Ecology Letters*, *16*(1), 112–125. http://doi.org/10.1111/ele.12009

Oakleaf, J. R., Kennedy, C. M., Baruch-Mordo, S., Gerber, J. S., West, P. C., Johnson, J. A., & Kiesecker, J. (2019). Mapping global development potential for renewable energy, fossil fuels, mining and agriculture sectors. *Scientific Data*, *6*(1), 101. http://doi.org/10.1038/s41597-019-0084-8

O'Hara, R. B., & Kotze, D. J. (2010). Do not log-transform count data. *Methods in Ecology and Evolution*, *1*(2), 118–122. http://doi.org/10.1111/j.2041-210X.2010.00021.x

Oliphant, A. J., Thenkabail, P. S., Teluguntla, P., Xiong, J., Congalton, R. G., Yadav, K., ... Smith, C. (2017). NASA Making Earth System Data Records for Use in Research

Environments (MEaSUREs) Global Food Security-support Analysis Data (GFSAD) Cropland Extent 2015 Southeast Asia 30 m V001. http://doi.org/10.5067/MEaSUREs/GFSAD/GFSAD30SEACE.001

OpenStreetMap. (2019). Elements. Retrieved from https://wiki.openstreetmap.org/wiki/Elements

OpenStreetMap. (2020). WikiProject Oil and Gas Infrastructure. Retrieved from https://wiki.openstreetmap.org/wiki/WikiProject%7B/_%7DOil%7B/_%7Dand%7B/_%7DGas%7B/_%7DInfrastructure

Orme, C. D. L., Davies, R. G., Burgess, M., Eigenbrod, F., Pickup, N., Olson, V. a, ... Owens, I. P. F. (2005). Global hotspots of species richness are not congruent with endemism or threat. *Nature*, *436*(7053), 1016–9. http://doi.org/10.1038/nature03850

Ostberg, S., Schaphoff, S., Lucht, W., & Gerten, D. (2015). Three centuries of dual pressure from land use and climate change on the biosphere. *Environmental Research Letters*, *10*(4), 044011. http://doi.org/10.1088/1748-9326/10/4/044011

Pacifici, M., Foden, W. B., Visconti, P., Watson, J. E. M., Butchart, S. H. M., Kovacs, K. M., ... Rondinini, C. (2015). Assessing species vulnerability to climate change. *Nature Climate Change*, *5*(February), 215–225. http://doi.org/10.1038/nclimate2448

Pacifici, M., Visconti, P., Butchart, S. H. M., Watson, J. E. M., Cassola, F. M., & Rondinini, C. (2017). Species' traits influenced their response to recent climate change. *Nature Climate Change*, (February). http://doi.org/10.1038/nclimate3223

Padgham, M., Rudis, B., Lovelace, R., & Salmon, M. (2017). Osmdata. *Journal of Open Source Software*, *2*(14). http://doi.org/10.21105/joss.00305

Pearson, R. G. (2016). Reasons to Conserve Nature. *Trends in Ecology and Evolution*, *31*(5), 366–371. http://doi.org/10.1016/j.tree.2016.02.005

Pearson, R. G., Stanton, J. C., Shoemaker, K. T., Aiello-Lammens, M. E., Ersts, P. J., Horning, N., ... Akçakaya, H. R. (2014). Life history and spatial traits predict extinction risk due to climate change. *Nature Climate Change*, *4*(3), 217–221. http://doi.org/10.1038/nclimate2113

Pebesma, E. (2018). Simple Features for R: Standardized Support for Spatial Vector Data. *The R Journal*. Retrieved from https://journal.r-project.org/archive/2018/RJ-2018-009/index.html

Pesaresi, M., Florczyk, A. J., Schiavina, M., Melchiorri, M., & Maffenini, L. (2019). *GHSL Data Package 2019, EUR 29788 EN*. Luxembourg: Publications Office of the European Union.

Pérez-Hoyos, A., Rembold, F., Kerdiles, H., & Gallego, J. (2017). Comparison of Global

Land Cover Datasets for Cropland Monitoring. *Remote Sensing*, *9*(11), 1118. http://doi.org/10.3390/rs9111118

Pillai, U. (2015). Drivers of cost reduction in solar photovoltaics. *Energy Economics*, *50*, 286–293. http://doi.org/10.1016/j.eneco.2015.05.015

Pimm, S. L., Jenkins, C. N., Abell, R., Brooks, T. M., Gittleman, J. L., Joppa, L. N., ... Sexton, J. O. (2014). The biodiversity of species and their rates of extinction, distribution, and protection. *Science*, *344*(6187), 1246752–1246752. http://doi.org/10.1126/science.1246752

Pogson, M., Hastings, A., & Smith, P. (2013). How does bioenergy compare with other land-based renewable energy sources globally? *GCB Bioenergy*, *5*(5), 513–524. http://doi.org/10.1111/gcbb.12013

Pollock, L. J., Thuiller, W., & Jetz, W. (2017). Large conservation gains possible for global biodiversity facets. *Nature Publishing Group*. http://doi.org/10.1038/nature22368

Pouzols, F. M., Toivonen, T., Di Minin, E., Kukkala, A. S., Kullberg, P., Kuusterä, J., ... Moilanen, A. (2014). Global protected area expansion is compromised by projected land-use and parochialism. *Nature*, *516*(7531), 383–6. http://doi.org/10.1038/nature14032

Ramankutty, N., Evan, A. T., Monfreda, C., & Foley, J. A. (2008). Farming the planet: 1. Geographic distribution of global agricultural lands in the year 2000. *Global Biogeochemical Cycles*, *22*(1), n/a–n/a. http://doi.org/10.1029/2007GB002952

Rand, J. T., Kramer, L. A., Garrity, C. P., Hoen, B. D., Diffendorfer, J. E., Hunt, H. E., & Spears, M. (2020). A continuously updated, geospatially rectified database of utility-scale wind turbines in the United States. *Scientific Data*, *7*(1), 15. http://doi.org/10.1038/s41597-020-0353-6

Randle-Boggis, R. J., White, P. C. L., Cruz, J., Parker, G., Montag, H., Scurlock, J. M. O., & Armstrong, A. (2020). Realising co-benefits for natural capital and ecosystem services from solar parks: A co-developed, evidence-based approach. *Renewable and Sustainable Energy Reviews*, *125*, 109775. http://doi.org/10.1016/j.rser.2020.109775

Rehbein, J. A., Watson, J. E. M., Lane, J. L., Sonter, L. J., Venter, O., Atkinson, S. C., & Allan, J. R. (2020). Renewable energy development threatens many globally important biodiversity areas. *Global Change Biology*, gcb.15067. http://doi.org/10.1111/gcb.15067

REN21. (2018). *Renewables 2018 Global Status Report*. Paris: REN21 Secretariat.

Ripley, B. D. (1977). Modelling Spatial Patterns. *Journal of the Royal Statistical Society: Series B (Methodological)*, *39*(2), 172–192. http://doi.org/10.1111/j.2517-6161.1977.tb01615.x

Robinson, T. P., Wint, G. R. W., Conchedda, G., Van Boeckel, T. P., Ercoli, V., Palamara, E., ... Gilbert, M. (2014). Mapping the Global Distribution of Livestock. *PLoS ONE*, *9*(5), e96084. http://doi.org/10.1371/journal.pone.0096084

Roddis, P., Carver, S., Dallimer, M., Norman, P., & Ziv, G. (2018). The role of community acceptance in planning outcomes for onshore wind and solar farms: An energy justice analysis. *Applied Energy*, *226*, 353–364. http://doi.org/10.1016/j.apenergy.2018.05.087

Ross, N. (2018). fasterize: Fast Polygon to Raster Conversion. R package version 1.0.0. Retrieved from https://cran.r-project.org/package=fasterize

Safi, K., Armour-Marshall, K., Baillie, J. E. M., & Isaac, N. J. B. (2013). Global Patterns of Evolutionary Distinct and Globally Endangered Amphibians and Mammals. *PLoS ONE*, *8*(5), e63582. http://doi.org/10.1371/journal.pone.0063582

Santangeli, A., Butchart, S. H. M., Pogson, M., Hastings, A., Smith, P., Girardello, M., & Moilanen, A. (2018). Mapping the global potential exposure of soaring birds to terrestrial wind energy expansion. *Ornis Fennica*, *95*, 1–14.

Santangeli, A., Di Minin, E., Toivonen, T., Pogson, M., Hastings, A., Smith, P., & Moilanen, A. (2016). Synergies and trade-offs between renewable energy expansion and biodiversity conservation - a cross-national multifactor analysis. *GCB Bioenergy*, *8*, 1191–1200. http://doi.org/10.1111/gcbb.12337

Santangeli, A., & Katzner, T. (2015). A call for conservation scientists to evaluate opportunities and risks from operation of vertical axis wind turbines. *Frontiers in Ecology and Evolution*, *3*(June), 2014–2016. http://doi.org/10.3389/fevo.2015.00068

Santangeli, A., Toivonen, T., Pouzols, F. M., Pogson, M., Hastings, A., Smith, P., & Moilanen, A. (2015). Global change synergies and trade-offs between renewable energy and biodiversity. *GCB Bioenergy*, *8*, 941–951. http://doi.org/10.1111/gcbb.12299

Sánchez-Bayo, F., & Wyckhuys, K. A. G. (2019). Worldwide decline of the entomofauna: A review of its drivers. *Biological Conservation*, *232*, 8–27. http://doi.org/10.1016/j.biocon.2019.01.020

Scheidel, A., & Sorman, A. H. (2012). Energy transitions and the global land rush: Ultimate drivers and persistent consequences. *Global Environmental Change*, *22*(3), 588–595. http://doi.org/10.1016/j.gloenvcha.2011.12.005

Scherer, L., & Pfister, S. (2016). Global water footprint assessment of hydropower. *Renewable Energy*, *99*, 711–720. http://doi.org/10.1016/j.renene.2016.07.021

Schuster, E., Bulling, L., & Köppel, J. (2015). Consolidating the State of Knowledge: A Synoptical Review of Wind Energy's Wildlife Effects. *Environmental Management*, *56*(2), 300–331. http://doi.org/10.1007/s00267-015-0501-5

Seppelt, R., Manceur, A. M., Liu, J., Fenichel, E. P., & Klotz, S. (2014). Synchronized peak-rate years of global resources use. *Ecology and Society*, *19*(4). http://doi.org/10.5751/ES-07039-190450

Slade, R., Saunders, R., Gross, R., & Bauen, A. (2011). *Energy from biomass: the size of the global resource*. London: Imperial College Centre for Energy Policy; Technology; UK Energy Research Centre.

Smil, V. (2008). *Energy in nature and society: general energetics of complex systems*. MIT press.

Smil, V. (2010). Power Density Primer: Understanding the Spatial Dimension of the Unfolding Transition to Renewable Electricity Generation. Retrieved from https://pdfs.semanticscholar.org/9fb0/7a8a4449ab6d8a773204d1ac31e8b98c50a2.pdf

Smith, A., Kern, F., Raven, R., & Verhees, B. (2014). Spaces for sustainable innovation: Solar photovoltaic electricity in the UK. *Technological Forecasting and Social Change*, *81*, 115–130. http://doi.org/10.1016/j.techfore.2013.02.001

Smith, P., Davis, S. J., Creutzig, F., Fuss, S., Minx, J., Gabrielle, B., ... Yongsung, C. (2016). Biophysical and economic limits to negative CO2 emissions. *Nature Climate Change*, *6*(1), 42–50. http://doi.org/10.1038/nclimate2870

Sonter, L. J., Dade, M. C., Watson, J. E. M., & Valenta, R. K. (2020). Renewable energy production will exacerbate mining threats to biodiversity. *Nature Communications*, *11*(1), 4174. http://doi.org/10.1038/s41467-020-17928-5

Stanton, J. C., Shoemaker, K. T., Pearson, R. G., & Akçakaya, H. R. (2015). Warning times for species extinctions due to climate change. *Global Change Biology*, *21*(3), 1066–1077. http://doi.org/10.1111/gcb.12721

Steffen, W., Broadgate, W., Deutsch, L., Gaffney, O., & Ludwig, C. (2015). The trajectory of the Anthropocene: The Great Acceleration. *The Anthropocene Review*, *2*(1), 81–98. http://doi.org/10.1177/2053019614564785

Steinbuks, J., & Hertel, T. W. (2013). Energy prices will play an important role in determining global land use in the twenty first century. *Environmental Research Letters*, *8*(1), 014014. http://doi.org/10.1088/1748-9326/8/1/014014

Sutherland, W. J., Barnard, P., Broad, S., Clout, M., Connor, B., Côté, I. M., ... Ockendon, N. (2017). A 2017 Horizon Scan of Emerging Issues for Global Conservation and Biological Diversity. *Trends in Ecology and Evolution*, *32*(1), 31–40. http://doi.org/10.1016/j.tree.2016.11.005

Sutherland, W. J., Broad, S., Caine, J., Clout, M., Dicks, L. V., Doran, H., ... Wright, K. E. (2016). A Horizon Scan of Global Conservation Issues for 2016. *Trends in Ecology and Evolution*, *31*(1), 44–53. http://doi.org/10.1016/j.tree.2015.11.007

Symes, W. S., Rao, M., Mascia, M. B., & Carrasco, L. R. (2016). Why do we lose protected areas? Factors influencing protected area downgrading, downsizing and degazettement in the tropics and subtropics. *Global Change Biology*, *22*(2), 656–665. http://doi.org/10.1111/gcb.13089

Thaxter, C. B., Buchanan, G. M., Carr, J., Butchart, S. H. M., Newbold, T., Green, R. E., ... Pearce-Higgins, J. W. (2017). Bird and bat species' global vulnerability to collision mortality at wind farms revealed through a trait-based assessment. *Proceedings of the Royal Society B: Biological Sciences*, *284*(1862), 20170829. http://doi.org/10.1098/rspb.2017.0829

Thomas, C. D., Jones, T. H., & Hartley, S. E. (2019). "Insectageddon": A call for more robust data and rigorous analyses. *Global Change Biology*, *25*(6), 1891–1892. http://doi.org/10.1111/gcb.14608

Thomas, C. D., Thomas, C. D., Cameron, A., Cameron, A., Green, R. E., Green, R. E., ... Williams, S. E. (2004). Extinction risk from climate change. *Nature*, *427*(6970), 145–8. http://doi.org/10.1038/nature02121

Thompson, M., Beston, J. A., Etterson, M., Diffendorfer, J. E., & Loss, S. R. (2017). Factors associated with bat mortality at wind energy facilities in the United States. *Biological Conservation*, *215*, 241–245. http://doi.org/10.1016/j.biocon.2017.09.014

Thornley, P., & Cooper, D. (2008). The effectiveness of policy instruments in promoting bioenergy. *Biomass and Bioenergy*, *32*(10), 903–913. http://doi.org/10.1016/j.biombioe.2008.01.011

Titeux, N., Henle, K., Mihoub, J. B., Regos, A., Geijzendorffer, I. R., Cramer, W., ... Brotons, L. (2016). Biodiversity scenarios neglect future land-use changes. *Global Change Biology*, *22*(7), 2505–2515. http://doi.org/10.1111/gcb.13272

Tittensor, D. P., Walpole, M., Hill, S. L. L., Boyce, D. G., Britten, G. L., Burgess, N. D., ... Ye, Y. (2014). A mid-term analysis of progress toward international biodiversity targets. *Science*, *346*(6206), 241–244. http://doi.org/10.1126/science.1257484

Trainor, A. M., McDonald, R. I., & Fargione, J. (2016). Energy Sprawl Is the Largest Driver of Land Use Change in United States. *PLOS ONE*, *11*(9), e0162269. http://doi.org/10.1371/journal.pone.0162269

Turner, B. L., Lambin, E. F., & Reenberg, A. (2007). The emergence of land change science for global environmental change and sustainability. *Proceedings of the National Academy of Sciences*, *104*(52), 20666–20671. http://doi.org/10.1073/pnas.0704119104

UN. (2020). Sustainable Development Goals. Retrieved from https://sustainabledevelopment.un.org/sdgs

UNEP-WCMC. (n.d.). Calculating protected area coverage. Retrieved from https://www.protectedplanet.net/c/calculating-protected-area-coverage

UNEP-WCMC & IUCN. (2020). Protected Planet: The World Database on Protected Areas (WDPA) [On-line]. Cambridge, UK: UNEP-WCMC; IUCN. Retrieved from http://www.protectedplanet.net/

UNEP-WCMC, IUCN, & NGS. (2018). *Protected Planet Report 2018*. Cambridge UK; Gland, Switzerland;; Washington, D.C., USA.

UNFCCC. (2016). Paris Agreement. Paris, France. Retrieved from https://treaties.un.org/pages/ViewDetails.aspx?src=TREATY%7B/&%7Dmtdsg%7B/_%7Dno=XXVII-7-d%7B/&%7Dchapter=27%7B/&%7Dclang=%7B/_%7Den

United Nations Convention to Combat Desertification. (2017). Energy and Climate. In *The global land outlook* (First, pp. 212–225). Bonn, Germany.

Urban, M. C., Bocedi, G., Hendry, A. P., Mihoub, J. B., Peer, G., Singer, A., ... Travis, J. M. J. (2016). Improving the forecast for biodiversity under climate change. *Science*, *353*(6304), aad8466–aad8466. http://doi.org/10.1126/science.aad8466

Van Asselen, S., & Verburg, P. H. (2013). Land cover change or land-use intensification: Simulating land system change with a global-scale land change model. *Global Change Biology*, *19*(12), 3648–3667. http://doi.org/10.1111/gcb.12331

Václavík, T., Langerwisch, F., Cotter, M., Fick, J., Häuser, I., Hotes, S., ... Seppelt, R. (2016). Investigating potential transferability of place-based research in land system science. *Environmental Research Letters*, *11*(9), 095002. http://doi.org/10.1088/1748-9326/11/9/095002

Václavík, T., Lautenbach, S., Kuemmerle, T., & Seppelt, R. (2013). Mapping global land system archetypes. *Global Environmental Change*, *23*(6), 1637–1647. http://doi.org/10.1016/j.gloenvcha.2013.09.004

Venables, W., & Ripley, B. D. (2002). *Modern Applied Statistics with S* (Fourth). New York: Springer. Retrieved from http://www.stats.ox.ac.uk/pub/MASS4

Venter, O., Sanderson, E. W., Magrach, A., Allan, J. R., Beher, J., Jones, K. R., ... Watson, J. E. M. (2016). Sixteen years of change in the global terrestrial human footprint and implications for biodiversity conservation. *Nature Communications*, *7*(1), 12558. http://doi.org/10.1038/ncomms12558

Verburg, P. H., Crossman, N., Ellis, E. C., Heinimann, A., Hostert, P., Mertz, O., ... Zhen, L. (2015). Land system science and sustainable development of the earth system: A global land project perspective. *Anthropocene*, *12*, 29–41. http://doi.org/10.1016/j.ancene.2015.09.004

Verburg, P. H., Ellis, E. C., & Letourneau, A. (2011). A global assessment of market

accessibility and market influence for global environmental change studies. *Environmental Research Letters*, *6*(3), 034019. http://doi.org/10.1088/1748-9326/6/3/034019

Visconti, P., Di Marco, M., Álvarez-Romero, J. G., Januchowski-Hartley, S. R., Pressey, R. L., Weeks, R., & Rondinini, C. (2013). Effects of Errors and Gaps in Spatial Data Sets on Assessment of Conservation Progress. *Conservation Biology*, *27*(5), 1000–1010. http://doi.org/10.1111/cobi.12095

Vuuren, D. P. van, Kok, M. T. J., Girod, B., Lucas, P. L., & Vries, B. de. (2012). Scenarios in Global Environmental Assessments: Key characteristics and lessons for future use. *Global Environmental Change*, *22*(4), 884–895. http://doi.org/10.1016/j.gloenvcha.2012.06.001

Waldman, J., Sharma, S., Afshari, S., & Fekete, B. (2019). Solar-power replacement as a solution for hydropower foregone in US dam removals. *Nature Sustainability*, *2*(9), 872–878. http://doi.org/10.1038/s41893-019-0362-7

Wang, P., Huang, C., Brown de Colstoun, E. C., Tilton, J. C., & Tan, B. (2017). *Global Human Built-up And Settlement Extent (HBASE) Dataset From Landsat*. Palisades, NY: NASA Socioeconomic Data; Applications Center (SEDAC). Retrieved from https://doi.org/10.7927/H4DN434S

Watson, J. E. M., Darling, E. S., Venter, O., Maron, M., Walston, J., Possingham, H. P., ... Brooks, T. M. (2016). Bolder science needed now for protected areas. *Conservation Biology*, *30*(2), 243–248. http://doi.org/10.1111/cobi.12645

Watson, J. J. W., & Hudson, M. D. (2015). Regional Scale wind farm and solar farm suitability assessment using GIS-assisted multi-criteria evaluation. *Landscape and Urban Planning*, *138*, 20–31. http://doi.org/10.1016/j.landurbplan.2015.02.001

Weiss, D. J., Nelson, A., Gibson, H. S., Temperley, W., Peedell, S., Lieber, A., ... Gething, P. W. (2018). A global map of travel time to cities to assess inequalities in accessibility in 2015. *Nature*, *553*(7688). http://doi.org/10.1038/nature25181

Wickham, H., François, R., Henry, L., & Müller, K. (2020). dplyr: A Grammar of Data Manipulation. Retrieved from https://cran.r-project.org/package=dplyr

Winemiller, K. O., McIntyre, P. B., Castello, L., Fluet-Chouinard, E., Giarrizzo, T., Nam, S., ... Saenz, L. (2016). Balancing hydropower and biodiversity in the Amazon, Congo, and Mekong. *Science*, *351*(6269), 128–129. http://doi.org/10.1126/science.aac7082

Wolfe, P. (2013). *Solar Photovoltaic Projects in the Mainstream Power Market* (1st ed., p. 240). Oxford, UK: Routledge.

Xu, C., Kohler, T. A., Lenton, T. M., Svenning, J.-C., & Scheffer, M. (2020). Future of the human climate niche. *Proceedings of the National Academy of Sciences*, *117*(21), 11350–11355. http://doi.org/10.1073/pnas.1910114117

Yohe, G. (2014). Some extending thoughts on "thinking globally and siting locally—renewable energy and biodiversity in a rapidly warming world". *Climatic Change*, *126*(1-2), 7–11. http://doi.org/10.1007/s10584-014-1205-1

Yu, J., Wang, Z., Majumdar, A., & Rajagopal, R. (2018). DeepSolar: A Machine Learning Framework to Efficiently Construct a Solar Deployment Database in the United States. *Joule*, *2*(12), 2605–2617. http://doi.org/10.1016/j.joule.2018.11.021

Zabel, F., Putzenlechner, B., & Mauser, W. (2014). Global Agricultural Land Resources – A High Resolution Suitability Evaluation and Its Perspectives until 2100 under Climate Change Conditions. *PLoS ONE*, *9*(9), e107522. http://doi.org/10.1371/journal.pone.0107522

Zalk, J. van, & Behrens, P. (2018). The spatial extent of renewable and non-renewable power generation: A review and meta-analysis of power densities and their application in the U.S. *Energy Policy*, *123*, 83–91. http://doi.org/10.1016/j.enpol.2018.08.023

Zuur, A. F., Ieno, E. N., Walker, N., Saveliev, A. A., & Smith, G. M. (2009). *Mixed effects models and extensions in ecology with R*. New York: Springer New York. http://doi.org/10.1007/978-0-387-87458-6